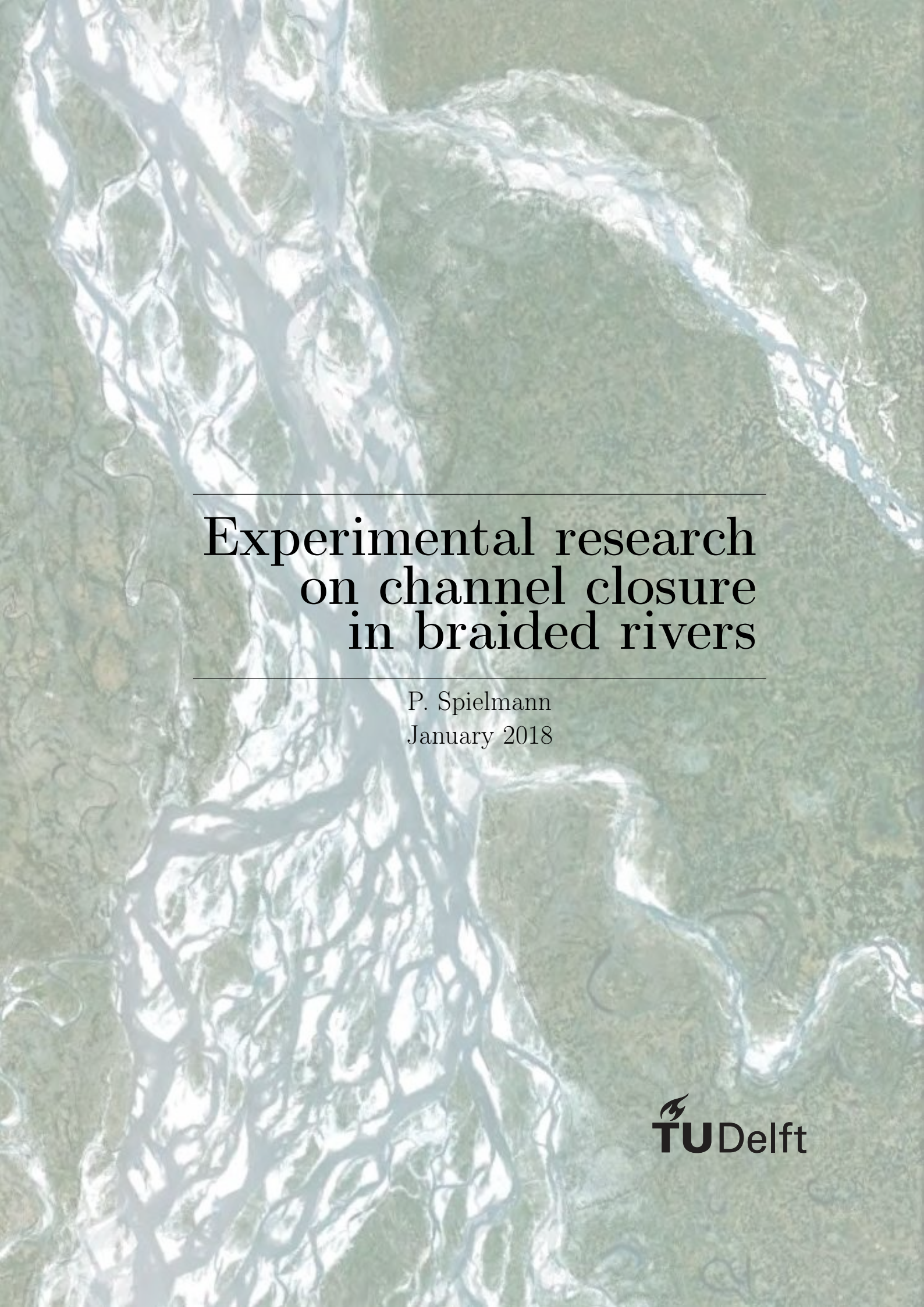

Experimental research on channel closure in braided rivers

P. Spielmann

January 2018

TU Delft

Cover photo: The braided Jamuna-Brahmaputra River (Bangladesh), from Google Earth™

Experimental research on channel closure in braided rivers

by

Peter Spielmann

to obtain the degree of Master of Science
at the Delft University of Technology,
to be defended publicly on Wednesday 31 January, 2018 at 10:00 AM.

Student number:	4144872	
Project duration:	March, 2017 – January, 2018	
Thesis Committee:	Prof. Dr. Ir. W.S.J. Uijttewaal	TU Delft
	Dr. Ir. A. Blom	TU Delft
	Dr. Ir. E. Mosselman	TU Delft, Deltares

An electronic version of this thesis is available at `http://repository.tudelft.nl/`.

TU Delft

Preface

This thesis is the final element of my Master study of Hydraulic Engineering at Delft University of Technology. The research on channel closure in braided rivers was carried out at the faculty of Civil Engineering and its adjacent Fluid Mechanics Laboratory. It was an interesting period with many challenges and I would like to thank everyone that contributed along the way.

First, I would like to thank my thesis committee for their guidance and critical feedback on my research. Especially the different perspectives of the committee members during meetings and individual conversations were very valuable. Further they often pointed out the importance of long term planning, which helped me to stay on track.

Furthermore, I would like to thank the staff of the Fluid Mechanics Laboratory. Their practical input and help with constructing the flume setup was important for successfully carrying out the laboratory experiments.

Finally, I would like to thank my family and friends for their support and great experiences during the last years.

Peter Spielmann
Delft, January 2018

Summary

The dynamic nature of braided rivers can lead to river bank erosion, bankline shifts and navigational hindrance. River training measures can be implemented in order to mitigate these problems. An alternative to conventional river training works is the closure of a channel within the braided network. Until recent there has been no systematic research on channel closure and guidelines or recommendations were absent. Recent simulations with numerical models on sand-bed braided rivers investigated both the effects of channel closure around the island and on the braided network. The results of these studies have their limitations and validation with physical models or pilot tests are necessary. Therefore, the objective of this thesis is to obtain a better understanding of the local morphodynamic effects of interventions aiming at channel closure in braided rivers.
This has been done by conducting flume experiments with a simplified section of a braided river with gravel-bed similarity. A section, consisting of a fixed Y-shaped confluence followed by an alluvial island surrounded by two channels and fixed outer banks, was used to systematically study the local effects of channel closure. For the experiments these local effects were divided into effects on island scale and effects on the downstream successive island. On island scale a weir was installed in one of the channels at three locations: the begin, middle and end. The closure effectiveness was analyzed both with a low and high discharge stage. The effects on the downstream successive island were analyzed by redistributing the discharge in the upstream confluence. This asymmetrical inflow was used to simulate the effects of channel closure upstream of the island.

The planform with an island surrounded by two channels was obtained by initially forming a mid-channel bar, which emerged with decreasing discharge. The mid-channel bar developed downstream of the confluence in the middle of the widened section with fixed banks. This so-called confluence-diffluence unit formed here due to the divergence of the streamlines and hence a decrease in sediment transport rate. By subsequently decreasing the discharge in phases the mid-channel bar emerged and the elevation increased in size by upstream addition of sediment. The formation of the planform with this method varied for the different experiments on channel closure of this study, however the final obtained planform was very similar. The initial planform for the different experiments was reproducible and stable enough to systematically study the local effects of channel closure.

For channel closure on island scale during the low-discharge stage it was most effective to install a closure measure at the upstream side of the island, at respectively the begin and middle. At these locations the sedimentation before the measure influenced the distribution at the bifurcation most. The closure measure at the end did not have as much effect, which agrees with the recommendations of the numerical study of Ostanek Jurina (2017). The effectiveness of the closure measure during the high-discharge stage could not be

analyzed properly for all experiments. As the discharge increased a large-scale reshaping of the upper half of the island was observed. This resulted in the direct bypassing of the closure measures at the begin and middle. For the closure measure at the end a bypass channel developed with headward erosion which was likely the result of the water level gradient. Similar results were obtained from numerical simulations with sand-bed braided rivers of Ostanek Jurina (2017), although the observed erosion mechanisms differed. This difference can be attributed to the difference in sediment mobility of gravel and sand-bed similarity.

For the experiments with the upstream closure measures it was observed that the asymmetrical inflow influenced the planform of the downstream successive island. The planform changes were more significant with higher discharge ratios of the two tributaries. The asymmetric discharge distribution over the tributaries resulted in the asymmetrical distribution of discharge over the bifurcation branches. As a result one of the channels became dominant and the island reshaped asymmetrically. This sequence of morphodynamic changes on the successive island corresponds with the numerical simulations of Schuurman et al. (2016). During the experiments two different reshaping mechanisms were observed, which differently influenced the distribution at the bifurcation. The first mechanism was the shift of the bifurcation and the second mechanism the deepening of the dominant channel. The separate observation of these mechanisms is probably due to the experimental setup, which prohibits the migration, rotation and reshaping of channels.

Contents

List of Figures

List of Tables

List of Symbols

β	Average aspect ratio	–
Δ	Relative submerged mass density	–
λ_b	Dimensionless wavenumber	–
λ_b^*	Wavenumber of width variation	m
ν	Kinematic viscosity	m^2/s
ρ_f	Density of fluid	kg/m^3
ρ_s	Density of sediment	kg/m^3
τ	Shear stress	N/m^2
θ	Shields number	–
θ_0	Dimensionless shear stress	–
B	Channel width	m
B_0^*	Average half-width of channel	m
C	Chézy Coefficient	$\mathrm{m}^{1/2}/s$
C_{90}	Grain roughness	$\mathrm{m}^{1/2}/s$
D	Sediment diameter	m
d_s	Dimensionless sediment diameter	–
Fr	Froude Number	–
g	Gravitational acceleration	m/s^2
h	Water depth	m
i_b	Channel slope	$1/\mathrm{m}$
$L_{1/2}$	Adaptation length (half)	m
L_b^*	Wavelength of width variation	m
Q	Discharge	m^3/s
Re	Reynolds Number	–
Re^*	Particle Reynolds Number	–

S	Sediment transport	m^3/s
u	Velocity	m/s
u_*	Shear velocity	m/s
w_s	Fall velocity	m/s
X_f	Distance upstream confluence to front elevation	m
Z	Bed level	mm

1 Introduction

1.1 Background

A braided river system is a complex network of multiple channels splitting and rejoining around alluvial bars or islands. These rivers are characterized as wide and shallow with an alluvial bed of non-cohesive sediment. Braided rivers are considered very dynamic with rapid planform changes that are difficult to predict, see Figure 1.1. Especially the dynamics of large braided rivers, with a combined channel width of one kilometre or more, can be a major threat to the surrounding population and impose challenges for river management.

The dynamic nature of braided rivers can lead to bank line shifts, river bank erosion and cause navigational problems. The bank line shift of the largest rivers may be in order order of hundreds of metres per year (Baki and Gan, 2012). River bank erosion and channel shifting leads to loss of homes, loss of fertile agricultural land, population displacement, destruction of infrastructure and flood protections. This adversely affect the livelihood of riparian population, agriculture, the environment and imposes socio-economic problems (Klaassen et al., 2002). Planform shifts and wide but relatively shallow channels also impose problems for navigation. Remaining sufficient navigational depth at some of its reaches is often difficult, especially during the dry season. In some cases vessels are forced to travel longer distances to their destination or even become stranded along the way. An often occurring problem after the wet season is the unknown position of the main navigable channel due to channel shifting (van der Velden, 2015). These properties of braided rivers hinder efficient use of the river for navigational purposes. This is especially a problem considering that navigation is often the most important mode of transport where these rivers are present (Karmaker and Dutta, 2016).

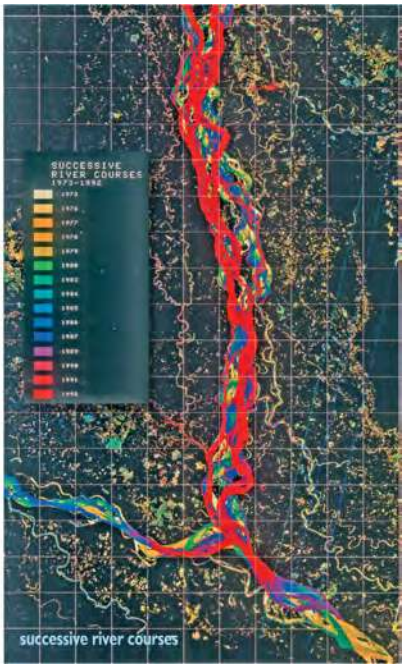

Figure 1.1: Successive river courses in the Jamuna River between years 1973-1992. Flow from N to S, from (Mosselman, 2006).

Channel closure as river training measure

River training measures can be implemented in order to mitigate the problems described. Conventional measures, such as groynes and spurs, are used in rivers in order to control meander migration and navigational depth. However, these measures are scarcely applied in large braided rivers and often not successful. Applying conventional measures results in high costs and large uncertainties of uncontrollable negative impacts, due to the enormous dimensions of these rivers (Schuurman et al., 2016). Problems encountered are the capability of the river to destroy measures or to completely bypass them as channels shift their position (Nakagawa et al., 2013). Predicting the large-scale effects of these river training works on the long term is difficult and often not fully understood.

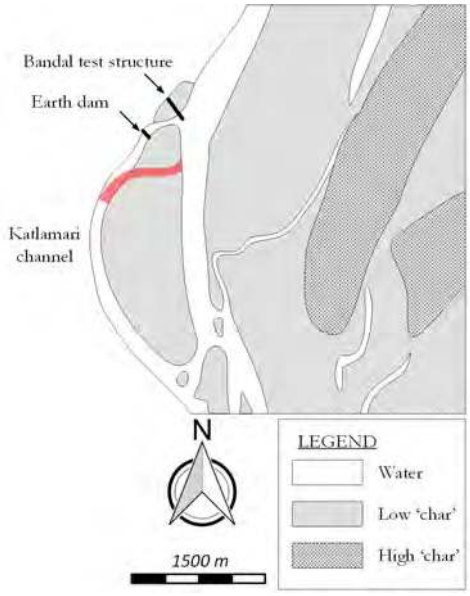

Figure 1.2: Reopening of the closed channel during the FAP22 pilot project in the Jamuna River, Bangladesh. Flow from N to S, after (Mosselman, 2006).

An alternative river training measure is closing off one of the channels in the braided network with interventions. By closing off one of the branches aggressive bank erosion can be mitigated and/or the navigational depth in the other branches can be increased during the dry season. Channel closure is often partially, meaning that during low water the flow is diverted while during high water the channel conveys water. This type of measure is planned or applied in several projects. Based on a multi-criteria analysis, Hooning (2011) concluded that narrowing (closing off channels) the Koshi River in Nepal is the most promising way for river management. For the Brahmaputra River system a similar management technique is proposed (Northwest Hydraulic Consultants & Mott MacDonald, 2014). Over the last decades the Brahmaputra system has been in a process of drastic widening and westward migration. It is therefore proposed to gradually narrow the river back to its original width. Another project is planned next to the port of Mandalay, along the Ayeyarwady River. Here the closure of a channel should improve the navigational conditions (Directorate of Water Resources and Improvement of River Systems, 2016).

Although channel closure is applied as river training measure in practice, guidelines or recommendations are absent. Moreover, only a few cases have been documented and were only partially successful. The formation of a bypass channel during the wet season caused the closed branch to reopen, see Figure 1.2. Similar problems with closing off channels occurred in the Ayeyarwady and Congo River. With numerical simulations for different research purposes, similar problems are encountered (Hooning, 2011) (Karmaker and Dutta, 2016) (Schuurman et al., 2016).

The effects of channel closure in large sand-bed braided rivers have been studied with numerical models (Ostanek Jurina, 2017) (Schuurman et al., 2016). The former study focused on effective channel closure on island scale. With a simplified planform, consisting of two branches separated by an island, systematic research was conducted in order to study the effects during the dry and wet season. The study concludes with guidelines

and recommendations for a successful channel closure. The latter study focused on the network response of disturbances in a braided river. With a self-forming braided river multiple river training works, including channel closure interventions, were simulated to evaluate the nearby and far-away effects. It was concluded that river training works can induce far downstream effects in the braided channel network.

1.2 Problem description

Management of braided rivers for navigational purposes or to mitigate bank erosion often leads to closing off one of its branches with interventions. However, channel closure measures are often not successful due to re-opening of the closed branch. In the few documented cases the re-opening was caused by the erosion of a bypass channel across the island during the wet season. Although channel closure is applied as river training measure in practice only recent systematic research provides some guidelines and recommendations. The numerical research of Ostanek Jurina (2017) and Schuurman et al. (2016) studied the effects of channel closure in large sand-bed braided rivers. The former focused on the effective closure on island scale, while the latter focused on the network response. Although the studies focused on different aspects and scales, the resulting guidelines, recommendations and conclusions can be used for the closure of a channel in a braided network.
However, it should be taken into account that both of these studies have been conducted with numerical models. Within the field of river engineering, models, numerical and physical, are used to research phenomena quantitatively and qualitatively. Both numerical as physical models have their advantages and disadvantages (de Vries, 1973). Using a combination of both types of models, so-called composite modelling, can lead to different forms of improvement.

1.3 Objective and research questions

The objective of this thesis is:
To obtain a better understanding of the local morphodynamic effects of interventions aiming at channel closure in braided rivers.

To reach this objective, three research questions are given below. Combined, these questions will set a next step in understanding the local effects of interventions aiming at channel closure in braided rivers.

1. How can a laboratory experiment be designed to study the local morphodynamic effects of interventions aiming at channel closure in a braided river?
2. What are the morphodynamic effects of interventions aiming at channel closure on island scale, during low and high water?
3. What are the morphodynamic effects of interventions aiming at channel closure on the downstream successive island?

1.4 Research methodology

This research consists of two main parts: selecting a setup of the laboratory experiments and conducting the experiments on channel closure. These experiments are designed and conducted in the Fluid Mechanics Laboratory of Delft University of Technology. With the selection of the setup of the laboratory experiments the first research question is addressed. The setup, with a simplified planform section of a braided river, is used to conduct experiments on channel closure. The main goal of the experiments is to answer the second and third research questions. These results are compared with the numerical simulations of Ostanek Jurina (2017) and Schuurman et al. (2016). In this thesis similar scenarios are tested to compare the obtained results in order to validate/complement the different models. The details of the design of the experiment and the conducted experiments on channel closure can be found in chapter 3 and chapter 4.

1.5 Outline of the thesis

Although the chapter titles should be self-explanatory, the following describes in short the contents of various chapters:

In *chapter 2* the theoretical background on morphodynamic processes and channel closure in braided rivers will be discussed on the basis of a literature review.

In *chapter 3* the design of the laboratory experiment is described. Here the selection of the setup, conditions and measurement equipment are discussed. The chapter is concluded with experiments relevant for selecting the setup.

In *chapter 4* the configurations, flow stages and results of the experiments conducted on channel closure are presented.

In *chapter 5* the results of the experiments are discussed.

In *chapter 6* the conclusions and relevant recommendations of this study are given.

2 Literature review

2.1 Braided rivers

Natural alluvial rivers can be distinguished based on their pattern or planform. In classical literature (Leopold and Wolman, 1957) straight, meandering and braided planforms are distinguished, see Figure 2.1. Since then many other river patterns have been identified such as anastomosing, anabranching and wandering.

(a) (b) (c)

Figure 2.1: Classical distinction of river patterns or planforms: straight (a), meandering (b) and braided (c).

Over the years several qualitative classifications and explanations for different channel patterns have emerged and are still debated. However, several authors do agree upon that a hard discrimination between different classes is less representative for natural rivers than a continuum of channel patterns with many intermediate classes (Leopold and Wolman, 1957) (Ferguson, 1987) (Vandenberghe, 1995).
Braided rivers systems are characterized as wide and shallow with an alluvial bed of non-cohesive sediments. They typically transport an abundance of non-cohesive sediment down a fairly steep slope. The channels form a complex network and split and rejoin around alluvial bars or islands. Braided rivers are considered dynamic systems with high

rates of fluvial activity and channel adaptation by erosional and depositional processes. The occurring flow stage is of large influence of the above characteristics and overall planform of a braided river. During bankfull conditions rivers may act as a single stream whereas at lower stages they exhibit a characteristic braided pattern. Also the number of bars or islands to be submerged or emerged varies with flow stage. These different flow stages cause complex sequences of erosion and deposition.

2.2 Morphodynamics of braided rivers

In this section the general hydro- and morphodynamic processes within braided rivers are discussed. For the purpose of this study the focus of these processes are related to channel closure.

2.2.1 Bifurcations and confluences

The morphodynamics of braided rivers are highly influenced by bifurcations and confluences within the network. At these nodes the sediment and discharge is distributed which determines the sediment availability and sediment transport capacity in the branches. Understanding the processes around bifurcations and confluences is of importance in order to determine the local effects of channel closure.

Bifurcations
A river bifurcation (or diffluence) is a node where a single stream divides into two or more downstream branches (or distibutaries). The evolution of the two downstream channels heavily depends on the distribution of water and sediment at the bifurcation. The distribution of sediment over the branches is mainly determined by the three-dimensional flow field, the local bed topography and the mode of sediment transport. Within a downstream branch a morphological equilibrium is obtained when the sediment transport capacity equals the sediment delivered into the branch at the upstream bifurcation. As the relation between flow velocity and sediment transport capacity is non-linear (e.g. $q_s \sim u^{4-5}$), minor adjustments in discharge distribution at the bifurcation may have a large influence on the sediment transport capacity in the downstream branches. Bifurcations in braided rivers are therefore often not in equilibrium and unstable. Moreover, they are often asymmetrical, causing one of the branches to be dominant (Bertoldi et al., 2009) (Egozi and Ashmore, 2008).
Bifurcation asymmetry is usually characterized by a difference in bed level and channel width of the branches. The dominant branch becomes deeper and wider, while the other slowly narrows and becomes shallower. The dominant channel usually has more or less the same direction as the upstream inflow. Another planform indicator of bifurcation asymmetry is the relative length and width of bar tail limbs (Koomen, 1992) (Schuurman and Kleinhans, 2015). The dominant channel, which is most morphologically active, creates the longest bar-tail limb, see Figure 2.2. This deposited sediment is often partly provided by upstream erosion of the bar, resulting in an increase in bifurcation angle. Furthermore, Schuurman and Kleinhans (2015) found that the bifurcation angle is an indicator of discharge division and shows the probability of entrance closure by migrating or expanding bars.

The distribution at a bifurcation can be influenced by the migration or formation of bars and a shift of the inflow channel (Schuurman and Kleinhans, 2015). Bars at the entrance can deflect the flow towards one of the channels, while bars within the branch can cause a backwater effect. The upstream shift of the inflow channel can change the distribution as well. These types of processes should be taken into account when considering channel closure.
In order to get some insight in the individual evolution of a bifurcation relatively simple analytically relations can be used. In 1D models sediment distribution is modelled with nodal point relations (Wang et al., 1995) (Bolla Pittaluga et al., 2003) (Kleinhans et al., 2013). Despite the simplifications, also acknowledged by the authors, these relations can be useful for analyzing specific cases. Schuurman and Kleinhans (2015) and Zolezzi et al. (2006) showed that the nodal point relations have limited predictive value. Especially the evolution of bifurcations in braided rivers where local three-dimensional effects and reach scale network effects dominate show their limitations.

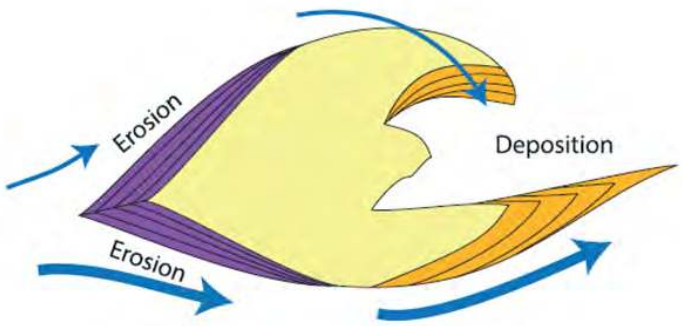

Figure 2.2: Concept of the evolution of bar-tail limbs according to the dominance of the bifurcation branch, from (Schuurman and Kleinhans, 2015).

Confluences
A river confluence (or conflux) is a node where two branches join into a single stream. Here the upstream branches provide the total water and sediment transport of the downstream channel. Due to variations in discharge ratio and the flow direction of converging channels, the planform of a confluence in a braided river can vary significantly over time. Ashmore (1993) studied the planform dynamics of confluences and observed a combination of migration, rotation, resizing and obliteration (abandonment of one of the confluencing channels).
The tributaries of a confluence will have a curved pathway as they re-align with the direction of the main channel. This curved pathway may cause secondary flow, similar as observed in river bends (Ashmore and Parker, 1983). The local secondary flow takes the form of two counterrotating flow cells with plunging flow in the centre, see Figure 2.3. Just after the confluence apex a stagnation zone can develop. Downstream of this stagnation zone a large portion of the mixing takes places in a shear layer between the two tributary flows. Often one, or both, of the confluent channels build an avalanche face due to flow deflection, acceleration and increased shear stresses (Best, 1987). A spoon-shaped scour hole can develop in the middle of the channel due to the local secondary flow (Mosley, 1976) (Ashmore et al., 1992). The depth of this confluence scour hole increases with increasing confluence angle or discharge ratio (Best, 1988). At the separation zone of the resulting flow field a bar may emerge, resulting in a combined confluence-bifurcation point. The relationship between confluence kinetics and subsequent braid bar sedimenta-

tion is a key element of braided river mechanics, which principle is used for designing the experimental setup in chapter 3.

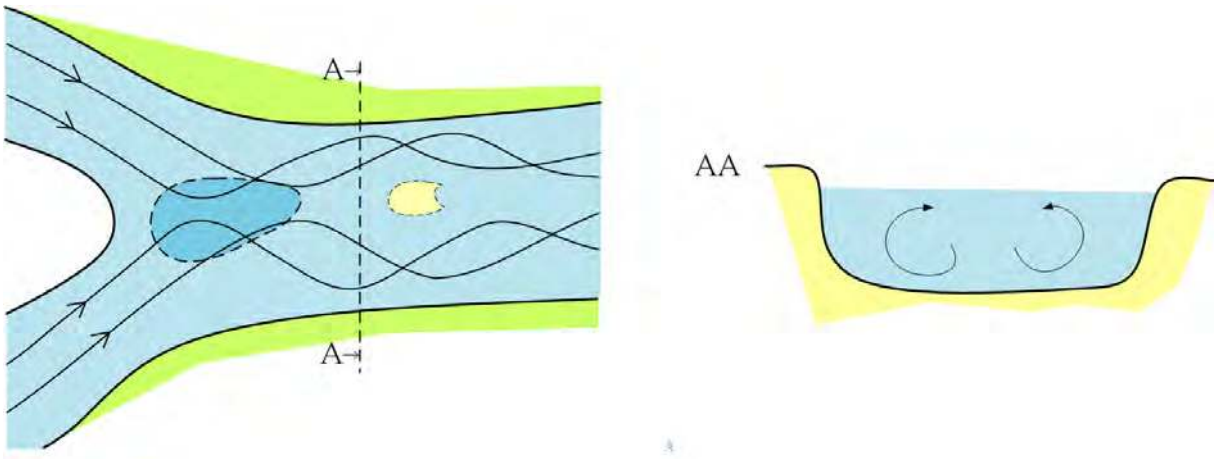

Figure 2.3: The flow field around a confluence: with scour hole, bar formation and helical secondary flow, after (Jagers, 2003).

When the tributaries are unequal in size, the avalanche face of the larger tributary often protrudes further than the face of the smaller one. The confluence moves towards and into the smaller channel through deposition (Klaassen and Masselink, 1992). This causes the direction of the downstream channels to adapt to the dominant flow direction from upstream. In addition, the long axis of the scour hole tends to parallel the dominant channel (Ashmore and Parker, 1983). The development of a bar-tail limbs from the dominant channel can affect this further, and possibly affect the next bifurcation (Schuurman and Kleinhans, 2015). These processes can propagate through the braided system and influence the redistribution of sediment far downstream (Schuurman et al., 2016).

2.2.2 River islands and bars

The different channels in braided rivers are separated from one another by morphological units: islands and bars. The difference between these two is identified by several authors (Brice, 1964) (Bridge, 1993) (Bristow and Best, 1993). The distinction between bars and islands is based on their size, age, vegetation and height with respect to bank full discharge. In general these factors can be linked to the stability; an island is more stable than a bar. The formation of bars and islands is inextricably linked with the formation of bifurcations and confluences, as described in the previous section.

River islands
Islands within the braided network are often vegetated, sometimes populated and are only submerged during floods. These morphological units are larger and higher than bars and their movement is limited. However, they are reworked by erosion, bar dissection and accretion. An island can be formed either by the growth of a large stable braid bar or by the river cutting a new channel through the flood plain. The first process leads to increasingly stable morphological units, while the second process is in general a starting point of a period with continuous erosion.

Bars

A river bar is an elevated area of sediment deposit within the watercourse, which is submerged or emerged depending on flow stage. Bars come in various shapes and were distinguished according to their origins and morphological features into free and forced bars (Seminara and Tubino, 1989), see Figure 2.4. Duró et al. (2015) improved this definition by introducing the hybrid bar, which has both free and forced properties. Free bars arise when an infinitesimally small perturbation of the flow or bed level is present within the morphodynamic instability range of the system. These bars are generally migrating and are classified as alternating bars and braid bars. Forced bars on the other hand are non-migrating. These sediment deposits are forced by a permanent deformation of the water flow, e.g. natural bend, a channel width variation or a structure. The hybrid bar forms both due to morphodynamic instability and the presence of some type of forcing.

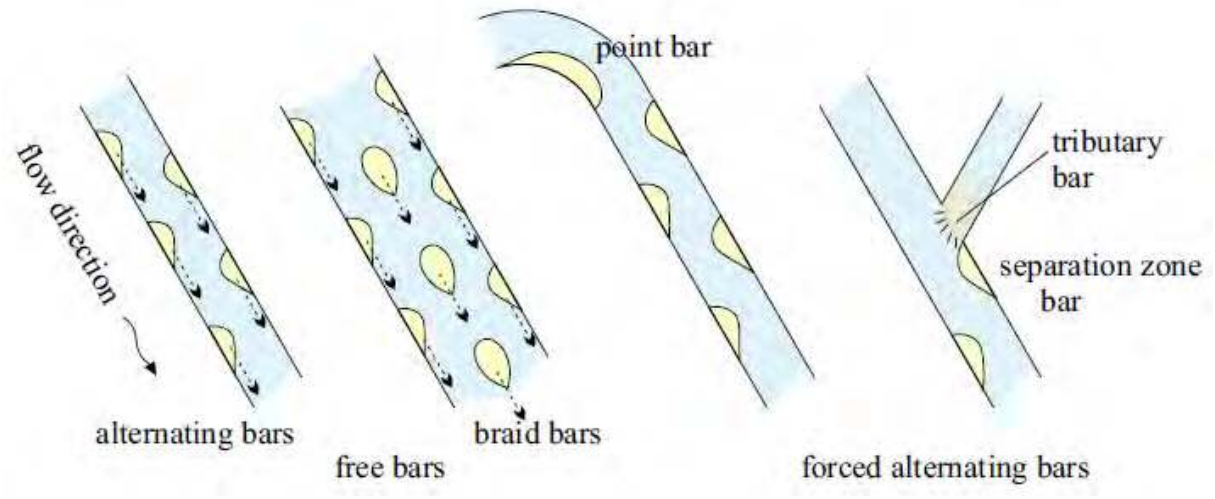

Figure 2.4: Sketches of the most commonly distinguished bar types, from (Jagers, 2003).

Braid bars are found in braided rivers and for the development and formation of these bars the width-to-depth ratio is of importance. With increasing width, the number of bars increase in transverse direction (Leopold and Wolman, 1957) (Engelund and Skovaard, 1973). One process that leads to the formation of such a bar is explained in subsection 2.2.3. The formation of braid bars can be accompanied with sediment sorting processes (Ashmore, 1991), which is mainly applicable in gravel-bed rivers. This results in a bar with coarse sediment at the upstream side and along the outer rim while fine sediment is found inside and at the downstream side, as indicated in Figure 2.5.

The secondary flow, or spiral flow, within river bends has a large influence on the flow and sediment dynamics in meandering rivers. Richardson et al. (1996) and Richardson and Thorne (1998) proposed a similar flow field in the two curved channels on both sides of a bar or island, see cross section AA in Figure 2.5. However, this secondary flow is in many cases too weak to be detected.

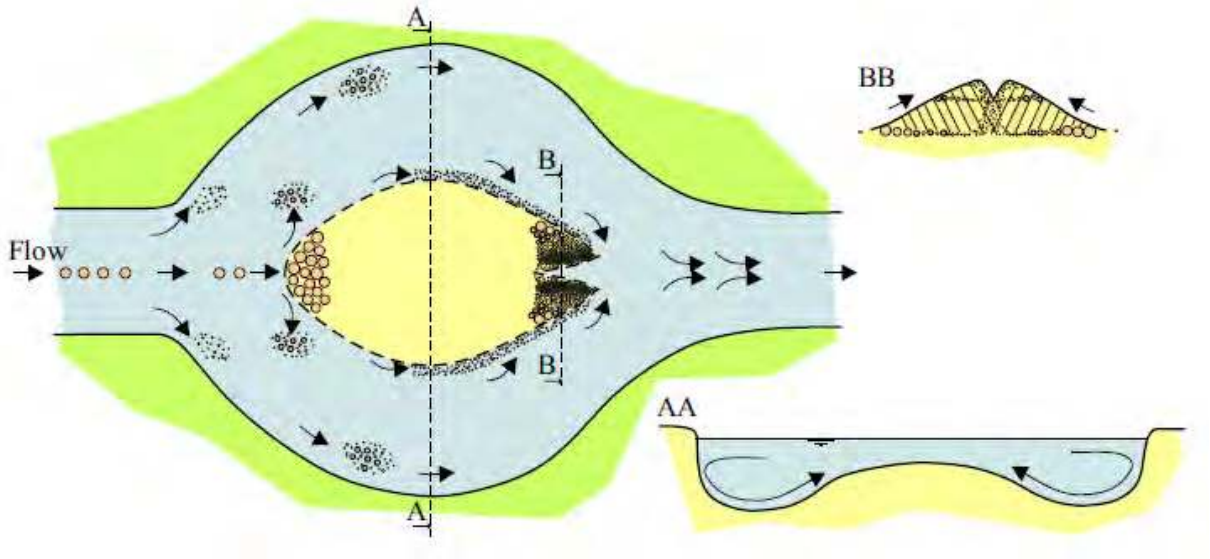

Figure 2.5: Sediment sorting processes and resulting grain size distribution within a braid bar as observed by (Ashworth et al., 1992), from (Jagers, 2003).

2.2.3 Channels shifts, formation and closure

The planform of braided rivers is dynamic as a result of the shifting, formation and closure of channels. The process of channel shifting is a complex process and difficult to predict. The shifting of a channel is accompanied with the abandonment of a channel and subsequent reoccupation of old channels, smaller channels or the formation of new channels. The abandonment of channels and formation of new channels is called avulsion and the reoccupation of previously abandoned channels is called secondary anastomosis (Ashmore, 1991) (Church, 1972). The natural formation and closure of channels in braided rivers is often initiated from the bifurcation point. Bifurcation asymmetry can be caused by bar dynamics, diverting flow and blocking one of the channels (Schuurman and Kleinhans, 2015). In addition. the initiation of bifurcations is closely linked to the initiation, growth and migration of bars (Ashmore, 1991).

Formation

The process of channel formation can be linked to the development of a bifurcation within the braided network. The different initiation mechanisms require high water levels and high rates of bed material transport, so they are often triggered by a flood (Kleinhans et al., 2013). From laboratory observations Ashmore (1991) identified three possible mechanisms through which bifurcations may occur:

Central bar mechanism and transverse bar conversion

The central bar mechanism occurs when a bedload sheet stalls, growing by downstream addition of sediment and forming a mid-channel bar. The stalling of the bed sheet is initiated by divergence of streamlines, causing a decrease in shear stress and hence in sediment transport rate. This divergence of streamlines is often observed downstream of confluences. This mechanism has also been observed by Leopold and Wolman (1957). A similar mechanism can be observed when transverse unit bars accumulate and form a mid-channel bar. The transport rates are higher than with the previous case, but both cases occur with the stalling of migrating bedforms in

a reach where the channel widens. The effects of width variations on the formation of central bars has been analyzed theoretically and experimentally (Repetto et al., 2002) (Wu and Yeh, 2005).

Chute cut-off mechanism
This mechanism occurs when a chute channel develops across alternate bars or point bars. The flow off the lee sides of the bars incise into chutes. This process is often initiated by a pulse of bed load that migrates into the neighbouring main channel. This causes a temporary rise of the water level and change in flow direction. Bifurcation initiation in a braided river occurs by over-bar flow forming cross-bar channels, and eventually a mature branch, see Figure 2.6. The same process can cause the formation of a channel in the floodplains. This mechanism was, besides scale experiments, observed in natural rivers (Bristow, 1987) and numerical models of braided rivers (Schuurman et al., 2013) (Schuurman and Kleinhans, 2015).

Figure 2.6: Formation of cross-bar channels in the Ganges River. Flow is from left to right, from (Schuurman and Kleinhans, 2015).

Simultaneous growth of multiple bars
This mechanism only has been observed in channels with high width/depth ratio. Bifurcations are initiated by the gradual converging of multiple row bars into fewer larger bars, leading to braiding.

For the analysis of the formation of the bypass channel around closure measures the processes of the second mechanism should be explored in more detail. Jagers (2003) found that in the braided Jamuna River channels often form from the upstream side. The results obtained from a numerical model mostly showed erosion starting from upstream as a propagating expansion wave, while headcut (upward) erosion could be only obtained with specific settings. Erosion from downstream was initiated for the situation with low water levels downstream and more cohesive sediment. The low downstream water levels resulted in accelerations of the flow and hence in increase in sediment transport capacity at the end of the bar. In scale experiments with gravel-bed braided rivers this downstream erosion has been observed as well (Leddy et al., 1993). This headcut erosion is caused by the decrease in sediment mobility. The bed is not easily erodible due to the sediment size.

Closure
Several mechanisms are responsible for the natural closure or abandonment of channels within the braided network. The bar dynamics play an important role in the closure of channels. When migrating bars stall in narrower channels one of the bifurcation branches can be closed off (Ashworth et al., 2011). This mechanism of bifurcation closure is dominant in channels with fixed banks (Burge, 2006) (Bertoldi et al., 2009). Another closure mechanism is observed when bar-tail limbs from the upstream bar expand towards one of

the branches (Schuurman and Kleinhans, 2015). This mechanism causes the merging and expansion of bars, which is also observed in nature (Ashworth et al., 2000) (Ashworth et al., 2011) (Best et al., 2003).
This expansion of bars in its turn may lead to the initiation of a bifurcation by (partial) blockage of the discharge through the channel. This impoundment of the local water level may form the potential for cross-bar flow and in the end bar dissection, as often observed in nature. This mechanism might be the reason for reopening of the channel. Channel closure also causes the partial blockage of the discharge and hence an impoundment of the local water level.

2.2.4 Erosion and sedimentation

In order to successfully close off a channel it is important to encourage sedimentation and prevent erosion at certain locations. Both erosion and deposition are caused by changes in sediment transport rate, which are caused by changes in the flow velocity. Large-scale erosion and sedimentation in braided rivers are affected by human interferences as they influence the hydrodynamics (Mosselman and Sloff, 2002).

Erosion
The erosion of sediment occurs as the transport capacity increases, which is caused by an increase in flow velocity. Erosion rates are influenced by the type of sediment and the presence of vegetation. In general two types of erosion are considered: bank erosion (horizontal) and scour of the channel bed (vertical).
The horizontal bank erosion is commonly distinguished in fluvial erosion, the entrainment of individual particles, and mass failure. Fluvial erosion occurs for example along the outer bank of a channel bend and the upstream end of an island or an emerged bar. Mass failure, or collapse, of the river bank is caused by a combination of reduction in strength and erosion processes. In large braided rivers the most common erosion process is a combination of the two described above. Large near-bank flow velocities are responsible for undercutting, which leads to bank failure. The cohesive nature of the banks is responsible for the mass failure. Bank erosion is common during the dry season and in smaller channels, it is not limited to extreme events (Sarker et al., 2014). The high rates of bank erosion can be mitigated with bank protection or by reducing the near-bank velocities. The presence of vegetation is negligible for the large-scale erosion as the roots do not effect the undercutting process (Klaassen and Masselink, 1992).
The vertical scour of the channel bed is induced by for example a change in flow stage (rising flood) or due to a change in planform (narrowing). Some specific planform characteristics cause local scour:

- Due to the secondary flow generated in channel bends a scour hole develops at the outer bed while sediment accumulates in the inner bend.
- Due to the helical flow generated at confluences a scour hole develops downstream of the point where the branches join, see Figure 2.3.
- Due to an obstruction in the flow, like a groyne head or bridge pier, a scour hole develops. The obstruction causes an increase in turbulence and accelerates the flow causing an increase in transport capacity.

The scour that develops near obstructions seems related with the eroding bypass channel

formed when channel closure measures are installed. This erosion around the river training prevents a successful closure of the channel.

Sedimentation

The deposition of sediment occurs as the transport capacity reduces, which is caused by a reduction in flow velocity. Other than erosion, deposition mainly occurs on the channel bed (vertical). The reduction in transport capacity can be caused for example by a change in planform (widening), falling stage of a flood or by a certain river training measure which increases roughness.

In order to close off channels sedimentation can be induced with for example porcupines and jack jetties to increase roughness. These permeable measures are situated in a specific lay-out in order to close off the channel initially. However, these can also be used near the eroded bypass channel during the falling stage, in order to prevent the reopening of the channel.

2.3 Channel closure in braided rivers

The dynamic behaviour of braided rivers imposes challenges for the management with river training works. A common management technique is the use of conventional hard permanent structures in order to stabilize and protect the most important reaches along the river. However, these river training measures are expensive and often lead to unexpected problems. For developing countries it is financially not possible to construct these measures along hundreds of kilometres of river reach, only some priority reaches can be protected. Along the Jamuna River several revetment-like and groyne-like structures have been constructed for protecting some important reaches. However, a significant part of these structures failed due to poor construction or lack of repair and maintenance (Uddin, 2010)(Hoque et al., 2008). In addition, the design is often based on the basis of experience in smaller rivers and extrapolated towards the larger rivers (Klaassen et al., 2002). By constructing river training measures at some priority reaches the entire river reach is changed on the long run by local changes, a stable river can never be formed. Further, due to shifting of channels these structures might be left with no purpose when the river changes direction (Nakagawa et al., 2013).

2.3.1 River training measures

Depending on the purpose of the closure, a channel can be closed off completely or partially. Complete closure means that both during dry season and wet season the channel will not convey water. Partial closure is used when the flow is forced into the other channel(s) by an obstruction during low flow, but during peak flow this obstruction is overtopped and the channel is used to convey water. For this study partial closure is of interest as complete closure only can be obtained with structures along the complete reach.
Partial closure can be realized with several measures, both permanent and recurrent. The former measures include the construction of a permanent dam or weir which is built to last multiple decades. In some cases the dredged material from the main channel can be used to provide material for such structures. The latter measures include the use of surface and bottom screens, porcupines or jack jetties. These measures are replaced more often due to their limited life-time, but provide more flexibility and are usually cheaper. Both permanent and recurrent measures use similar principles to close off channels in braided rivers: (1) by decreasing the discharge and sediment transport within the channel (2) by increasing roughness within the channel, which decreases flow velocity and hence induces sedimentation, and (3) by diverting flow away and sediment towards the channel, which induces sedimentation.

Dams and weirs
A branch can be closed off with the construction of a dam or weir. This simple obstruction can be used to reduce the flow in the closed branch. The reduction in discharge depends on the water level difference across the weir, the downstream water level and the crest shape. The suspended sediment may be transported over the weir while the bed load is deposited before the weir. This deposition continuous until the bed reaches the weir crest. Dams or weirs can be constructed as permanent measures, from concrete, or as recurrent

measure, from bed material.

Bandals

Already since the British Colonial Period the bandalling system has been used as river training measure on the Indian subcontinent along the Ganges and Brahmaputra River (Schmuck-Widmann, 2001). Bandals consist of a frame which is open at the lower half and closed off at the upper half by a screen, so in principle a surface screen. The bandals are placed with an angle with the main flow and as rule of thumb fifty percent of the flow area is blocked. The screen separates the sediment-laden flow near the bed from the clearer water near the surface, see Figure 2.7. The sediment-laden flow passes under the screen in the flow-direction whereas the clearer water is guided in a direction parallel to the screen. This results in sediment deposition behind the structure and scour in its vicinity due to the acceleration of the flow. Traditionally, bandals are used during the dry season to assure navigation with low water levels. Recent research shows that bandals also are capable of preventing bank erosion and stabilize river reaches (Rahman et al., 2003).

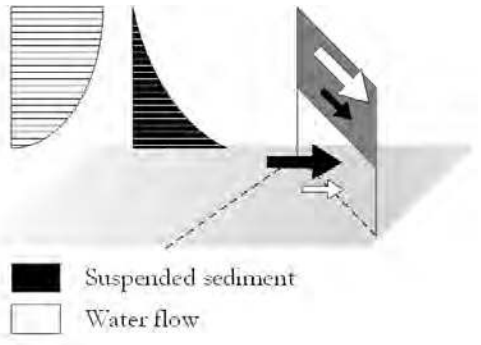

Figure 2.7: Schematic of the working principle of bandals.

Bottom vanes

Submerged vanes are relatively small river training structures installed in fields in the river bed. Bottom vanes redistribute the flow and sediment transport within a channel cross-section as a result of the generation of secondary circulation in the flow (Odgaard, 2009). These structures are installed at an angle with the flow, typically 10 to 20 degrees. The height of the vanes is as a design rule 0.2 to 0.4 times the local water depth at design stage. Submerged vanes have a broad range of applications which have been verified by both laboratory and field tests (Odgaard and Kennedy, 1983) (Odgaard and Spoljaric, 1986) (Douma and Mosselman, 2005): stabilization of river bank and river bed, sediment control at water intake or diversion and stabilization of river channel alignment. In Odgaard (2009) and Odgaard (2015) it is suggested that submerged vanes can be a useful tool for stabilizing reaches of braided rivers. By using the mentioned guidelines, vanes have the potential to reduce lateral extension of braided rivers. Indeed, vanes have been used to close off channels in the past (Chabert et al., 1961), with good results. Figure 2.10a schematically shows how submerged vanes can help to close off channels. The vanes are orientated such that they intercept and deflect sediment into the entrance region of the secondary branch, closing off the entrance by aggregation.

Figure 2.8: Vane pilot project, from (Douma and Mosselman, 2005).

Porcupines and jack jetties

Both porcupines and jack jetties locally increase roughness, decrease flow velocity and hence induce sedimentation (Nayak et al., 2016) (Yu et al., 2011). These river training measures are stable, all-round symmetrical elements with a rigid frame. The typical dimension of both elements is 2 to 3 metre, which can be applied for maximum water depth twice the height. As rule of thumb 15% to 33% is used for obstruction, otherwise undesired scour will take place along the proposed structures (Jha, 2014). They are used to train the river along the desired course, divert flow away from the bank, prevent erosion or enhance sedimentation. Both porcupines and jack jetties are used to close off channels, see Figure 2.9 (Nayak et al., 2016). In Flood Management Organisation (2012) the general design features of a porcupine screen are shown, together with a layout plan, see Figure 2.10b. Here it can be seen that as rule of thumb the screen is extended for 1/3 on both sides and that two screens are constructed. The experience with these types of measures to close off channels is not documented well. Hooning (2011) observed a failed channel closure of this type along the Koshi River in Nepal. According to the author this closure failed due to floating debris, damaging the porcupines.

Figure 2.9: Jack Jetty screen for channel closure, from (Nayak et al., 2016).

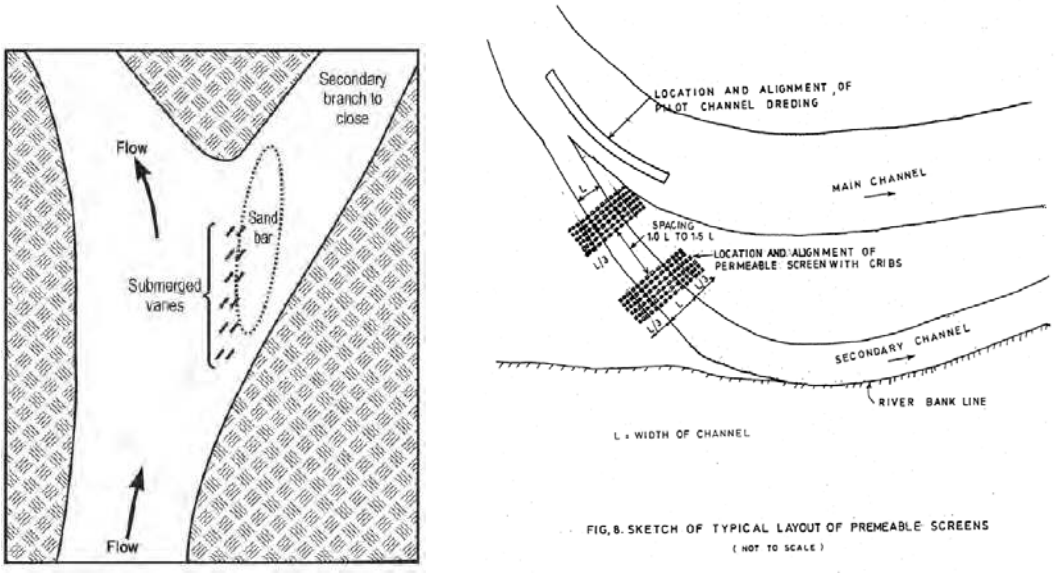

(a) Submerged vanes, from (Odgaard, 2009)

(b) Porcupine screen, from (Flood Management Organisation, 2012)

Figure 2.10: Different layout plans for closing channels with river training measures.

2.3.2 Pilot projects and research

Channel closure measures in braided rivers have been poorly documented. One of the documented projects is a pilot test to close a smaller secondary channel along the Jamuna River in Bangladesh: the Katlamari channel. This pilot project was conducted during the Flood Action Plan (FAP) 21/22. For this project efficient and potentially affordable solutions to the problem of bank erosion have been developed and tested (Mosselman, 2006). In order to close the channel a combination of bandals and an earth dam were constructed near the bifurcation point, see Figure 2.11b. The combination of these measures caused the flow to be diverted away from the channel and increased sedimentation. For a while the project seemed successful, however, during the flood period the river eroded a bypass channel downstream of the river training works, see Figure 2.11a and Figure 1.2. Analysis of the hydrodynamic data showed that a local water elevation difference, the water level gradient, over the river island caused the erosion of the bypass. In the evaluation report it was therefore proposed to change the location of the plug along the river island or impose measures on top of the island for a successful closure (Northwest Hydraulic Consultants & Mott MacDonald, 2014). The latter measures could include vegetation development or raising the elevation of the island/bar with dredged material. The local population in Bangladesh often uses catskin to stabilise river banks and increase siltation. Mosselman (2006) proposed that the deployment of the recurrent measures over a larger area, including the seasonally flooded bars and islands, would lead to a more complete closure. Similar problems with closing off channels occurred in the Ayeyarwady and Congo River.

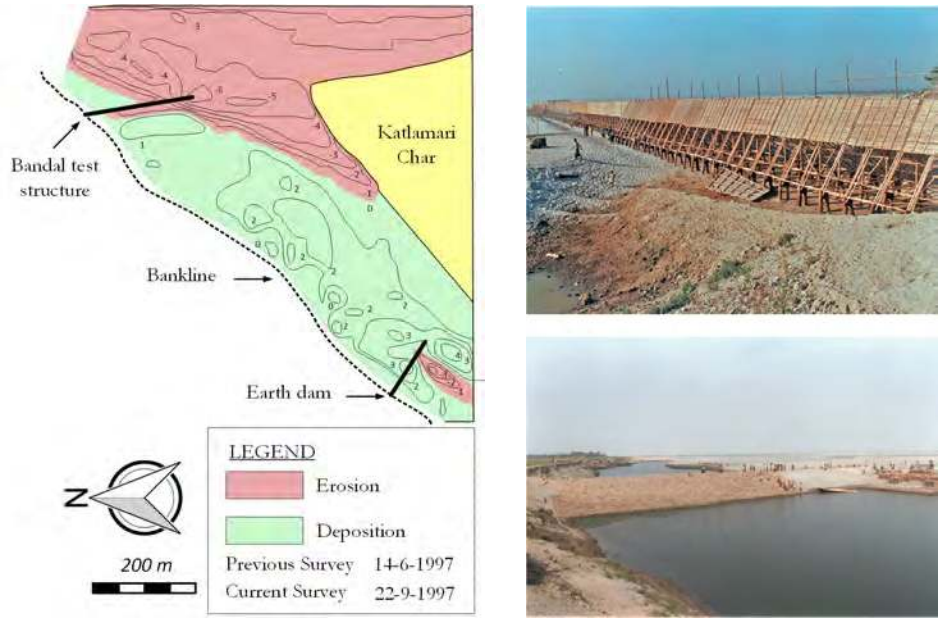

(a) (b)

Figure 2.11: Overview of bandals and earth dam of the Katlamari channel pilot test, figures after and from (Mosselman, 2001).

In numerical models similar problems with channel closure have been observed. Schuurman et al. (2016) investigated several perturbations in a self-formed braided river, including channel closure. The results of the simulation show resemblance with the pilot test: scour at the sides of the structure and channel reopening across the bar. A study on flood and sediment management of the braided Koshi River concluded that narrowing

the river (closing of channels) with recurrent measures was the most promising way to manage sediment (Hooning, 2011). When this was implemented in the numerical simulation, all structures were bypassed when time progressed. Hooning suggested to extend the structures to prevent the bypassing. Karmaker and Dutta (2016) experienced similar problems when trying to close off a channel with different groyne configurations. They discussed that the eroding channel might be caused by erosion at the tip of the groyne.
Ostanek Jurina (2017) conducted research on channel closure in large sand-bed braided rivers with a numerical model. Various simulations were conducted with a simplified planform, consisting of two branches separated by an island. Different types of closure measures at different locations along one of the channels were modelled. A hydrograph was used to simulate the effects of the dry and wet season. The different simulations were evaluated based on the effectiveness of the closure. In various simulations a bypass channel was formed over the braided island during the wet season, causing a failure of the closure, see Figure 2.12. From the research it was concluded that two types of channels formed: around the measure and across the island to the other channel. From Figure 2.12 it can be seen that the former forms with a measure at the begin of the channel, while the latter forms for the cases with a measure in the middle and final part of the channel. It was analyzed that the water level gradient, around the closure structure and across the island, is the main cause of the channel formation.
The research concludes with recommendations on channel closure based on the outcomes of the model study. Different layout plans are suggested depending on the pursued goals of the closure measure and the conditions in the particular river section, see Appendix F. Here it is mentioned that the use of a long embankment perpendicular to the closure measure, parallel to the island banks, is recommended in order to decrease the water level gradient around the structure. Further the results show that closure measures at the end of the channel are less effective than measures at the begin and middle.

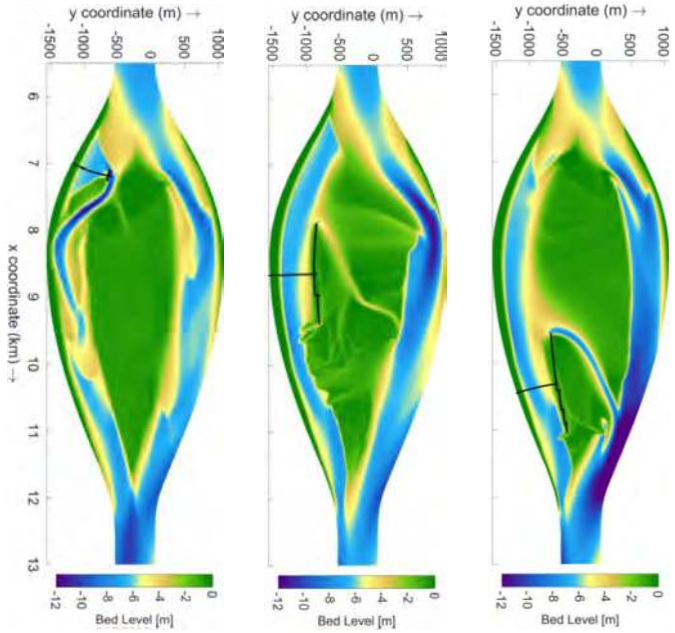

Figure 2.12: Numerical simulation of Ostanek Jurina (2017) show channel reopening for the cases with a closure measure at the begin (a) in the middle (b) and at the final part (c) of the channel.

2.3.3 Network response to channel closure

Installing a closure measure in a braided river affects the network both upstream and downstream. By closing a channel the river is locally narrowed, reducing the cross-sectional area. For predicting the short and long term morphodynamic effects equations exist based on the assumptions of quasi-steady non-uniform flow. On the short term the narrowed section of the river deepens, as sediment transport capacity is increased. Downstream of the narrowed section sediment is deposited, as here the transport capacity remains unaltered. The upstream section is influenced by the backwater curve induced by the river narrowing. Here a gradual reduction in velocities causes the deposition of sediment due to a decrease in transport capacity. On the long term the narrowing causes a reduction in the bed slope due to erosion in the narrowed section and overall bed degradation upstream caused by a lower downstream water level boundary condition.
From numerical simulations Schuurman et al. (2016) found that channel closure can induce far downstream effects in the braided channel network. Several disturbances in the form of river training works were simulated to evaluate the nearby and far-away effects. The results show that a disturbance, in the form of an adjustment to a bar, bifurcation or branch, initiates a sequence of adjustments in the downstream direction. This sequence of adjustments is (1) asymmetrical division of discharge and sediment over the bifurcation branches, (2) the elongation of the bar tail limb along the dominant branch, and (3) the change in approaching flow towards the successive bifurcation. The unequal division of discharge and sediment over a bifurcation induced the asymmetrical reshaping of mid-channel bars. This reshaping was found to have a crucial effect on the downstream propagation of disturbances.
In Figure 2.13 four regions of morphological effect of disturbances identified by Schuurman et al. (2016) are shown. In the case of channel closure as disturbance the following morphological response is initiated (green line in Figure 2.13):
The first region shows the direct effect in the vicinity of the closure structure. Here local incision takes place due to the compensation for width loss. In the second region, the compensation region, local deposition is initiated in response to the incision near the structure. The third region is influenced indirectly by bifurcation instability and asymmetrical reshaping of bars. The fourth region shows the upstream backwater effects, where deposition takes places.

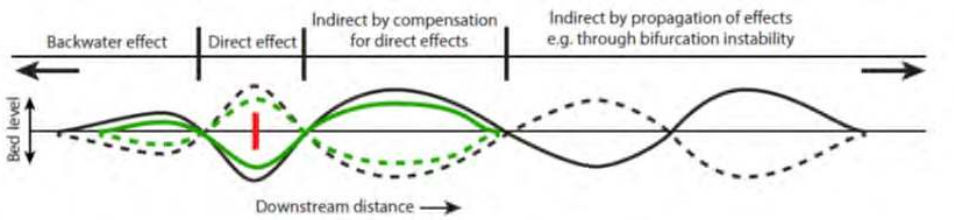

Figure 2.13: The four regions of morphological response to a disturbance, red line, in a braided river, from (Schuurman et al., 2016).

3 Design of laboratory experiment

3.1 Method

3.1.1 Selection of experimental setup

In order to study the local morphodynamic effects of channel closure in a laboratory flume, a relatively simple system is considered. In reality the braided river system is a complex network which constantly changes. However, for the purpose of this study only a small section of this network is considered. This simplified system consists of a channel, splitting (bifurcation) and re-joining (confluence) around an alluvial island. In one of the two channels closure measures are installed during the experiment in order to study the local effects.
In order to obtain this planform in a laboratory experiment some considerations should be taken into account. First of all the planform should be reproducible in order to systematically study the local morphodynamic effects. The starting point of all the experiments should be similar. Further the obtained planform should be stable to the hydrodynamic forcing and to small perturbations. With an unstable planform it would be practically impossible to distinguish the effects of channel closure.
Based on these considerations some practical characteristics of the experimental setup were determined. In order to find a suitable experimental setup the different considerations and practical characteristics were taken into account.

- The outer banks of the setup should be non-erodible. Without these fixed banks the hydraulic forcing would cause bank erosion of the adjacent banks. This will results in lateral migration of the branches, island aggradation and possible downstream migration of the island. By using non-erodible banks the overall planform of the island and its surrounding branches become more stable.

- The island should be self-forming with use of hydraulic forces. A stable system is obtained by using the interaction between the fixed outer banks, the formed island and the flow around the island. When this system is constructed by hand this interaction and the resulting system is influenced.

- The self-forming island should be obtained by initially forming a mid-channel bar. Sediment is deposited under water, forming an elevation in the middle of the planform. By decreasing the discharge the self-formed island emerges.

Widened section with fixed banks

The research conducted by Repetto et al. (2002) and Wu and Yeh (2005) was initially used for the formation of a mid-channel bar. These studies focused on the role of width variations in producing channel bifurcations in braided rivers. Both studies used a channel geometry with periodic width variations, see Figure 3.1 on the left. Theoretical models were used to obtain an analytical solution of the bed level deformation and flume experiments were conducted to verify these results. Within the wider section of the planform elevations formed.

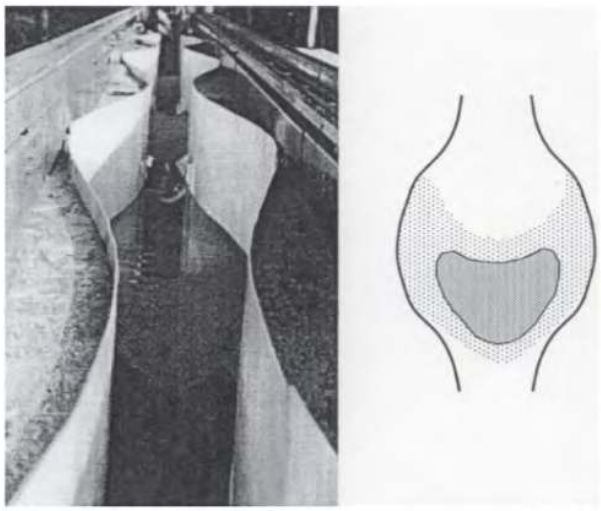

Figure 3.1: Experiments with sinusiodally varying channel width and elevation within the widened section. Flow is from top to bottom, from (Repetto et al., 2002).

The resulting theoretical models of Repetto et al. (2002) and Wu and Yeh (2005) were used to design an experimental setup to form a mid-channel bar. A planform was used with a single width variation, where the outer banks were fixed with stainless steel strips. The theoretical model of Wu and Yeh (2005) distinguishes four types of bars formed by the width variations, namely central, side and two types of transverse bars. These bars are classified according to the locations of peak deformations. It was concluded that the width to depth ratio (β) is the main factor controlling the transition from one type to another. Other important parameters are the dimensionless wave number of width variations (λ_b), dimensionless shear stress (θ_0) and dimensionless sediment diameter (d_s). These last two parameters mainly influence the bar height, not the bar pattern. From the research a specific shape of the widening is proposed in order to form the first bar mode, the central bar. The width to depth ratio was chosen such that ($\beta < \beta_{c1}$) and the shape of the widening was designed such that $\lambda_b = 0.3$. Several preliminary experiments were conducted with the proposed shapes of the widening based on the dimensionless wave number of width variations and the width to depth ratio.

However, during multiple tests with different shapes and sizes of this planform the formation of a central mid-channel bar was not obtained. In the final section of the widening a clear elevation was formed, similar to the results of Repetto et al. (2002), see Figure 3.1 on the right. In Wu and Yeh (2005) the obtained central bars are similar and have peak value bed levels in the region covering a 1/4 wavelength immediately downstream of the widest section (named Region 1 in the study). So the obtained central bar is very similar. However, at the first section of the widening no elevation was formed in the middle. The flow was mainly directed in the middle of the flume, which made it impossible for the

sediment to settle here. During lower flow regimes sediment was deposited at the sides, forming side bars at the first section of the widening. This finally obtained planform was not appropriate for the formation of a self-forming island in the middle of the widening. Wu and Yeh (2005) mention that the development of central bars upstream of the widest section (Region 2) has not been observed in laboratory flumes. Moreover, this type of bar due to width variations was, to their best knowledge, never reported in the literature.

In order to obtain an elevation at the first section of the widening several smaller tests were conducted. A first test was the deposition of some sediment at this location. It was observed that due to the direction of the flow most of the sediment at the front eroded as time proceeded. From this test it was concluded that the flow entering the widening should be diverged in order to form an island in the upper section. The streamlines should be diverged to redirect the main flow towards the sides of the widened section. Several methods were used to diverge the streamlines at this location: small plastic vegetation, toothpicks, clay and a wooden stick. The final method, a wooden stick with a diameter of 6 mm, was suitable for the formation of a mid-channel bar in the first section of the widening. The flow around the wooden stick was characterized by a horseshoe vortex, where the flow diverged. Approximately 10 cm downstream of the measure a stable mid-channel bar was obtained. Island or bars formed by such an obstruction are called lee deposition types. Sediment is deposited behind the obstruction due to a local zone of shallow depth with reduced velocity. Similar experiments with PVC tubes were done by Wyrick (2005) in order to create such an island. However, by using this measure for the simplified planform a different system was obtained. Another method should be used to form an island within the widened section.

Upstream confluence
Finally, the research conducted by Ashworth (1996) was used for the successful development of a mid-channel bar in the widened section. In this study several experiments were conducted in order to improve the model of mid-channel bar growth. The predominantly qualitative description was elaborated with quantitative results and the link with braiding processes was established. The conducted experiment were based on the qualitative description of the model, as can be seen in Figure 3.2. This description of the model comes from observations of laboratory flume work done by Leopold and Wolman (1957), Yalin (1992) and Mosley (1976).

The qualitative model describes the evolution of a mid-channel bar downstream of a symmetrical Y-shaped confluence, a so-called confluence-diffluence unit. Initially two channels join at the confluence, where a central scour hole is formed. The channels are characterized by steep avalanche faces at the scour hole. The beginning of bar growth and modification of the local flow structure is induces by the selective deposition of the coarser fractions. Eventually the bar is large enough to deflect flow towards the adjacent banks. Due to the divergent flow the maximum flow velocity shift from over the bar to the distributaries, causing bank erosion. The cycle repeats downstream with the formation of a scour hole and X shaped interconnected channels.
The experiments of Ashworth (1996) were conducted with an upstream Y-shaped confluence with fixed location and angle (95°). Downstream of the confluence a straight channel was dredged with erodible banks. The two tributaries were designed as half-width equivalents of the post-confluence channel. During the experiments a mid-channel bar developed with the processes described above, see Figure 3.2. The process of bar growth was accompanied with an increase in width and decrease in mean water depth. It was found that

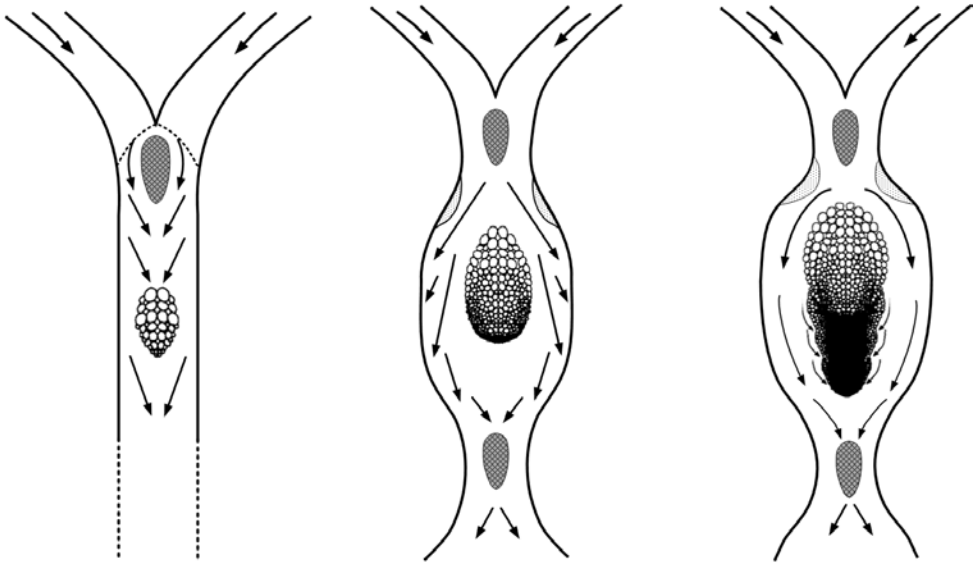

Figure 3.2: The model for the formation of a mid-channel bar, after Ashworth (1996).

the mid-channel bar developed approximately at the same location downstream of the confluence for the different experiments, which was consistent with the findings of Mosley (1976) and Yalin (1992). Both studies concluded that tributary discharge ratio, junction angle and total tributary width are some key factors controlling scour development and the position of downstream bar growth. An increase in discharge ratio caused an decrease in scour depth, while an increase in confluence angle was accompanied with an increase in scour depth. For the design of the experiments a generic modelling approach was followed, so the experimental model was not constricted to a specific field case. For the experiment quite coarse sediment was used with a D_{50} of 2.2 mm. The sediment feed rate was ranging from 60 to 480 g/min. The velocity and water depth were measured at different locations, ranging from 0.30 to 0.65 m/s and 0.0065 to 0.023 m. The resulting Froude and Reynolds number ranged accordingly from 0.64 to 1.89 and 3580 to 145000. The slope was 0.016.

Some preliminary experiments were performed with the experimental setup with upstream Y-shaped confluence and post-confluence straight channel. A small deviation from the setup of Ashworth (1996) was the confluence angle, which was 90°instead of 95°. This deviations was mainly for practical reasons. During these experiments the evolution from the above described model could be observed as a mid-channel bar developed. The shape of the planform obtained from the tests was used to design the shape of the fixed banks. From multiple experiments it was concluded that the combination of the Y-shaped confluence and widening with fixed outer banks provides the right conditions to form a stable mid-channel bar. Different discharge phases, ranging from 2.1 L/s to 0.7 L/s, were used to form and finally emerge a stable island planform. By decreasing the discharge the submerged bar slowly emerged and became larger as additional sediment was deposited at the front. This planform was also reproducible in multiple experiment. In Figure 3.4 a schematic of the development of the mid-channel bar as the discharge decreases is shown. During the preliminary experiments the effects of asymmetrical tributaries was noticeable. The confluencing channels should be constructed with great precision in order to assure a symmetrical development of the bar/island. Minor deviations or imperfections in confluence angle, channel width or discharge ratio resulted in one of the channels becoming dominant and hence the formation of an asymmetrical bar/island. In Figure 3.3

the developed island of one of the failed preliminary experiments is shown.

Figure 3.3: The asymmetrical formation of the bar/island due to the asymmetrical tributaries of the upstream confluence.

During multiple tests with the above setup the planform of Ashworth (1996), with an post-confluence straight channel, was compared with an initial flat bed in the widened section. From these test it was concluded that an initial flat bed has the preference. It was visually determined that the final shape of the bed was very similar. Moreover, with the post-confluence straight channel the floodplains slowly erode till reaching the fixed outer banks. This process took approximately 150 minutes with floodplains 1.5 cm higher than the dredged channel. In Appendix B, section B.1, photo's of this experiment can be seen.

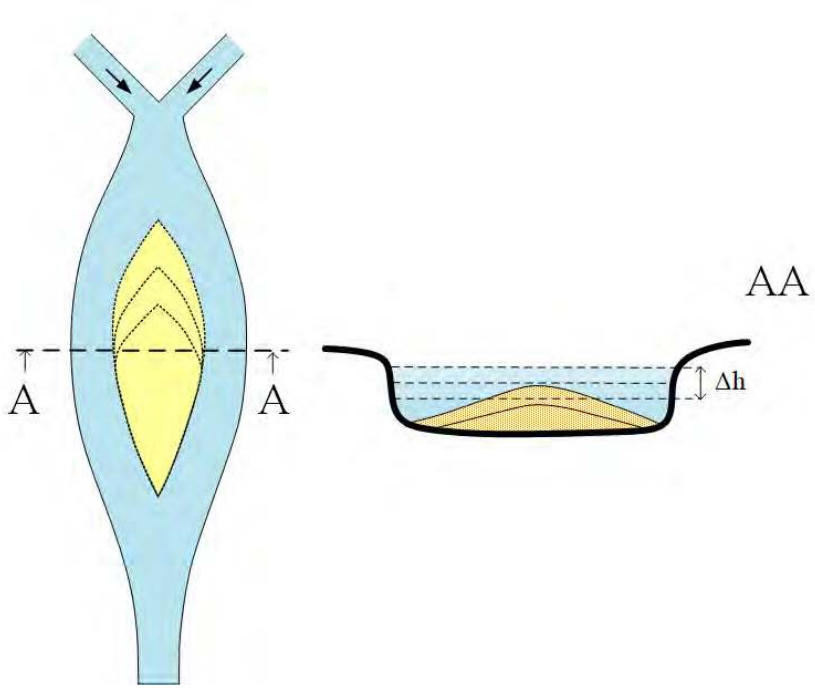

Figure 3.4: Schematization of the development of the mid-channel bar as it emerges with decreasing discharge/water level.

3.1.2 Experimental conditions

For small-scale experiments it is important to reproduce the flow pattern and general processes of the larger scale 'prototype', in this case natural braided rivers. During the experiments certain conditions have to be complied in order to have meaningful results. Dimensionless numbers can be used for proper scaling.
In this section the conditions for the laboratory experiment are discussed. A distinction can be made between the hydraulic flow conditions and the properties of the sediment. In the following section an overview of the final parameters of the experiments are shown.

Subcritical flow
The Froude number is used to determine whether a flow is respectively sub- or supercritical. When this dimensionless number reaches unity the flow is in a critical state, lower values indicate subcritical flow and higher values supercritical flow. The number indicates the ratio between inertial and gravitational forces, see Equation 3.1.

$$Fr = \frac{u_0}{\sqrt{g \cdot h_0}} \tag{3.1}$$

u_0	= characteristic flow velocity	[m/s]
g	= gravitational acceleration	[m/s^2]
h_0	= characteristic water depth	[m]

The flow regime in braided rivers is in general between sub- and supercritical flow, with a Froude number close to unity (Ashmore, 1982).

Turbulent flow
The Reynolds number indicates whether a flow is considered laminar ($Re < 2000$) or turbulent ($Re > 2000$). This dimensionless number is the ratio between inertial and viscous forces of the flow, see Equation 3.2. The flow is considered turbulent when inertial forces dominate, the flow is chaotic and undergoes irregular fluctuations. On the other hand, when viscous forces dominate the flow is considered laminar the flow moves smoothly and in regular paths.

$$Re = \frac{u_0 \cdot h_0}{\nu} \tag{3.2}$$

u_0	= characteristic flow velocity	[m/s]
h_0	= characteristic water depth	[m]
ν	= kinematic viscosity	[m^2/s]

where $\nu = 1 \cdot 10^{-6}$ m^2/s for water at 20°C. The large dimensions of rivers give rise to turbulent phenomena, which should be reproduced in the model. However, due to the reduction in dimension here it is only aimed to have a fully turbulent regime. Hence the model should facilitate a Reynolds number that is greater than 2000.

Sediment mobility
Flowing water begins to transport sediment particles when the shear stresses exceed the critical shear stress for the initiation of motion. The Shields parameter is used to calculate the initiation of motion of sediment in flowing water. Sediment is in motion when the Shields number is larger than the critical Shields number. The dimensionless number is the ratio of bed shear stresses and gravity, see Equation 3.3.

$$\theta = \frac{\tau}{(\rho_s - \rho_f) g D_{50}} \tag{3.3}$$

τ	= shear stress	[N/m^2]
ρ_s	= sediment density	[kg/m^3]
ρ_f	= fluid density	[kg/m^3]
g	= gravitational acceleration	[m/s^2]
D_{50}	= the median sediment diameter	[m]

with $\tau = \rho \cdot g \frac{u^2}{C^2}$, with C the Chézy value. For small-scale experiments downscaling sediment can impose problems, due to the change in cohesion and threshold mobility (Kleinhans et al., 2010). Therefore the sediment cannot be much smaller than in nature. This restriction causes a decrease in sediment mobility, as shear stresses within the model are considerably lower due to a decrease in depth. This decrease in sediment mobility is usually counterbalanced by steepening (increasing the slope) of the model.

Bed load transport
The transport of entrained sediment in a flow is commonly distinguished into two mechanisms: bed load and suspended load transport. Bed load is transported along the bed in the form of sliding, hopping and rolling while suspended load is transported as suspension. Due to the decrease in sediment mobility, the dominant transport mechanism will be bed load transport.

Gravel bed
As mentioned before is the experiment conducted with natural sediment, which decreases the mobility. This experiment is therefore representative for natural gravel-bed rivers.

Hydraulic roughness
When sediment particles are emerged or submerged in the laminar (viscous) sublayer, the flow is considered respectively hydraulic rough or smooth. The particle Reynolds number is used to determine the hydraulic roughness of a flow. This dimensionless number is the ratio between inertial and viscous forces at the bed, see Equation 3.4.

$$Re^* = \frac{u_* \cdot D_{50}}{\nu} \tag{3.4}$$

u_*	= shear velocity	[m/s]
D_{50}	= the median sediment diameter	[m]
ν	= kinematic viscosity	[m^2/s]

with $u_* = \sqrt{\frac{\tau}{\rho}}$. The hydraulic roughness influences the occurrence of certain bedforms. During hydraulic smooth conditions ripples or scour holes form, which provide unrealistic morphology. For hydraulic rough conditions the bed remains planar or dunes form. For the purpose of this experiment hydraulic rough conditions are needed.
The transition from hydraulic smooth to rough flow is gradual, $Re^* = 3.5 - 70$. According to Kleinhans et al. (2010) the particle Reynolds number should be larger than 11.63 to reproduce hydraulic rough conditions.

3.1.3 Parameters

The parameters used for the different stages of the experiments were designed based on the range of experimental conditions discussed in the previous section. In Table 3.1 an overview is shown of the parameters. It can be seen that three different flow stages are distinguished. These coincide with different stages of the experiments: (1) formation of island (2) low discharge and (3) high discharge. These experimental stages are further discussed in subsection 3.3.2 and subsection 4.1.2.

Parameter	**Flow stage**			**Unit**
	1	*2*	*3*	
Discharge (Q)	0.7-2.1	0.7	1.0-1.4	m^3/s
Sediment input rate (S)	180-450	140	200-280	g/min
Water depth (h)	0.013-0.027	0.013	0.015-0.019	m
Velocity (u)	0.27-0.39	0.27	0.30-0.37	m/s
Channel Slope (i_b)	0.008	0.008	0.007	m/m
Chézy value (C)	26-27	26	29-32	$m^{1/2}/s$
Froude number (Fr)	0.75-0.79	0.75	0.78-0.85	-
Reynolds number (Re)	3500-10500	3500	4500-7000	-
Particle Reynolds number (Re^*)	33-47	33	32-36	-
Shields number (θ)	0.07-0.14	0.07	0.06-0.08	-

Table 3.1: The parameters for the different flow stages of the experiments.

The parameters shown in Table 3.1 are based on measurements and calculations upstream and downstream of the widened section. In the upstream confluence and downstream straight channel the cross-section is constant and approximately rectangular. In the widened section the cross-section constantly changes due the emerging bar. The measurements and calculations of the water depth and velocity are therefore representative for these locations. The average water velocity can be calculated with Q/bh. During the first flow stage plastic floaters and a timer were used to approximate the velocity (further explained in subsection 3.2.2). This was done during this stage as no bed elevation would stop or decelerate the floater. An average velocity of 0.41 m/s was estimated. Using the 8/10 rule from Whipple (2004) results in $0.40 \cdot 8/10 = 0.33$ m/s. This estimated value is close to the value 0.39 m/s in Table 3.1. The roughness is indicated with the Chézy value, which was calculated with, $C = v/\sqrt{hi_b}$. The slope is, similar to the width of the planform, not constant in longitudinal direction. The slope in Table 3.1 is an average

slope which was determined based on the upstream and downstream boundary conditions. For stage three the downstream boundary condition is raised, which results in a less steep slope.
The sediment used during the experiment has a has D_{50} of 1 mm and D_{90} of 1.55 mm. The grain size distribution can be seen in Appendix E. As mentioned will this sediment result in a gravel-bed similarity. This representation has to be taken into account with the comparison with numerical models, which mostly simulate large sand-bed braided rivers. The formula of sediment transport rate of Meyer-Peter and Muller (1948), Equation 3.5, can be used for estimating the bed load transport.

$$S = 8 \cdot D_{50}^{3/2} \sqrt{g\Delta} (\mu\theta - 0.047)^{3/2} \tag{3.5}$$

Δ = relative submerged mass density [-]
μ = ripple factor [-]

with $\mu = (C/C_{90})^{3/2}$ (where C_{90}=grain roughness=$18 \cdot log(12h/D_{90})$) and $\Delta = \frac{\rho_s - \rho_f}{\rho_f}$. The formula is valid for $w_s/u_* > 1$, $D_{50} > 0.4$ mm and $\mu\theta < 0.2$, with w_s the fall velocity. The theoretical bed load transport capacity calculated with this formula gives 0.06 g/min and underestimates the transport capacity in the experiment.

3.2 Overview of setup

3.2.1 Flume characteristics

The laboratory experiments were conducted in a flume in the Fluid Mechanics Laboratory of Delft University of Technology. The flume was made of wood and had a length of 7.0 m, width of 1.2 m and height of 0.25 m, see Figure 3.5. The water was circulated from the downstream basin to the upstream stilling basin and back to the basin again. A submersible pump was used which was controlled with a frequency controller. A constant water level in the downstream water basin assured a constant discharge output from the pump. This was done by using a combination of a constant external water supply and an overflow pipe. An upstream and downstream weir were used as boundary conditions, with heights of respectively 13 and 8 cm. Additional weirs were installed at the distribution point of the tributaries for the confluence, with heights of 12.5 cm. These were installed in order assure and even distribution of discharge at this location. The downstream installed weir imposes critical flow at this boundary condition. At the final section therefore a $M2$ backwater curve forms. The backwater curve effects only a limited reach at the downstream section, and does not influence the widened section. The upstream confluence had an angle of 90°. The two channels witch join at the confluence had a width of 0.10 m and a length of 0.70 m. The confluence was followed by the widened section, which was 0.95 m at its widest and has a length of 3.30 m. The final straight section has a width of 0.20 m, double the width of the upstream channels, and had a length of 1.30 m. More details of the experimental setup, including photo's and the exact shape of the widened section, can be found in Appendix A.

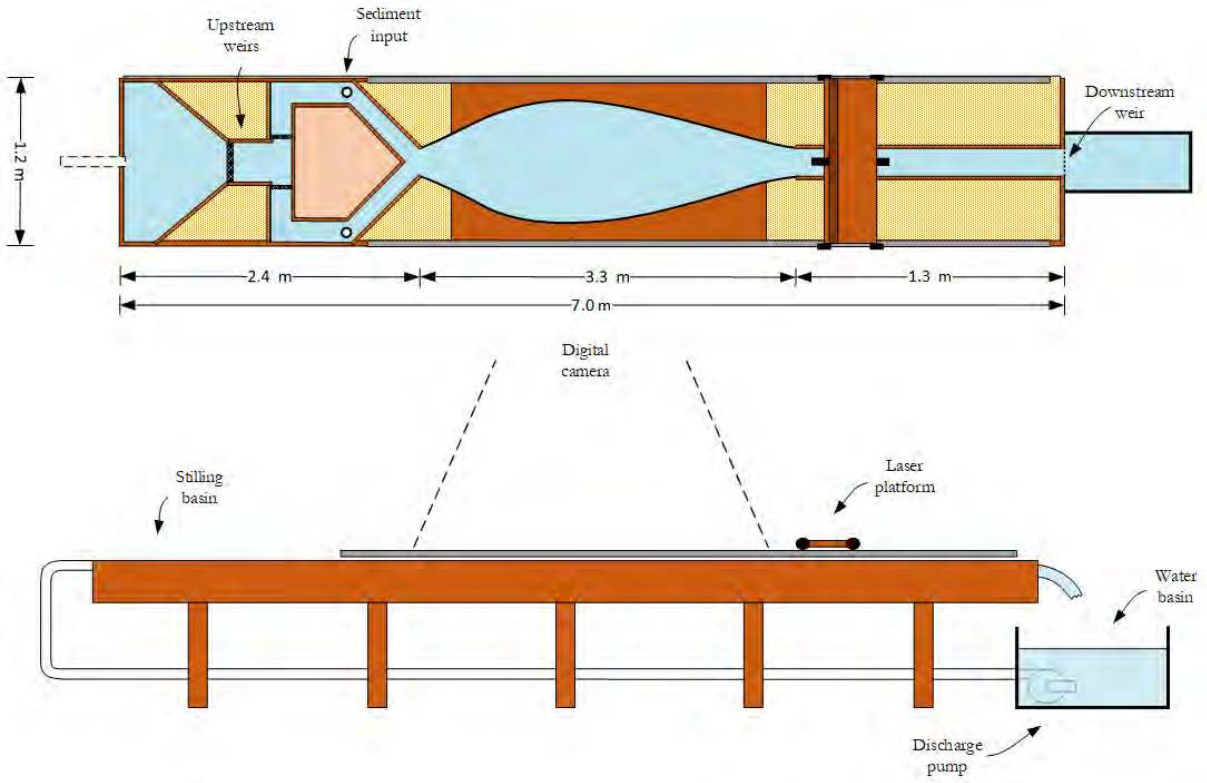

Figure 3.5: Top and side view of the laboratory flume used during the experiment. Flow is from left to right (figure not to scale).

The experiments were conducted with a movable sediment bed and dry sediment was deposited into the water by hand. The sediment has a D_{50} of 1 mm and a D_{90} of 1.55 mm, the GSD can be seen in Appendix E. The bed of the flume consisted out of a layer of sediment approximately 20 cm thick. Within this layer the channel geometry as described previously was constructed. The sediment was deposited approximately 70 cm upstream of the confluence, see Figure 3.5. Initially some tests were conducted with a sediment feeder, which divided its output over the two different locations. However, after these tests it was concluded that over time the sediment output was not divided equally over the two channels. Moreover, the sediment taps used occasionally clogged and were difficult to adjust. The use of a vibrating device to prevent clogging was discouraged, as this might influence the experiment to much. Further it was tested whether it was possible to deposit the sediment directly at the confluence, so at one location. This also did not result in the wanted sediment deposition in the system. Therefore it was decided to deposit the sediment manually. This was done in batches within a time interval, depending on the discharge stage.

3.2.2 Measurement techniques

In this section the different measurement techniques conducted before, during and after the experiment are discussed. In order to measure specific characteristics of the laboratory experiment, several measurement techniques and devices were used. It should be taken into account that systematic and stochastic errors are made with experimental research. These can be minimized by respectively carefull calibration of the instruments

and repeating measurements and calculating the average values.

Grain size distribution [mm]
The grain size distribution of the sediment was determined with a sieving analysis. For this analysis a scale and sieves were used. From this analysis the characteristic parameters D_{50}=1 mm and D_{90}=1.55 mm were determined. The grain size distribution is shown in Appendix E.

Sediment feeding rate [g/min]
The sediment was deposited manually in batches within a certain time interval. The sediment input differed per stage of the experiments.

Discharge [dm^3/s]
The discharge was measured with a ultrasonic flow meter from Prosonic. The measuring system consists of one transmitter and two sensors. The two sensors are clamped outside the pipe between the pump and the upstream basin. In this measurement method, acoustic (ultrasonic) signals are transmitted between two sensors. In Appendix A more information and photo's can be found.

Water level [mm]
The water level was measured with measuring tape installed at multiple locations along the flume. As mentioned before were these locations upstream and downstream of the widened section. From these measurements the average water depth at these locations was determined. Together with the measurements of the discharge and average flow velocity could be calculated.

Flow velocity [m/s]
The flow velocity was approximated using plastic floaters and a timer. Over a certain distance these floaters were timed in order to estimate the surface velocity. This was repeated three times and an average velocity was calculated. The rule of thumb of Whipple (2004) was used to convert the surface velocity to a dept averaged velocity, with $u_{avg} = 8/10 \cdot u_{surf}$. For the experiments with closure measures pink dye was used in order to observe the difference in flow velocity between the channels. This was done as plastic floaters stranded around the closure measure. This difference in velocity was only used for qualitative analysis.

Bed profile [mm]
The bed profile was measured with the use of two lasers, one for the longitudinal direction and one in the lateral direction.

- The bed profile in the longitudinal direction was measured with a laser which was installed in the middle of the moveable laser platform. The laser could be moved in the streamwise direction over a distance of 4 m. The location of the laser was measured with a rotating wheel. One rotation of the wheel was accompanied with 5000 measurements of the bed laser.
- The bed profile in the lateral direction was measured with a laser which could be moved in the lateral direction on the movable laser platform. Therefore this laser could be moved in the streamwise direction and perpendicular to that. Here another rotating wheel was installed to measure the location in the 1.0 m lateral direction. These cross-section were measured over a longitudinal distance of 3.2 m every 0.05 m, resulting in 65 cross-sections. The full 3.3 m

of the widening was not possible to measure due to the constraints of the laser platform.

The flume should be drained for a correct measurement of the bed level. With flowing water in the flume the bed laser alternated between the water and bed level, giving distorted data. The output of the bed lasers was in Volt. By calibrating the device this data was converted into millimeters. The setup, see Figure 3.6a, was used to measure the bed profile multiple times during the experiments: (1) after the formation of the bar/island, (2) after the low-discharge stage and (3) after the high-discharge stage. The first measurement is used to verify the similar starting conditions of the experiments. The second and third measurement are used to analyze the morphodynamic effects of a closure measure.

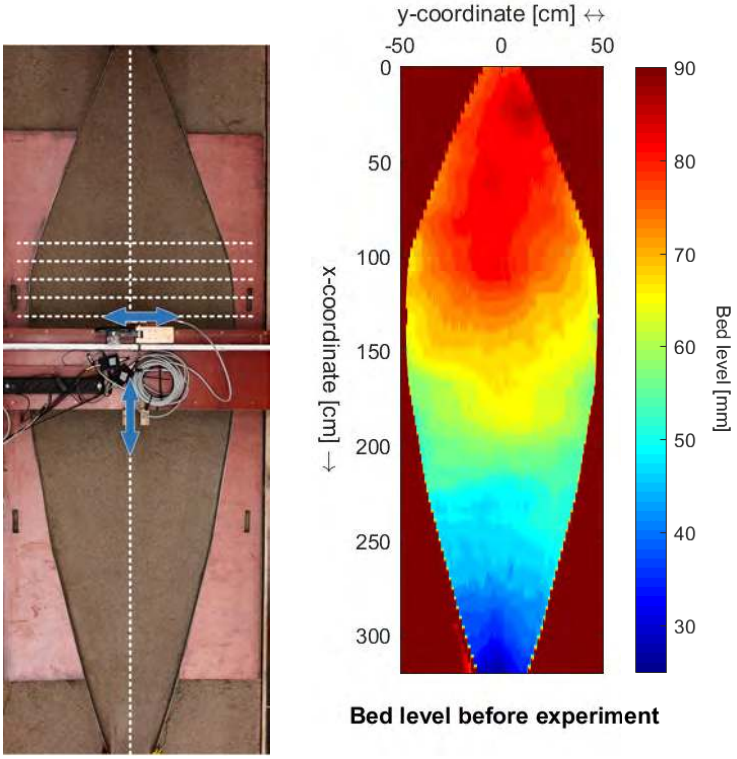

(a) (b)

Figure 3.6: Setup to measure the bed level in the longitudinal and lateral direction (a) and the obtained results of the bed level profile (b).

The data from the lasers was retrieved by using the data acquisition software of DASYlab®. This data was used in MATLAB® R2016a to create graphs for analyzing the data of the bed profile. For the two-dimensional plots a script was used which interpolated the bed level between the 65 cross-sections, see Figure 3.6b. In Appendix A more information and photo's can be found.

Observations [pixels]

The developments of the experiments were observed both optical and digital. A digital camera was installed approximately 6 m above the flume, on a movable crane. The morphological evolution during the experiment was captured with images and videos. During the experiments the camera took an image every 30 seconds.

3.2.3 Simplified conditions

With the design of this small-scale experiment it was attempted to replicate the flow conditions of the real-life prototype. However, some simplifications were necessary, which are shortly discussed here and more elaborated in the Discussion in chapter 5.

- **Wall roughness**
  At the first section of the flume the banks were made of wood and along the remainder banks stainless steel strips were installed. The roughness of the wood and steel is considerably less than in natural rivers. However, because of the limited depth of the experiment the influence on the experiment and hydraulic conditions is thought to be limited. Further it should be noted that the connections between the different sections were not perfect, see Figure 3.7. Because of this some local effects influenced the processes.

- **Non-erodible banks**
  Along the channels the outer banks were fixed with wood and stainless steel sides. This was done in order to prevent the bank erosion, island aggradation and possible downstream migration of the island/bar. However, the fixed outer banks prevent the branches from re-aligning, rotating and migrating, which are processes representative in natural braided rivers. By fixing the outer banks the system was influenced. However, it is thought that the general processes of channel opening and closure were mostly unaffected.

- **Steady flow conditions**
  For this experiment the flow stages used after the island formation, Q_{low} and Q_{high}, were designed as steady flow conditions. In natural rivers the discharge shows much variation over the year, which is not taken into account here.

- **Simplified planform**
  The planform of the setup, with straight sections upstream and downstream of the widened section, is a simplification of natural rivers. Natural rivers are usually not straight, and if this is the case not longer than ten times the width (Leopold and Wolman, 1957). In addition, the system with two similar sized channels surrounding an island is also a simplification. As mentioned in chapter 2 is one of the channels often dominant due to the asymmetrical distribution at the bifurcation.

Figure 3.7: The overlap and connection between the different sections causes some local perturbations.

3.3 Description of experiments

3.3.1 Configurations

In the process of finding a suitable experimental setup, see subsection 3.1.1, it was found that the planform upstream of the widening was important for the development of a mid-channel bar. By using an upstream Y-shaped confluence a mid-channel bar developed in the middle of the widening, while with a straight channel a bar developed at the final section of the widening. As the discharge decreased the former resulted in a planform which was appropriate for the experiments on channel closure, while the latter was not. The outcome of these preliminary experiments was analyzed in more detail in two experiments.
In order to compare the influence of the upstream forcing on the morphological development within the widened section the rest of the setup remained identical. The only changing variable was the upstream planform, which was a straight channel in the first experiment and a Y-shaped confluence in the second experiment, see Figure 3.8. Both planforms had the same initial widths, $B = 20$ cm in total. For the confluence planform the tributaries were half-width equivalents of the single straight channel. The location of the sediment input was also identical, 70 cm upstream of the start of the widening section. For both experiments the first flow stage, as described in subsection 3.3.2, was used. The abbreviations *Str* and *Con*, are used for respectively the straight upstream channel and the upstream confluence.

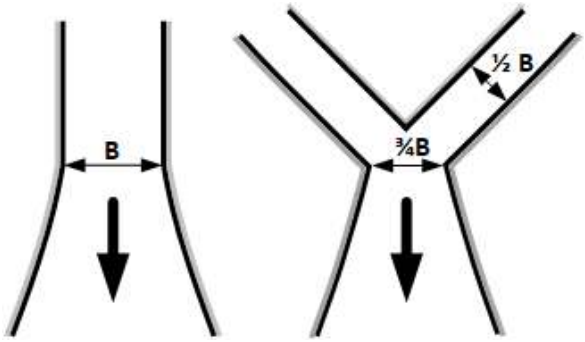

Figure 3.8: The configuration upstream of the widening for the experiments conducted for the selection of the experimental setup.

3.3.2 Flow stage

As mentioned in subsection 3.1.1 develops a self-forming island by using a falling discharge stage in combination with the discussed planform. On the basis of various preliminary experiments it was determined to use four different phases for the formation of the island. Figure 3.2 shows the discharge, which ranges from 2.1 to 0.7 L/s, and the sediment input, which ranges from 140 to 450 g/min, for the four phases. Figure 3.9 shows a graphical representation of the decrease in discharge over time. In the remainder of this report these four phases are referred to as the first flow stage: the island formation. The following paragraph describes the different steps of the flow stage in more detail.

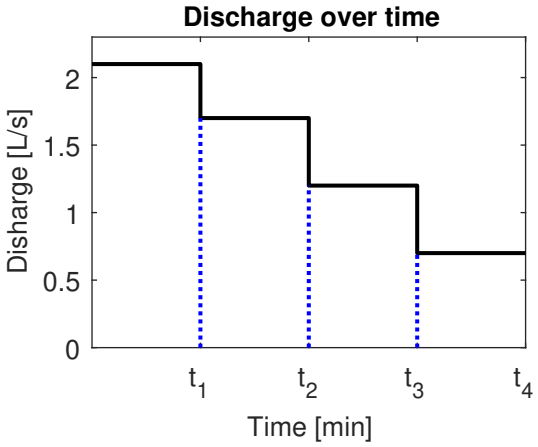

Figure 3.9: Discharge over time of the first flow stage, the island formation.

Phase	Discharge [L/s]	Sediment input [g/min]	Time [min]
1	2.1	180	0 - t_1
2	1.7	450	t_1 - t_2
3	1.2	370	t_2 - t_3
4	0.7	140	t_3 - t_4

Table 3.2: The four phases of the first flow stage, the island formation.

1. Island formation

At first the bed in the flume was smoothed by hand with the use of a trowel. In the lateral direction the bed profile was made flat, while in the longitudinal direction a slope was made. The first phase, 2.1 L/s, was mainly used to remove any perturbations within the flume after it was flattened by hand. During this phase the sediment within the flume rearranged due to the forcing of the planform and the water forcing. The following two phases, of 1.7 L/s and 1.2 L/s, had a relatively high sediment input of respectively 450 and 370 g/min. During these two phases the mid-channel bar became larger as sediment was deposited at the upstream side. The final phase had a discharge of 0.7 L/s and a sediment input of 140 g/min. During this phase the water level dropped to a minimum and the bar emerges further.

It can be seen that no time constrain was used for the phases. This is because the development of the mid-channel bar was different for each experiment. Sediment was deposited and eroded at different locations during the same phase for different experiments. Therefore the transition to the next phase was determined on the basis of some indicators. From various preliminary experiments some experience had been gained on the time scale, development and emerged area of the bar of each phase. This experience was used to determine the qualitatively indicators for the transition to the next phase. The first and most important indicator was the shape and location of the front and back of the bar/island. During a phase sediment was deposited at the upstream side of the bar, which over time formed a clear front. For the transition to the next phase it was important that the front and back of the island are approximately in the middle of the flume and that the overall shape was symmetrical. During the preliminary experiments it was observed that the island shapes asymmetrical when this indicator is neglected. In addition, the location of the front was in a similar range after each phase, as can be seen in Appendix C in Table C.1. The development of the front in the middle and within this range was an indicator for the transition to the next phase. A second indicator was the morphological activity. For the transition to the next phase it was important that for a longer period no large-scale erosion or depositions was observed. The transition to the next phase was thus based on qualitatively indicators, and is not determined quantitatively.

3.4 Results

3.4.1 General

The time of the different phases for the two conducted experiments are shown in Table 3.3. It can be seen that the total time needed for the experiments is in the same order of magnitude. This total time needed for the first flow stage increases significantly when the bed level is drained after each phase. This was done in order to measure the bed level after each phase. The transition to the next phase for experiment *Str* was mainly determined on the basis of the morphological activity, as no front developed. The results and overall observations of the two experiments are discussed separately in the remainder of this section.

Experiment	**Time per phase [min]**				
	1	*2*	*3*	*4*	*total*
Str	38	68	64	53	223
Con	24	85	58	41	208

Table 3.3: The time per phase for the experiments on selecting the setup.

3.4.2 Straight channel

In Figure 3.10 the bed level in longitudinal direction for the four different phases is shown, including the bed level before the water. This longitudinal bed level was measured in the middle of the flume, where $y = 0$. The figure shows the evolution of the bed level as the discharge decreases (Phase 1 to 4). It can be seen that the bed level increases at the upstream side with decreasing discharge. Further the effect of the width variations can be seen in the variations in gradient of the longitudinal slope. The widened section is at its widest around $x = 140$ cm and stops around x=320. A drop in bed level can be seen at the end of the widening, which develops further downstream with decreasing discharge.
In order to analyze the development of the bed level and the planform, the results obtained from each phase will be discussed separately. In Figure 3.12 the bed level of the widened section per phase is shown. More photo's of the experiment can be found in Appendix B section B.2.

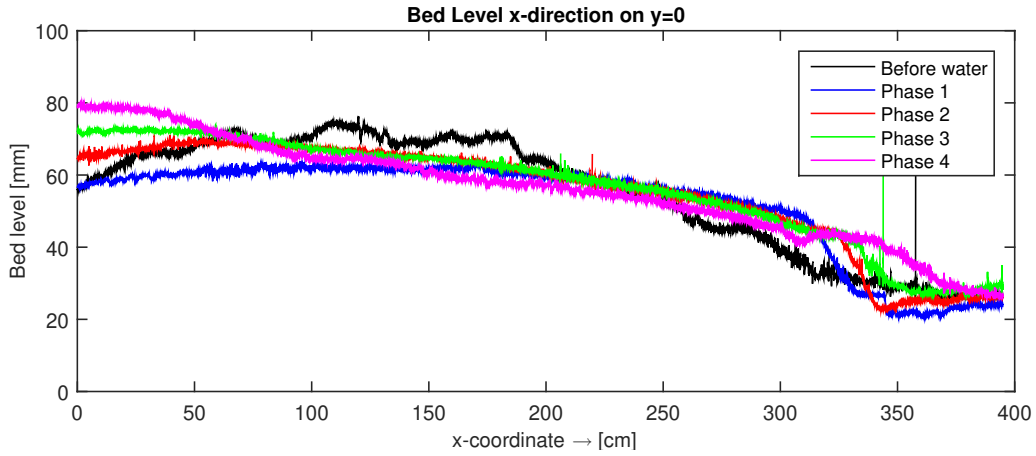

Figure 3.10: The bed level in the longitudinal direction for the four different phases of experiment *Str*.

Phase 1
At the beginning of the experiment the bed was made flat, with a longitudinal slope. By introducing the water into the flume perturbations were removed and the bed level smoothened. The final bed level obtained from this phase, see Figure 3.12a, shows that the upper and lower half of the widened section develop different. In the cross-sections in Figure 3.12e this difference is even more evident. In the upper half of the widened section side bars developed. During the phase it was observed that the main flow was in the middle, while sediment was deposited at the sides. In the lower half of the widening an elevation formed in the middle, with lower bed level on the sides. Here the flow was more divided over the width of the widened section. The elevation formed in the shape of the widening and moved downstream. The elevation formed approximately 5 cm from the edges of the setup. The elevation formed until the end of the widened section, which is visible in the drop in bed level in Figure 3.10. The elevation developed as sediment from upstream settles. During the phase the planform remained submerged.

Phase 2
During the second phase no significant changes took place and the overall shape of the bed level remained the same. From Figure 3.12b and Figure 3.12e it can be seen that some sedimentation took place. The deposition of sediment was mainly in the upper half of the widening, where it can be seen that the side bars are elevated compared to the previous phase. In combination with a lower water level this caused the main flow to be in the middle. During the phase the planform remained submerged.

Phase 3
During the third phase the overall shape of the bed level remained very similar. From Figure 3.12c and Figure 3.12e it can be seen that sedimentation was again mainly in the upper half of the widening. Here the increase in the bed level of the side bars caused the flow at the sides almost to stagnate. The planform remained submerged, although the water level at the side bars was very shallow, see Figure 3.11a.

Phase 4
From Figure 3.12d and Figure 3.12e it can be seen that the bed level increased again. The deposition of sediment was mainly at the sides, as the main flow was concentrated in the middle. This resulted in an increase in the bed level of the sides bars and evened out

the elevation in the lower half of the widened section. In the lower half there was some erosion in the middle, as here the main flow is concentrated.
During the final stage the side bars emerged, as can be seen in Figure 3.11b. The bars had a similar length of approximately 135 and 140 cm. It can be seen that the main flow was in the middle.

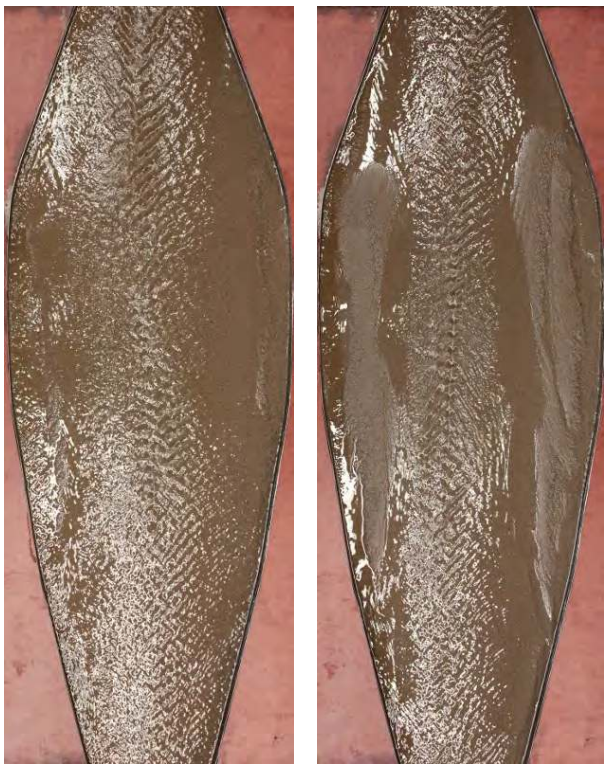

(a) (b)

Figure 3.11: The development of the elevation widened section for Phase 3 (a) and Phase 4 (b) of experiment *Str*.

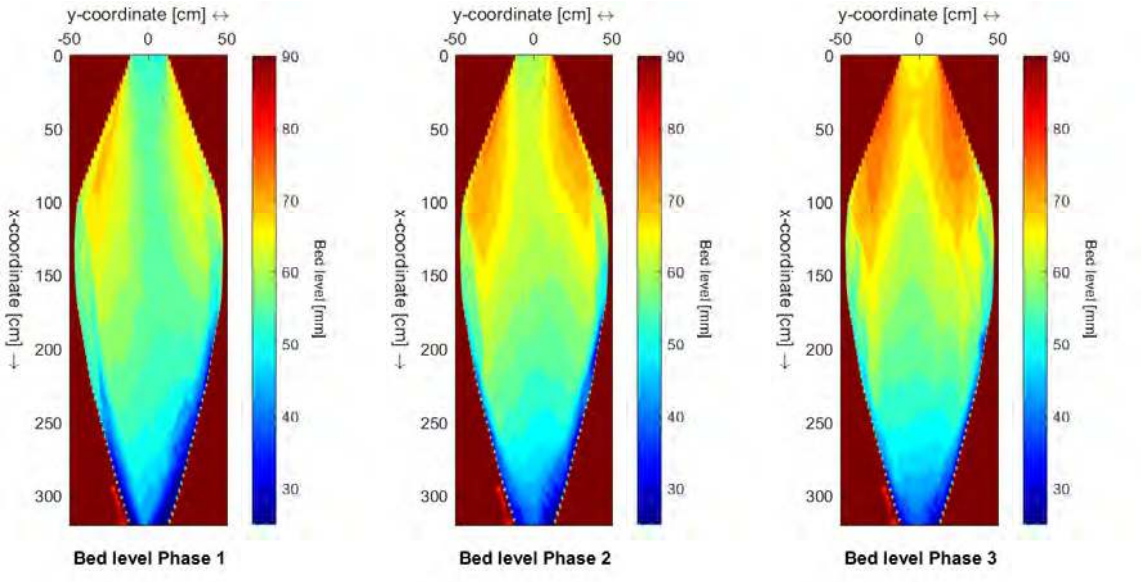

(a)

(b)

(c)

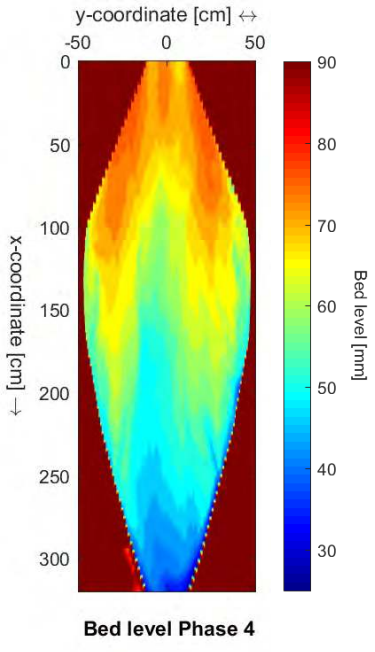

(d)

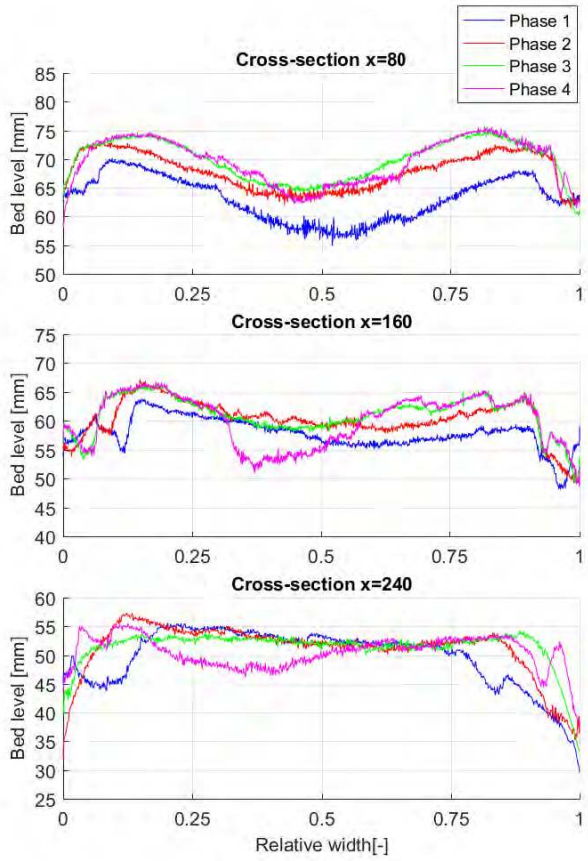

(e)

Figure 3.12: The overview of the bed levels after Phase 1 (a), Phase 2 (b), Phase 3 (c), and Phase 4 (d) of experiment *Str*. Cross-sections at $x = 80$, $x = 160$ and $x = 240$ cm show the evolution of the bed level per phase.

3.4.3 Y-shaped confluence

In Figure 3.13 the bed level in longitudinal direction for the four different phases is shown, including the bed level before the water. This longitudinal bed level was measured in the middle of the flume, where $y = 0$. The figure shows the evolution of the bed level as the discharge decreases (Phase 1 to 4). It can be seen that the bed level increased at the upstream side with decreasing discharge. The effect of the upstream confluence can be seen in the form of the scour hole at the upstream section. This scour hole decreased in depth with decreases discharge. Further the effect of the width variations can be seen in the variations in gradient of the longitudinal slope. The final section of the widening, at x=320, is characterized by a drop in bed level. It can be seen that this drop remains at this location for the different phases.
In order to analyze the development of the bed level and the obtained planform, the results obtained from each phase will be discussed separately. In Figure 3.16 the bed level of the widened section per phase is shown. More photo's of the experiment can be found in Appendix B section B.3.

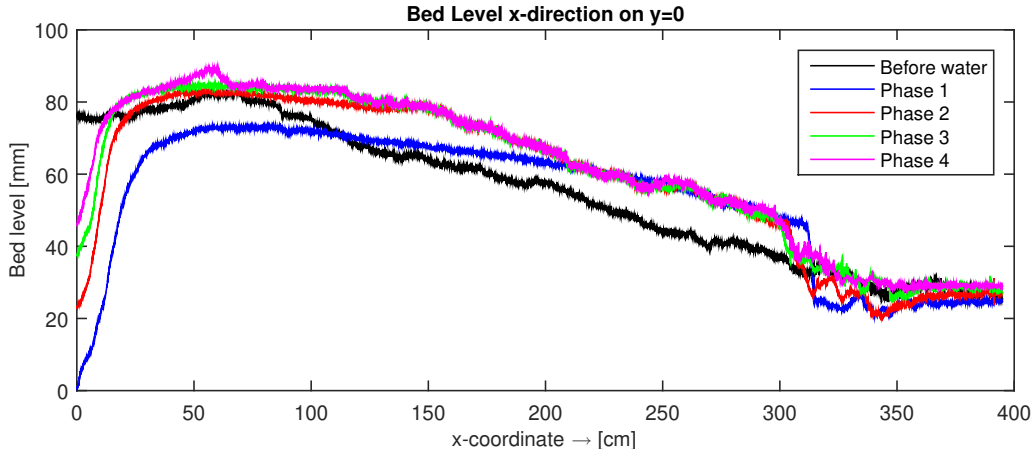

Figure 3.13: The bed level in the longitudinal direction for the four different phases of experiment *Con*.

Phase 1
At the beginning of the experiment the bed was made flat, with a longitudinal slope. By introducing water into the flume perturbations were removed and the bed level smoothened. In accordance with the analyses of experiment *Str*, see subsection 3.4.2, difference is made between the upper and lower half of the widened section. The upper half of the widening was characterized by the formation of the confluence scour hole, see Figure 3.16a. The flow downstream of the scour hole diverged when it entered the widened section, dividing the flow over the cross-section. From Figure 3.16e it can be seen that the main flow was concentrated in the middle. However, the difference in elevation between the middle and sides is considerably less than for experiment *Str*. At the lower half of the widening an elevation formed with deeper parts at the sides. This elevation developed as it moved downstream in the shape of the widening. The elevation formed until the end of the widened section, which is visible in the drop in bed level in Figure 3.13. The build-up of the elevation was from sediment at the sides and from upstream. During the experiment is was observed that a large portion of the flow was concentrated at the fixed banks. At

these outer banks the development of bedforms in the form of ripples was observed, see Figure 3.14a. The planform remained submerged during this phase.

(a) (b)

Figure 3.14: The development of bed forms at the sides during Phase 1 (a), image taken from upstream. The front of the elevation after Phase 2 and 3 (b).

Phase 2
During the second phase the elevation in the final section of the widening emerged and became larger in upstream direction. During this phase sediment was deposited mainly in the upper half of the widened section, see Figure 3.13. Sediment was deposited arbitrarily in the middle, forming an elevation. At one point during this process multiple nucleus merged and a clear front developed at the final section of the widening. This front became larger in upstream direction and developed until approximately x= 155 cm, see Figure 3.16b. The elevation in the final section of the widening had a length of approximately 150 cm and a width of 40 cm. However, only the front part of the island emerged, while the last 40 cm was submerged by shallow water, see Figure 3.15a. The channels surrounding the elevation became deeper as the water was forced towards the sides.

Phase 3
During this third stage the elevation in the middle became longer and wider, see Figure 3.16c and Figure 3.16e. This increase was caused by the drop in water level and deposition of sediment. The front of the elevation formed further upstream as sediment settled in the middle. More sediment was deposited as time proceeded and eventually a triangular shaped front formed, see Figure 3.14b. From the figure it can be seen that the fronts mainly developed from the large sediment particles.
The final development of the elevation formed approximately at $x = 105$ cm till x=290, resulting in a total length of 185 cm. From Figure 3.15b it can be seen that a part of the front of the island was submerged, approximately 30 cm of the front. The flow was concentrated at the sides while the flow over the front was almost stagnant. Two channels surrounded the elevation in the middle, these channels had a width of approximately 15 cm.

Phase 4

During the final stage the emerged area in the middle became longer and wider again, see Figure 3.16d and Figure 3.16e. During the experiment the elevation became larger due to a drop in water level and the deposition of some sediment at the front. Further it can be observed that some sediment was eroded at the sides of the upper edges. During the experiment a clear elevation in the middle was observed with surrounding channels.
The final development of the elevation emerged at approximately $x = 65$ cm until $x = 285$, resulting in a total length of 220 cm. The elevation was at its widest 65 cm (1/3 length island from front). It can be seen that the channels surrounding the island did not have a consistent width, see Figure 3.15c. At the front of the island the channel had a width of 27 cm, where the island was its widest 12 cm, and at the end 20 cm. Further it can be seen that the elevation was not homogeneous, as it was self-forming. Some parts were a bit more elevated while other were a bit lower.

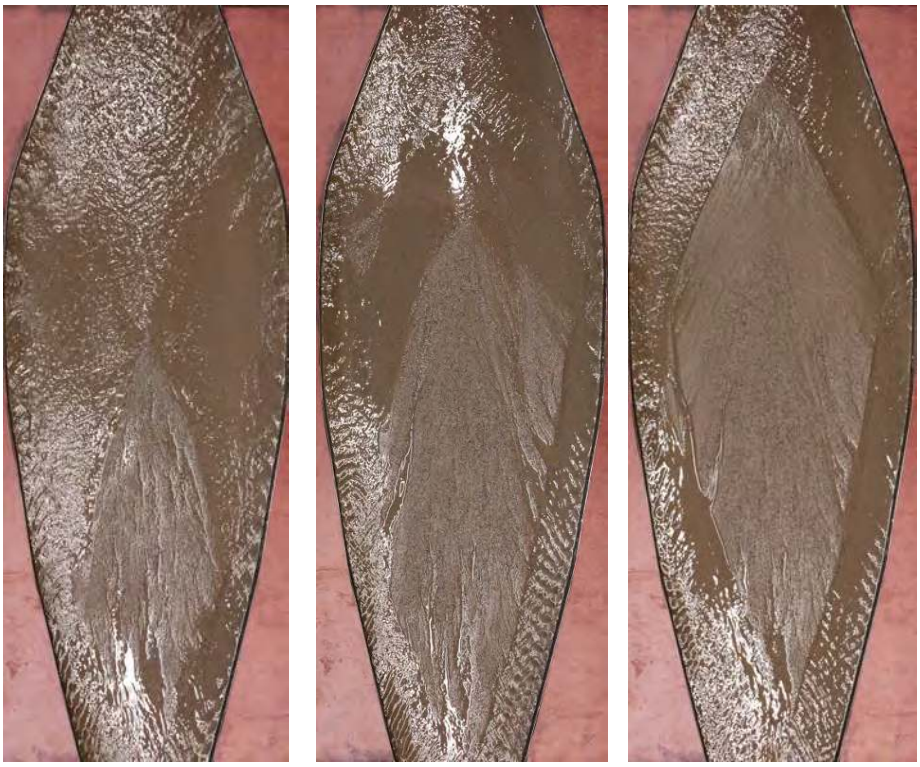

(a) (b) (c)

Figure 3.15: The development of the elevation in the middle of the widened section for Phase 2 (a), Phase 3 (b) and Phase 4 (c) of experiment *Con*.

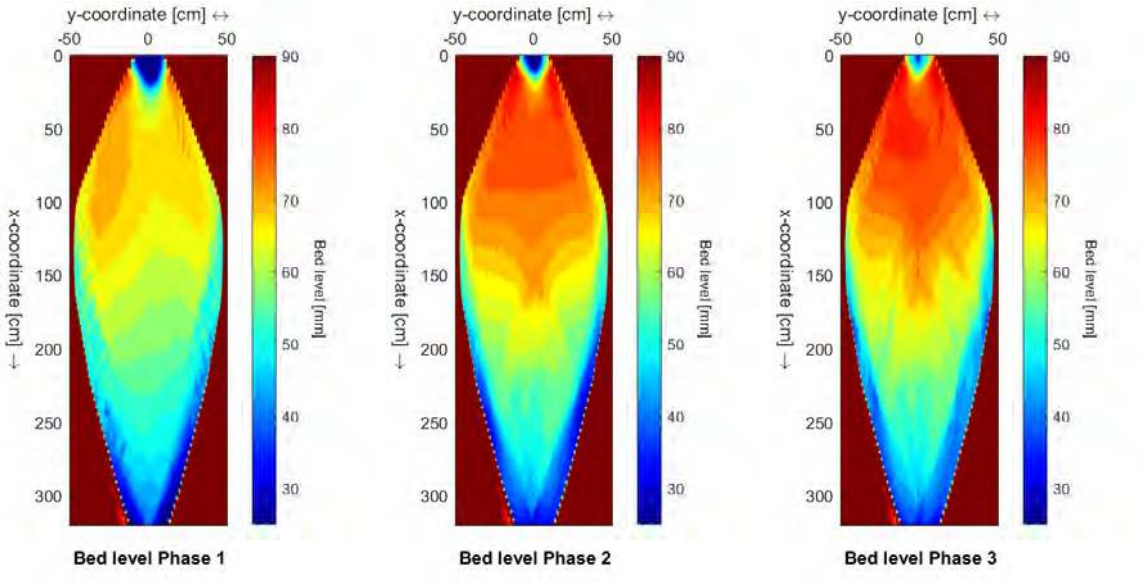

(a) (b) (c)

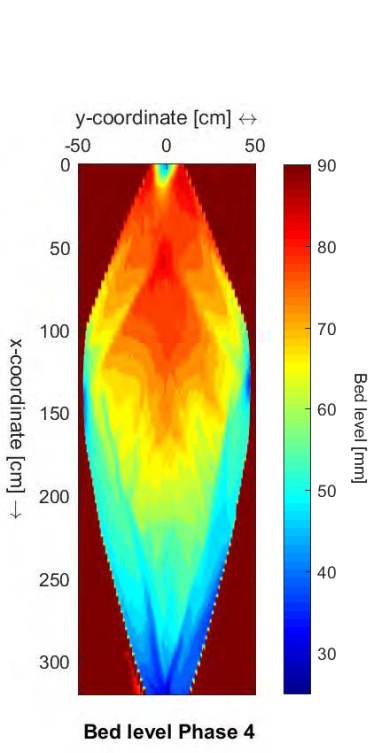

(d)

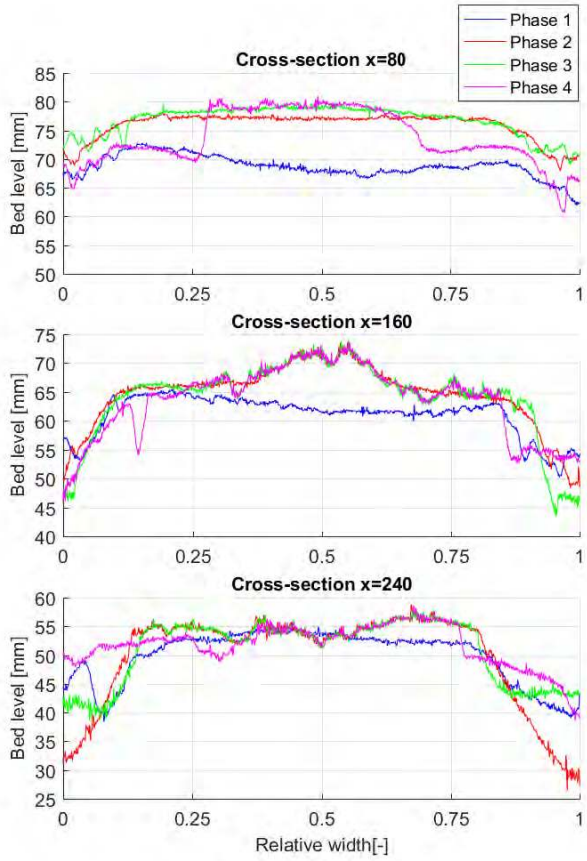

(e)

Figure 3.16: The overview of the bed levels after Phase 1 (a), Phase 2 (b), Phase 3 (c), and Phase 4 (d) of experiment *Con*. Cross-sections at $x = 80$, $x = 160$ and $x = 240$ cm show the evolution of the bed level per phase.

4 Experiments on channel closure

4.1 Method

In order to analyze the morphodynmic effects of channel closure, both on island scale as for the successive island, several experiments were conducted. These experiments were done with the same experimental setup as described in chapter 3. The starting point of these experiments was the formation of an island with the flow stage previously described in subsection 3.3.2. The different configurations and flow stages for these experiments are described below.

4.1.1 Configurations

The different experiments conducted on channel closure, with the location and type of closure, are shown in Table 4.1. Figure 4.1 gives an overview of the different experiments within the experimental setup. It can be seen that all the experiments on channel closure had the same starting point, with an island in the middle of the widened section.

Experiment	**Closure measure**		
	Location		*Type*
Reference			
W1	Along island	Begin	Weir
W2		Middle	
W3		End	
I20	Confluence	Inner bend	20% width reduction
I40			40% width reduction
O20		Outer bend	20% width reduction
O40			40% width reduction

Table 4.1: The location and type of closure for the experiments on channel closure.

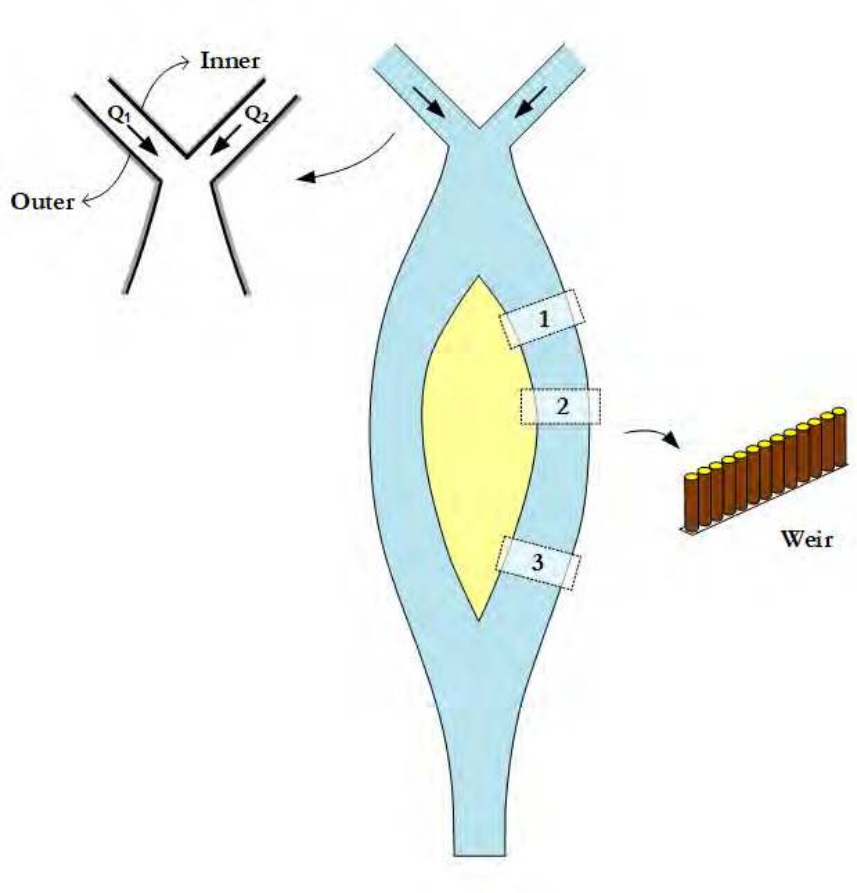

Figure 4.1: Overview of the locations of the different closure measures within the experimental setup.

With the reference experiment no closure measures were installed. This experiment therefore shows the evolution of the island without measures. For this experiment all the flow stages were used, as can be seen in Table 4.3. The remainder of the experiments can be subdivided into two categories; closure measures along the island and at the upstream confluence.

The experiments with measures along the island are used to get a better insight in the local morphodynamic effects of channel closure on island scale. In total three experiment were conducted. For these experiments a weir was installed at three location along the island: (1) the begin, (2) middle and (3) end of the right channel, see Figure 4.1. Determining the exact location of the measures was not so straight forward, as the island was not symmetrical. Installing the measures on the limits of the island, i.e. the bifurcation or confluence, is not practical. With little erosion the measure is easily bypassed and becomes useless. The closure measures at the begin, middle and end were installed at approximately $\frac{1}{8}$,$\frac{3}{8}$ and $\frac{6}{8}$ on the island from the front.
There are several structures to close off a channel which often have similar working principles. For this experiment the simple weir construction was used as measure. The weir was constructed out of small wooden sticks with a diameter of 2 mm, and height of 8 cm. This type of construction was chosen because the closure measure should be constructed in phases. When a obstruction is installed within a short period local scour causes the experiment to fail as the flow directly bypasses the measure. The length of the closure

measure was extended for 33% on the island, similar to the rule of thumb for porcupines and jack jetties from Flood Management Organisation (2012). The weir was installed at approximately the water level of the low flow discharge stage (further explained in subsection 4.1.2). When the wooden sticks were installed water flowed over the weir due to backwater effects.
Because the island formed itself, it was not homogeneous and slightly different after every formation. In order to compare the different closure measures it is of importance that no local weaker locations might cause erosion. Therefore the island was patched during the final stage of the island formation. For these experiments all the flow stages were used as can be seen from Table 4.3.

The experiments with measures at the upstream confluence are used to get a better insight in the morphodynamic effects of channel closure on the successive island. In total four experiments were conducted. For these experiments the width in the left channel of the confluence was reduced. Wooden 2 centimeter thick boards were used to reduce the width of the channel. The boards were fixed along the channel using glue clamps. This width reduction was constructed along the complete left branch, all the way to the point where the discharge is distributed over the two tributaries. By installing one or two boards in the 10 centimeter wide tributary, the width reduction was respectively 20% or 40%. For the experiments the influence of the location, inner and outer bend, and amount of width reduction, respectively 20% and 40%, were evaluated.
This width reduction caused relatively more discharge in one of the channels (Q_2) and less in the other (Q_1), as total discharge remained the same. Thus, by installing these measures an asymmetry of the inflow of the widening was created. In Table 4.2 the ratio of the discharge over the tributaries is shown. The sediment input was also adjusted for the channels according the amount of discharge. For these experiments the first two flow stages were used as can be seen from Table 4.3.

Width reduction	**Discharge**	
	Q_1	Q_2
20%	4/9	5/9
40%	3/8	5/8

Table 4.2: The distribution of discharge over the left (Q_1) and right (Q_2) tributaries in the upstream confluence per width reduction.

4.1.2 Flow stages

The different experiments conducted on channel closure with the executed flow stages are shown in Table 4.3. Here the first flow stage correspond with the formation of the island as described in subsection 3.3.2. The second and third flow stage correspond with respectively the low-discharge and high-discharge stage.

Experiment	**Flow stage**		
	1	*2*	*3*
Ref	√	√	√
W1	√	√	√
W2	√	√	√
W3	√	√	√
I20	√	√	
I40	√	√	
O20	√	√	
O40	√	√	

Table 4.3: The flow stages, as discussed in subsection 3.3.2 and subsection 4.1.2, for the different experiments.

2. Low discharge
After the falling flow stage used to form the island a steady discharge stage was used to conduct experiments on channel closure. This low-discharge stage was used to see the effects of channel closure during the dry season. This stage used a discharge of 0.7 L/s and a sediment input of 140 g/min. These are the same settings as the final phase of the island formation stage. This flow stage was continued for 75 minutes. When the time was passed the bed level was drained and the bed level measured.

3. High discharge
After the steady low-discharge stage a high-discharge stage was used to conduct some further experiments on channel closure. This high stage was used to see the effects of channel closure during the wet season. In order to simulate the wet season the island should be submerged, similar to the simulations done by Ostanek Jurina (2017) and the pilot project of FAP22. The water level was increased by using a combination of increasing the downstream weir and increasing the discharge.
Increasing the height of the downstream weir had its limitations as the imposed backwater curve should not influence the processes in the widened section. By installing the weir a $M1$ backwater curve was induced which influences the water and bed level in upstream direction. It is important to limit the influence in the widened section as it influences the processes around the island. The distance from the downstream weir to the widened section is approximately 130 cm. With the empirical fit to the analytical solution Equation 4.1 (Bresse, 1860), the distance that is influenced can be determined. Further it should be noticed that increasing the discharge also had its limitations as the island changes shape with higher discharge. Therefore the discharge was slowly increased to a certain limit.

$$L_{1/2} = 0.24 \frac{h_e}{i_b} \frac{h_0}{h_e}^{4/3} \tag{4.1}$$

with $h_e = q^2/C^2 i_b$ the equilibrium depth. Eventually an increase of 8 mm of the downstream weir and a discharge as shown in Table 4.4 was used for this flow stage. Figure 4.2 shows a graphical representation of the increase in discharge over time. The discharge was increased every 7.5 minutes in order to increase from 1.0 L/s till 1.4 L/s 30 minutes later. Then the closure measure was exposed to a steady discharge for 60 minutes.
The sediment input was increased accordingly during this period. The initial 0.7 L/s was accompanied with 140 g/min while the final 1.4 L/s has an input of 280 g/min. In practice the time between the deposits was reduced, from 2 minutes to 1 minute. After the final stage the flume was drained and the bed level measured.

Phase	**Discharge [L/s]**	**Sediment input [g/min]**	**Time [min]**
1	1.0	200	0 - 7.5
2	1.1	220	7.5 - 15
3	1.2	240	15 - 22.5
4	1.3	260	22.5 - 30
5	1.4	280	30 - 90

Table 4.4: The five different phases used in the high-discharge stage.

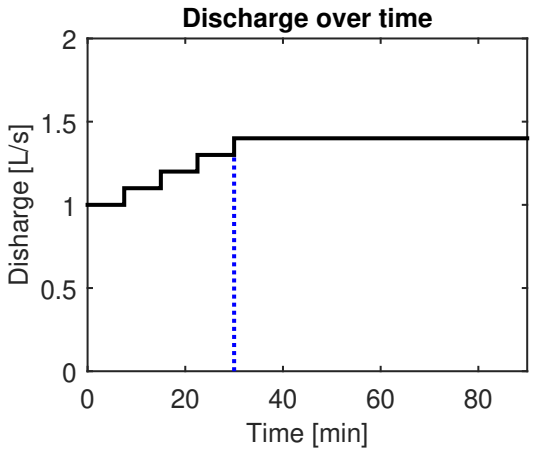

Figure 4.2: Graphical representation of the high-discharge stage over time.

4.2 Results

4.2.1 Island formation

For all the experiments the initial stage focused on the formation of an island in the middle of the widened section. The four different phases as described in subsection 3.3.2 were conducted. In Table 4.5 an overview of the time needed for the different phases is shown. The total time varied between the 130 and 152 minutes, with an average of 139 minutes. The variation can be attributed to the random formation of the island for each experiment. As no bed level measurements in between the different phases are conducted, which was the case for the experiments on selecting the setup, the time needed for the formation of the island significantly reduces. Further it can be seen that the formation for the experiments W1, W2 and W3 is slightly longer. This is the results of the patching in the final phase.

Experiment	**Time per phase [min]**				
	1	*2*	*3*	*4*	*total*
Ref	25	51	22	42	140
W1	27	62	23	40	152
W2	23	57	34	38	152
W3	17	52	28	42	139
I20	29	46	28	27	130
I40	22	51	25	33	131
O20	18	68	26	24	136
O40	28	42	26	36	132

Table 4.5: The time per phase of the first flow stage for the experiments on channel closure.

Figure 4.3 shows the bed levels in longitudinal direction after the formation of the island for the experiments on channel closure. From the graph it can be seen that the obtained bed levels were quite similar. The sub-figure below shows the standard deviation of the bed level in longitudinal direction. The standard deviations is used in order to quantify the amount of variation of the longitudinal bed level. The standard deviation, σ, is defined as the square root of the variance of X, $\sigma = \sqrt{E[(X-\mu)^2]}$. From the figure it can be seen that the highest deviations of the mean bed level are around $x = 280$ to $x = 320$, so at the final part of the widened section. In Appendix C the formation of the island, both per phase and the final obtained planform, is discussed in more detail. Here the two-dimensional bed levels of the different experiments are compared as well. From this analysis it is concluded that the final obtained planform is very similar. The right channel at the begin and the left channel at the final section show the most deviation from the mean. It is therefore important to take these locations into consideration when the results are analyzed.

Discharge distribution
Besides comparing the planform after the formation of the island, the discharge distribution over the two channels should be analyzed. The discharge over the two branches was

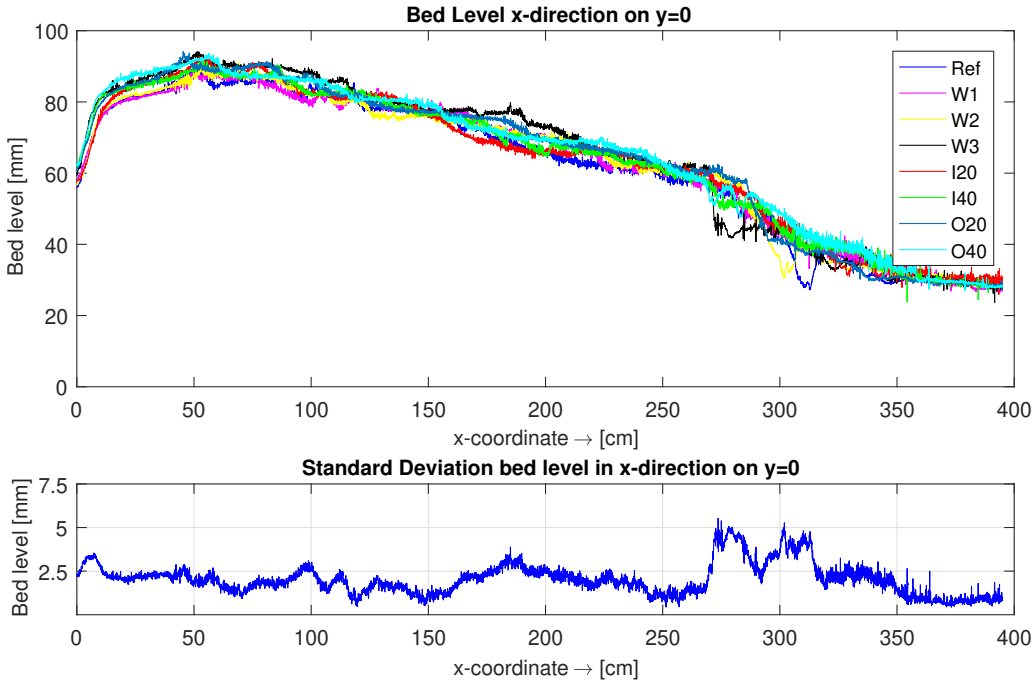

Figure 4.3: Longitudinal bed level after the formation of the island for the experiments conducted om channel closure. The figure below shows the standard deviation of the bed level in longitudinal direction.

not measured during the experiments. However, other parameters were measured which give a good indication of the distribution. For the estimate of the discharge distribution the cross-sectional areas of the two channels are compared. It should be taken into account that with this estimate the water velocities are assumed equal. The cross-sectional area can be calculated from the water depth and channel width. However, as the water depth is not known within the widened section, both parameters can be determined from the bed level measurements. At the location with similar water levels, the bifurcation and confluence, the cross-section can be analyzed. An average bed level is determined for each channel on the basis of two cross-sections at the bifurcation and confluence of the island. The channel widths are also determined based on these cross-sections. More details of the calculation can be found in Appendix D.

From Figure 4.4 an indication of the discharge distribution can be obtained. The figure shows the difference of the average bed level of the right and left channel on the vertical axis. The horizontal axes shows the width ratio of the left and right channel. The filled markers represents the front (bifurcation) of the island, while to open markers represents the final section of the island (confluence). The figure can be interpreted as following: positive bed level differences indicate a deeper left channel and width ratio values larger than 1 indicate a wider left channel. Meaning that a marker located in the upper right corner indicates that the discharge is mainly distributed to the left channel. It should be taken into account that the bed level difference is an average taken over the width of the channel. Although the width differences are more significant for the discharge distribution, this parameter also is of importance.

The figure shows that the bifurcation and confluence are approximately in the middle for all experiments after the formation of island. This agrees with the qualitative indicator for the transition to the next phase as mentioned in subsection 3.3.2. The width ratio

scatters between the 0.9 and 1.1. However, it can be seen that for all the markers the right channel is deeper at both the bifurcation and confluence. This estimate of the discharge distribution shows that the right channel is dominant, although the difference is not significant. The reason for this asymmetry is probably the forcing of the planform. Small deviations of the upstream confluence and the shape of the widening result in the obtained elevation in the middle. However, the results show that the asymmetry is obtained for all the different experiments. Therefore the different experiments on channel closure can be compared as the starting points are similar.

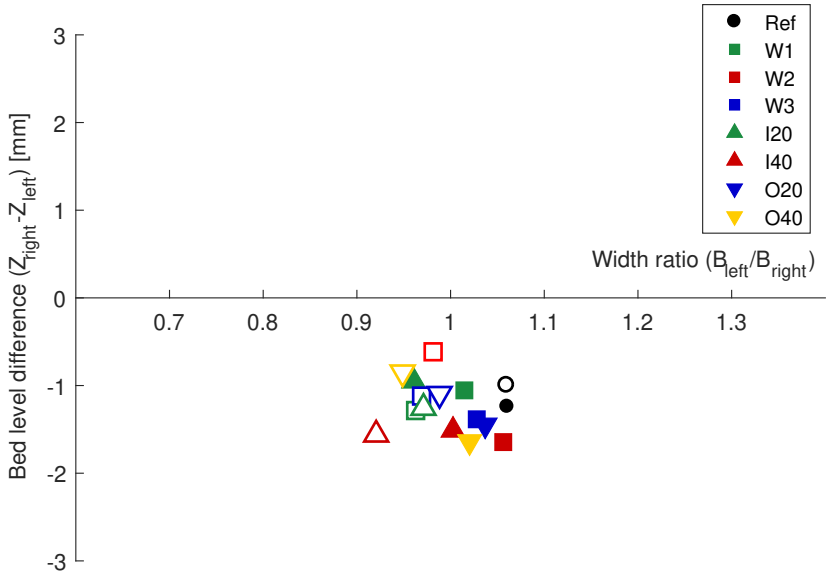

Figure 4.4: The difference of the average bed level and width ratio of the left and right channel at the bifurcation (filled markers) and confluence (open markers). The results are obtained after the island formation for all experiments.

4.2.2 Reference

The first experiment conducted on channel closure was the reference experiment. During this experiment all three flow stages were used: the island formation (1), the low-discharge stage (2) and the high-discharge stage (3). The details of the island formation are discussed in subsection 4.2.1.

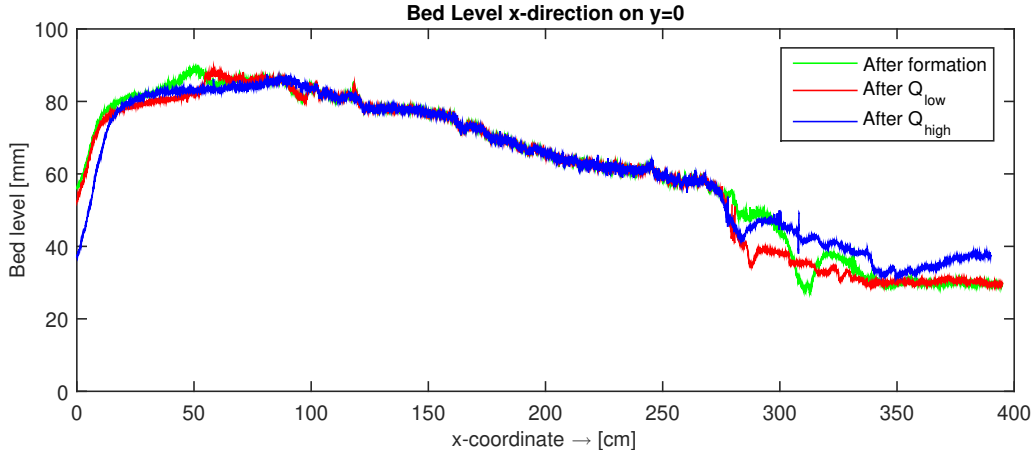

Figure 4.5: Longitudinal bed level after the formation of the island, Q_{low} and Q_{high} for the reference experiment.

In Figure 4.5 the longitudinal bed levels after the island formation, Q_{low} and Q_{high} are shown. It can be seen that after the low flow stage the front of the island, around $x = 50$ cm, moved downstream for approximately 5 cm. At the final section of the island a drop in bed level is visible at approximately $x = 275$ cm. The confluence scour hole developed here as the final section of the island moved upstream for approximately 15 cm. After the high flow stage the upstream confluence scour was deeper and the front of the island moved further downstream. Further the influence of the downstream weir is clearly visible. It can be seen that the bed level was raised in the final section until the downstream confluence scour hole.

In Figure 4.6 the bed levels after the low and high-discharge stage are shown for the widened section. During the low-discharge stage the island changed shape, however the front and back of the island remained approximately in the middle. The main erosion took place around the front and back of the island. The erosion at the left and right side of the front of the island resulted in a smaller bifurcation angle.
During the final high-discharge stage the island slowly submerged as the discharge increased. At its peak almost the complete island was submerged, however there was hardly any flow over the island. Therefore no erosion took place on the island, only the front section was affected. This resulted in a complete reshaping of the island during this flow stage, see Figure 4.7. It can be seen that front moved further downstream and the bifurcation angle decreased further as the width of the island decreased. Figure 4.7b shows the development of the bed level in the right branch for the first 50 minutes of the high-discharge stage. Both channels around the island remained approximately equal in width during the stage. However, in the left channel ripples formed which are visible from the bed level measurements and images.
More images of the experiment can be found in Appendix B section B.4.

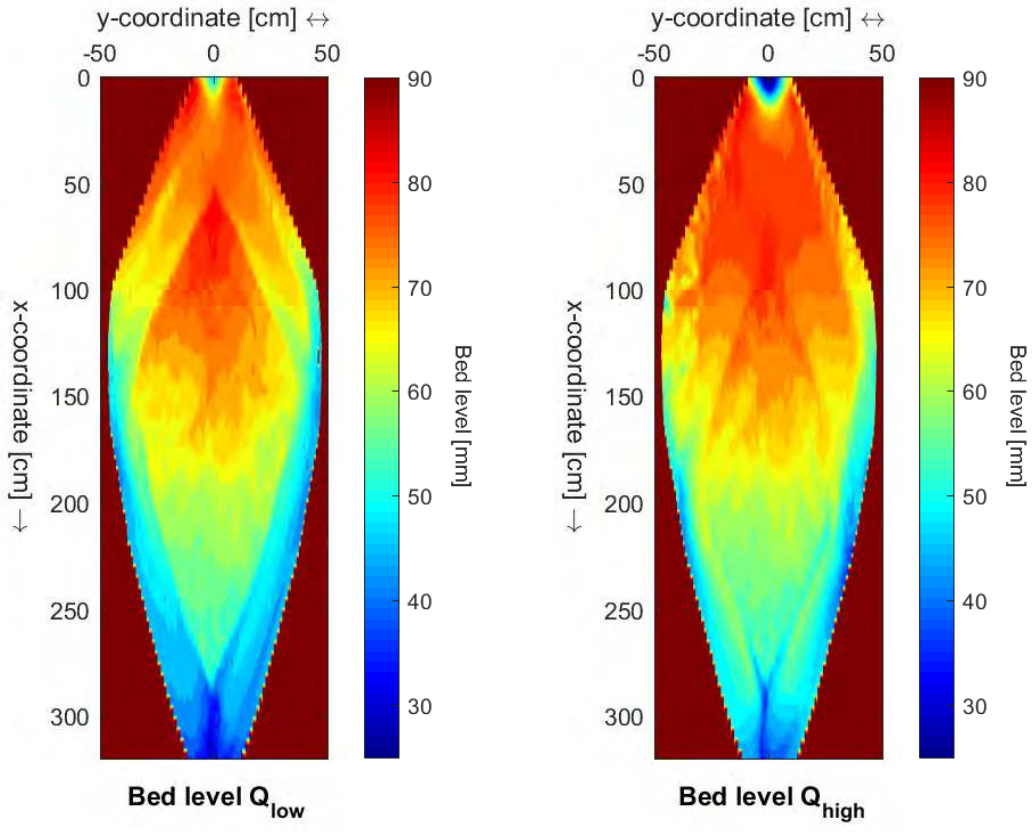

Figure 4.6: The bed level in the widened section after Q_{low} and Q_{high} for the reference experiment.

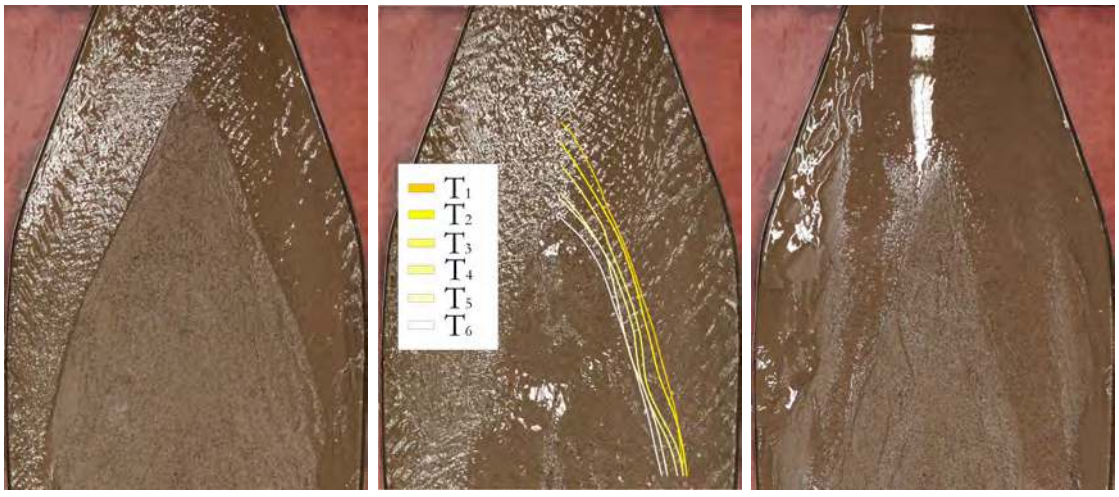

(a) (b) (c)

Figure 4.7: The reference experiment after the low-discharge stage (a) during the high-discharge stage (lines indicate development bed level over 50 minutes) (b) after the high-discharge stage (c).

4.2.3 Measures at island

In total three experiments were conducted with an installed weir at three location along the island: the begin, middle and end of the right channel. Both the length of the weir, 133% of channel width, and the location, respectively at 1/8, 3/8 and 6/8 of the island from upstream, depended on the final planform obtained after the island formation. In Table 4.6 these parameters for the experiments are shown.
For these experiments the three flow stages as earlier described are used to analyze the channel closure. The details of the first flow stage, the island formation, are discussed in subsection 4.2.1.

Experiment	**Closure weir**	
	Length [cm]	*x-coordinate* [cm]
W1	26.66	90
W2	16	140
W3	20	225

Table 4.6: The location and length of the installed weir during the experiments.

Closure at begin
In Figure 4.8 the longitudinal bed level after the island formation and after the measure with respectively Q_{low} and Q_{high} are shown. The resulting bed level after the low-discharge stage is very similar to the reference case, the front moved downstream and the final section upstream. After the high flow stage the bed level shows some differences compared to the reference case. An additional elevation of the bed level is visible from $x = 260$ to $x = 325$ cm. This increase is caused by a shift of the confluence scour downstream of the island, see Figure 4.10.

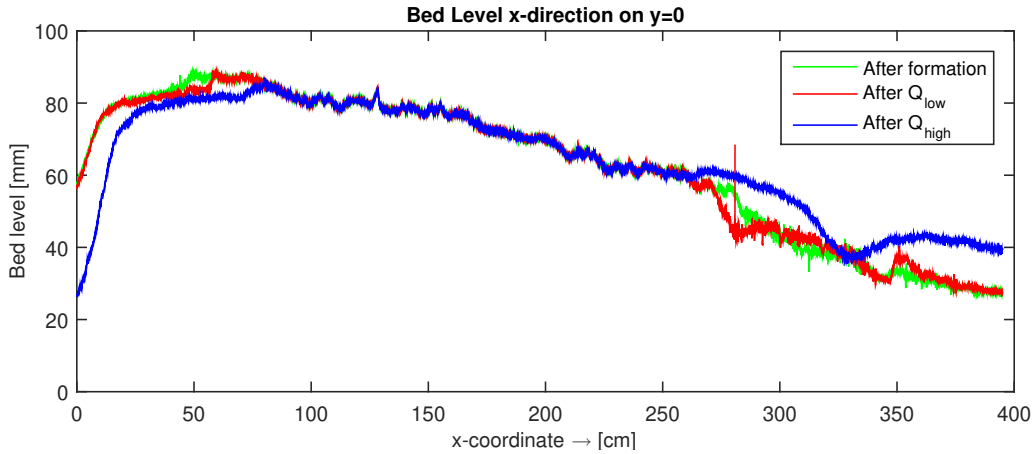

Figure 4.8: Longitudinal bed level after the formation of the island, Q_{low} and Q_{high} for experiment W1.

During the low flow stage a weir was installed at the begin of the right channel. The exact location and length of the weir are shown in Table 4.6 and are good visible in Figure 4.9 and Figure 4.10. During the installment of the weir a local increase in water

depth before the measures was visible. This increase in water depth resulted in an increase of channel width, submerging the front part of the island just before the measure. After the installment sediment was deposited at the inner bend, while sediment was eroded at the outer bend. Behind the measure some incision was visible at the inner bend, while sedimentation was visible at the outer bend. From the final bed obtained level it can be seen that a clear elevation formed from the upstream confluence to the front of the island, blocking a large part of the flow to the right channel. Further it can be seen that some sedimentation took place at the final section of the right channel. In addition, the confluence scour downstream of the island clearly points towards the right, in line with the dominant left branch. The left channel clearly became dominant during this stage, as erosion took place in the left channel while sedimentation took place in the right branch. From adding dye to the flow it was observed that the flow velocity in the right channel was reduced.

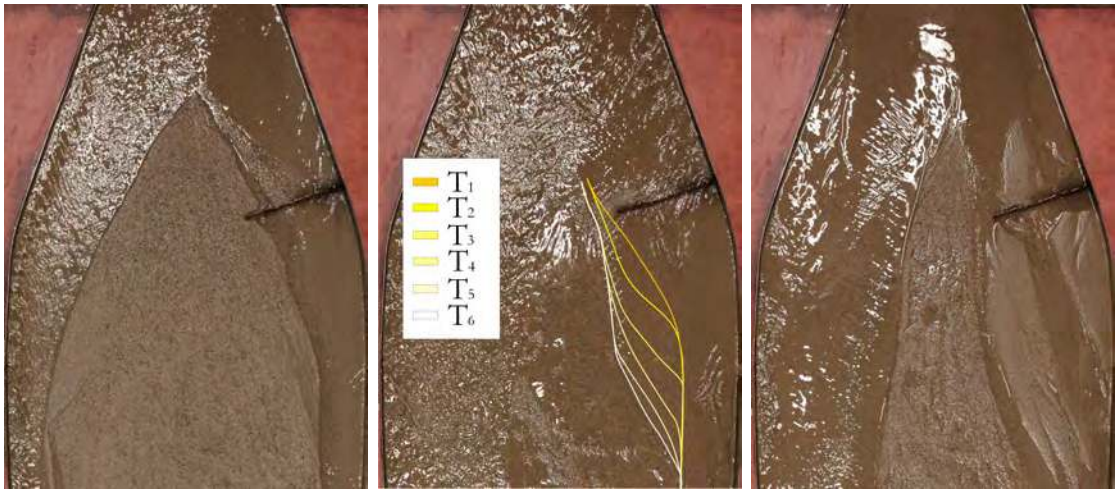

(a) (b) (c)

Figure 4.9: The closure measure for W1 after the low-discharge stage (a) during the high-discharge stage (lines indicate development bed level over 50 minutes) (b) after the high-discharge stage (c).

During the high-discharge stage the closure measure was exposed to an increase in discharge. As the discharge slowly increased the island changed shape accordingly. Initially the increase in discharge caused sediment to be deposited higher in front of the measure, approximately at the same level as the island. However, after approximately 15 minutes the formation of a bypass channel was initiated, see Figure 4.9b. This bypass channel slowly became larger and moved further downstream. In addition, a bar developed just after the tip of the measure which became larger as the bypass channel moved further downstream. This resulted in two channels, one from to outer bend and one from the bypass channel. The left channel remained dominant during this stage as an increase in width and depth is visible and the overall elevation shifted towards the closed off branch. During this stage the development of ripples was observed at the upper left branch and just downstream of the weir.
More images of the experiment can be found in Appendix B section B.5.

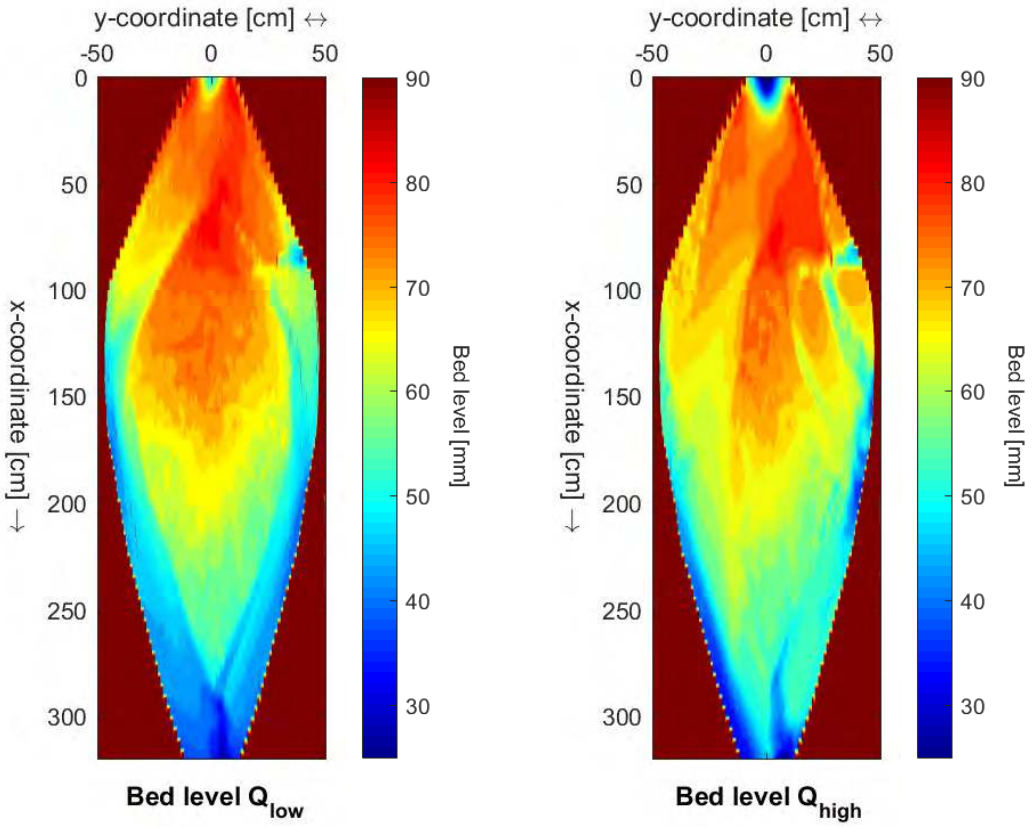

Figure 4.10: The bed level in the widened section after Q_{low} and Q_{high} for experiment W1.

Closure at middle

In Figure 4.11 the longitudinal bed levels after the island formation and after the measure with respectively Q_{low} and Q_{high} are shown. The resulting bed level after the low-discharge stage is very similar with the reference case at the front, however at the final section a deviation is visible. It can be seen that the drop in bed level at $x = 275$ cm is considerably less than with the reference case. This is due to the shift of the downstream confluence scour hole towards the right, see Figure 4.13. After the high flow stage the scour hole remained shifted, which explains the increase in bed level from $x = 260$ to $x = 325$ cm. During the low flow stage a weir was installed at the middle of the right channel. The exact location and length of the weir are shown in Table 4.6 and are good visible in Figure 4.12 and Figure 4.13. During the installment of the weir the water depth locally increased, resulting in the submergence of the island around the measure. After the installment sediment was deposited at the inner bend, while erosion took place at the outer bend. Behind the measure erosion took place at the inner bend for approximately 60 cm. On the other hand a bar formed in the outer bend. From the final bed level it can be seen that a clear elevation was formed from the upstream confluence to to front of the island, blocking a large part of the flow to the right channel. Some sedimentation was observed in the final section of the right channel. The confluence scour hole upstream and downstream of the island are in line with the dominant channel. The left channel clearly became dominant during this stage, as erosion took place in the left branch while sedimentation took place in the right branch. From adding dye to the flow it was observed that the flow velocity in the right channel was reduced.

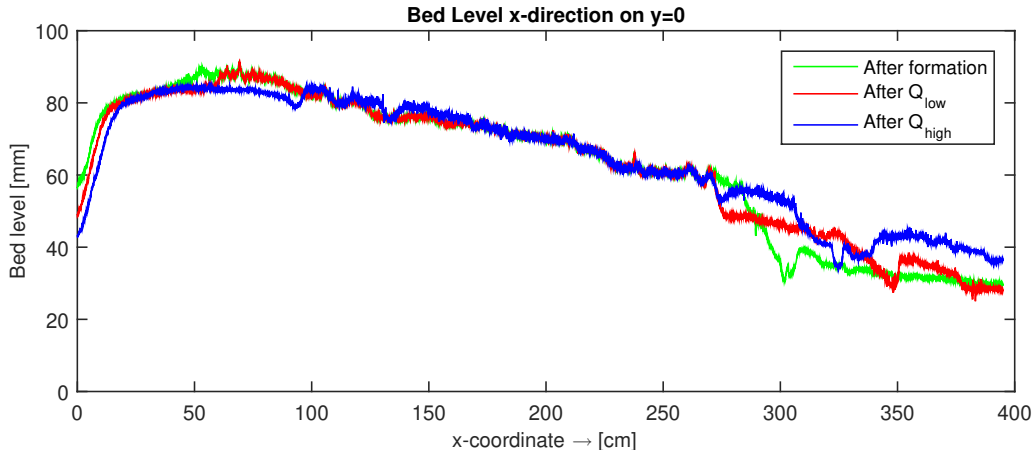

Figure 4.11: Longitudinal bed level after the formation of the island, Q_{low} and Q_{high} for experiment W2.

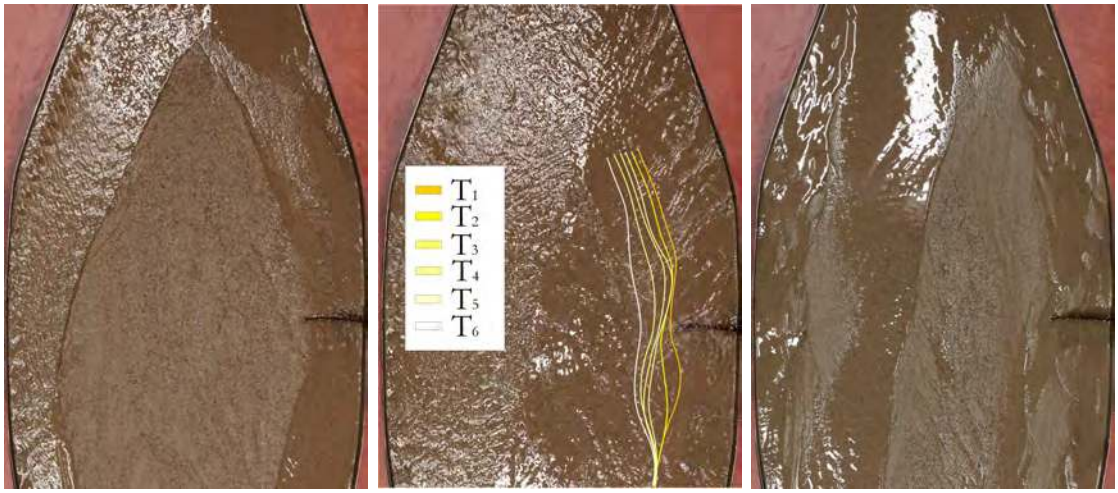

(a) (b) (c)

Figure 4.12: The closure measure for W2 after the low-discharge stage (a) during the high-discharge stage (lines indicate development bed level over 50 minutes) (b) after the high-discharge stage (c).

During the high-discharge stage the closure measure was exposed to an increase in discharge. As the discharge slowly increased the island changed shape accordingly. Initially, the increase in discharge, and thus water level, was accompanied with a higher deposition of sediment before the measure. This deposition process continued and the bed level became roughly the same as the elevation of the island. However, as this deposition before the measure formed erosion took place at the inner bend around the structure. The bypassed flow increased with time and the eroded area slowly increased, see Figure 4.12b. In the inner bend a bar developed behind the weir. During this stage the left channels remained dominant as the channel becomes wider and deeper and the overall elevation shifted towards the closed branch. During this stage the development of ripples was observed at the at the upper left branch and just downstream and upstream of the weir. More images of the experiment can be found in Appendix B section B.6.

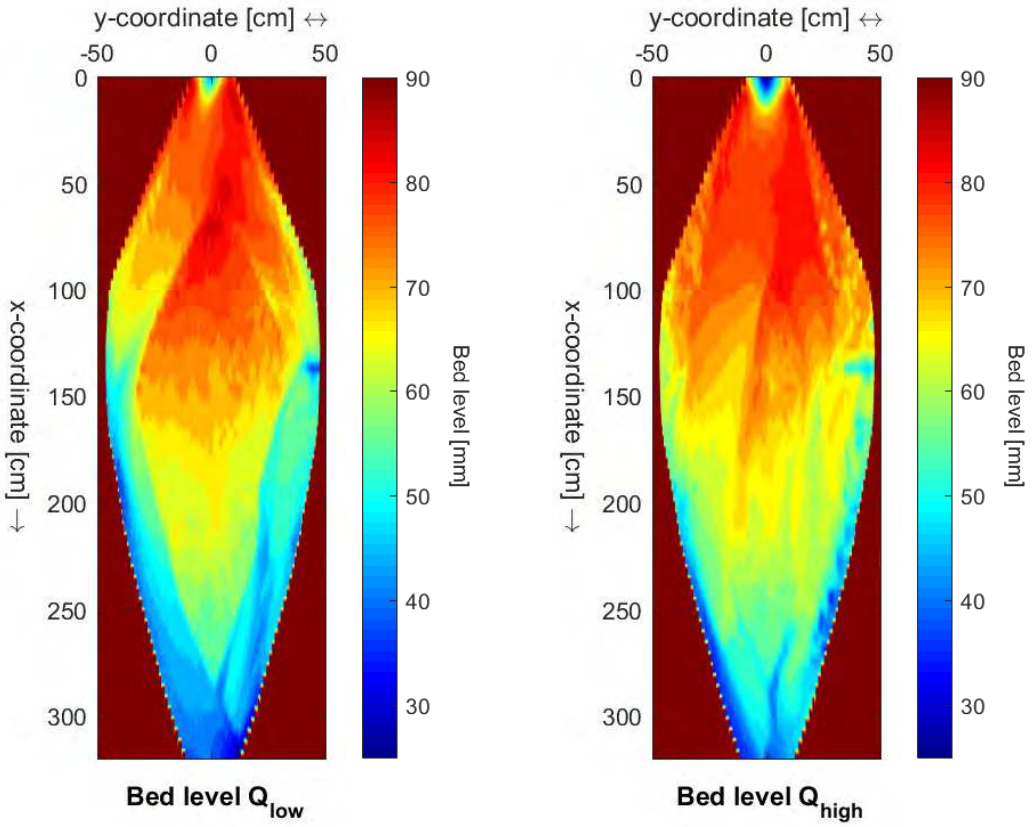

Figure 4.13: The bed level in the widened section after Q_{low} and Q_{high} for experiment W2.

Closure at end

In Figure 4.14 the longitudinal bed levels after the island formation and after the measure with respectively Q_{low} and Q_{high} are shown. The resulting bed level after the low-discharge stage is very similar with the reference case. A small deviation can be seen at $x = 320$ cm, here a small increase in bed level is visible. This deviation is caused by a shift in the direction of downstream confluence scour hole. After the high flow stage the development of the longitudinal bed level is similar as the reference case.

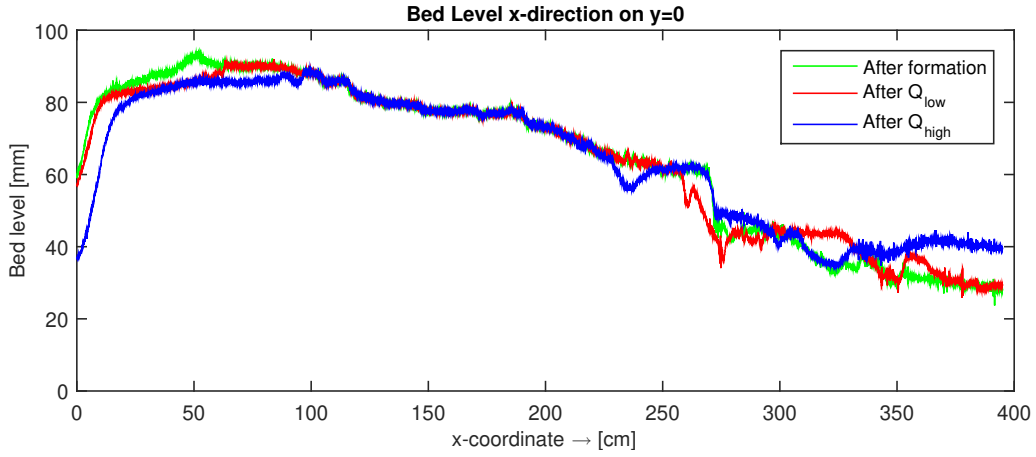

Figure 4.14: Longitudinal bed level after the formation of the island, Q_{low} and Q_{high} for experiment W3.

During the low flow stage a weir was installed at the end of the right channel. The exact location and length of the weir are shown in Table 4.6 and are good visible in Figure 4.16 and Figure 4.15. During the installment of the weir the water depth locally increased, resulting in submergence of the island around the measure. Around the measure it could be observed that the main flow was concentrated in the outer bend, where erosion took place. In the inner bend some sedimentation took place. In the outer bend behind the measure sedimentation was observed and the main flow was concentrated at the inner bend. Several indicators show that the left channel became dominant during this stage. The direction of the downstream confluence scour hole is in line with the left channels. Moreover, it was can be observed that erosion took place in the left channel while sedimentation took place in the right branch. From adding dye to the flow it was observed that the flow velocity in the right channel was reduced.

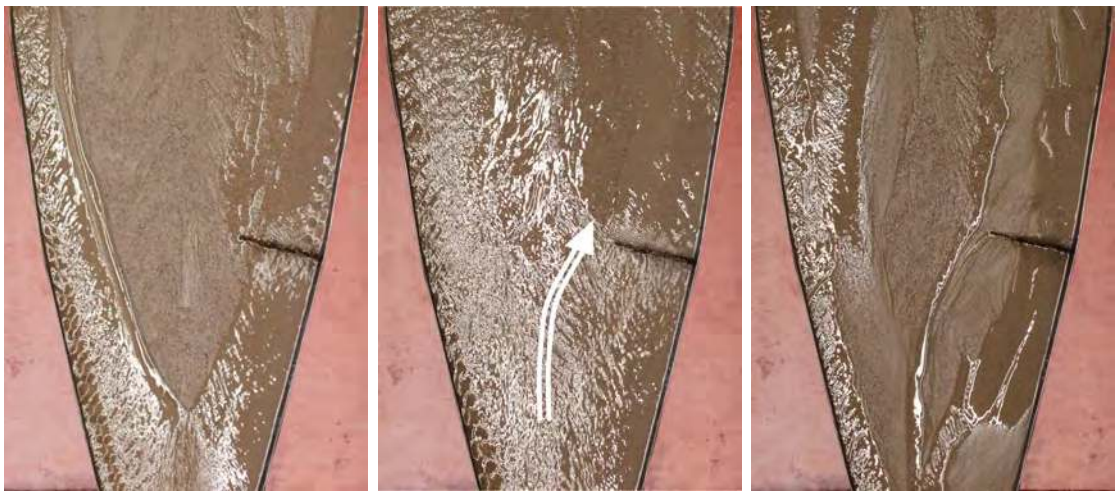

(a) (b) (c)

Figure 4.15: The closure measure for W3 after the low-discharge stage (a) during the high-discharge stage (see text) (b) after the high-discharge stage (c).

During the final stage the discharge was doubled with the measure at the final section of the island. As the discharge slowly increased the island changed shape accordingly. During this experiments sediment was deposited again before the measure. A clear phenomenon during this phase was the rapid water flowing over the final section of the island just downstream of the weir. At the beginning some sediment transport was visible here, but no erosion. However, after some time erosion took place forming a channel from the confluence to just upstream of the closure measure, creating a third branch, see Figure 4.15b. This channel was formed by headward erosion and fully developed near the end of the high-discharge stage. Unfortunately the development of the bed level was only obtained from observations. Due to the rapid water flow over this section the development of the bed could not be retrieved from images of the digital camera. Further it was observed that the left channel remained dominant during this stage. The left channel was wider and the elevation moved towards the closed branch. During this experiment ripples developed upstream of the weir.
More images of the experiment can be found in Appendix B section B.7.

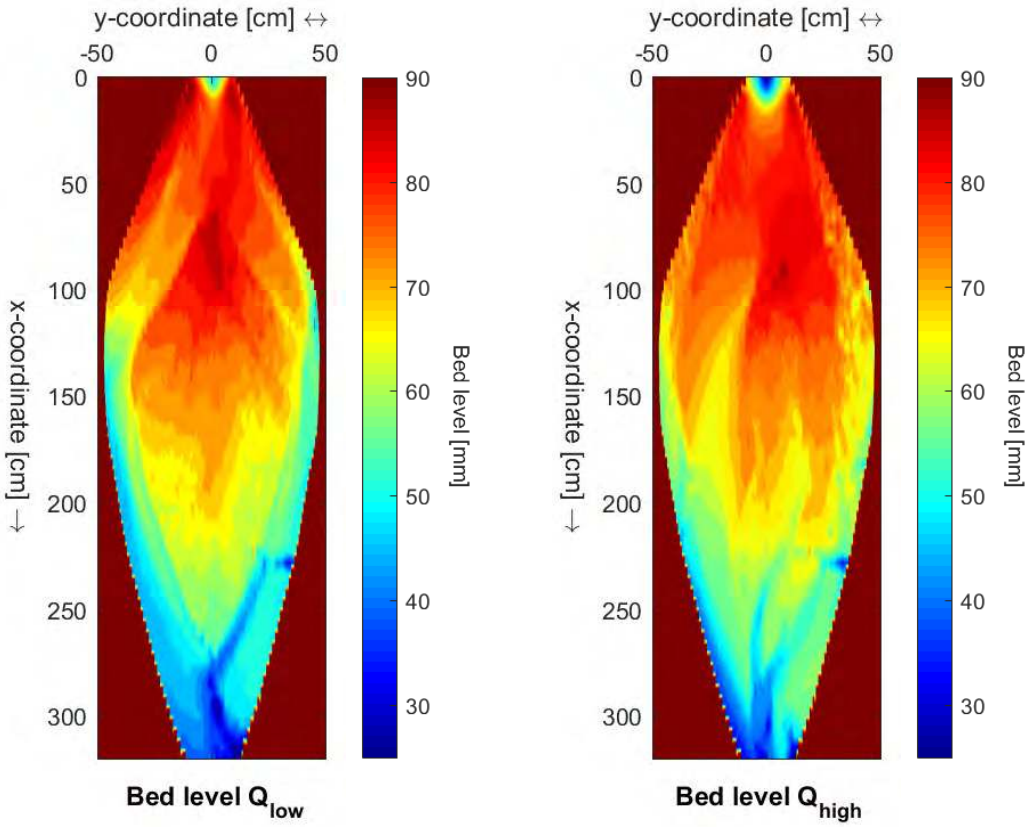

Figure 4.16: The bed level in the widened section after Q_{low} and Q_{high} for experiment W3.

Discharge distribution

Besides the planform changes observed during and after the experiments, the discharge distribution over the two channels should be analyzed. An estimate of the discharge was obtained as explained in subsection 4.2.1. More details of the calculation can be found in Appendix D. Figure 4.17 shows the estimate of the discharge distribution for the considered experiments after the low flow stage. The figure can be interpreted as followed: positive bed level differences indicate a deeper left channel and width ratio values larger than 1 indicate a wider left channel. Meaning that a point located in the upper right corner indicates that the discharge is mainly distributed to the left channel.

From the figure it can be seen that the initial bed level difference, after the island formation, is almost absent for the reference experiment. It seems that as time proceeds the distribution is almost equal, although the width of the channels show some differences. Further it can be seen that for all experiments with closure measures at the island the left channels becomes dominant. This outcome agrees with the observations of the planform. The figure shows that the distribution at the bifurcation differs from the distribution at the confluence. In addition, it can be observed that the closure measure at the final section is less effective than at the other locations. It should be noted that for this analysis it was assumed that the velocities of both channels were similar. However, as mentioned before was there a clear difference observed in the velocities of the open and closed branch. This difference in velocity could not be measured very precisely, however it was observed that the difference was in the same order of magnitude for the different experiments. It can be concluded that the estimate of the discharge distribution in Figure 4.17 underestimates the discharge ratio of the two channels.

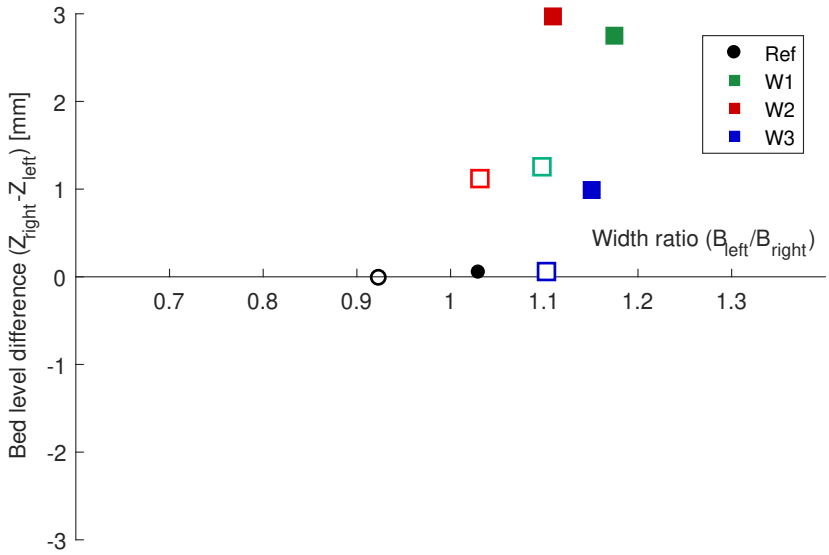

Figure 4.17: The difference of the average bed level and width ratio of the left and right channel at the bifurcation (filled markers) and confluence (open markers). The results are obtained after low-discharge stage for the closure measures around the island.

4.2.4 Measures at confluence

In total four experiments were conducted with a width reduction in the upper confluence. Width reductions of 20% to 40% were installed, both in the inner and outer bend. For these experiments the first and second flow stage were used to analyze the effects of channel closure on the successive island. The details of the first flow stage, the island formation, are discussed in subsection 4.2.1.

Inner bend width reduction

In Figure 4.18 the overview of the longitudinal bed levels before and after the 20% and 40% width reduction of the upstream inner bend are shown. The bed levels before the width reductions shows the longitudinal slope after the island formation. For both measures there was some erosion at the front of the island, around $x = 50$ cm, which is similar with the reference case. Around the final section of the island, around $x = 275$, there is a difference between the 20% and 40% case. The bed level for the 20% width reduction shows a drop in bed level as the final section moved upstream, approximately 15 cm, which is similar with the reference case. However, the 40% width reduction does not show this drop in bed level. This is because the final section of the island moved upstream approximately 30 cm and shifted towards right channel, see Figure 4.19.

From the bed level profiles after the width reduction measures in Figure 4.19 other observations are made. During both experiments the upstream confluence scour was influenced by the width reduction. As expected the dominant upstream channel mainly influenced the direction of the scour hole. During the 20% reduction the scour hole alternated from direction, but eventually remained centered. During the 40% reduction the scour hole clearly pointed towards the left, in line with the upstream dominant channel, during the whole experiment. Further it was noticed that the avalanche face of the left channel changed location, which is probably due to the location of the narrowing.

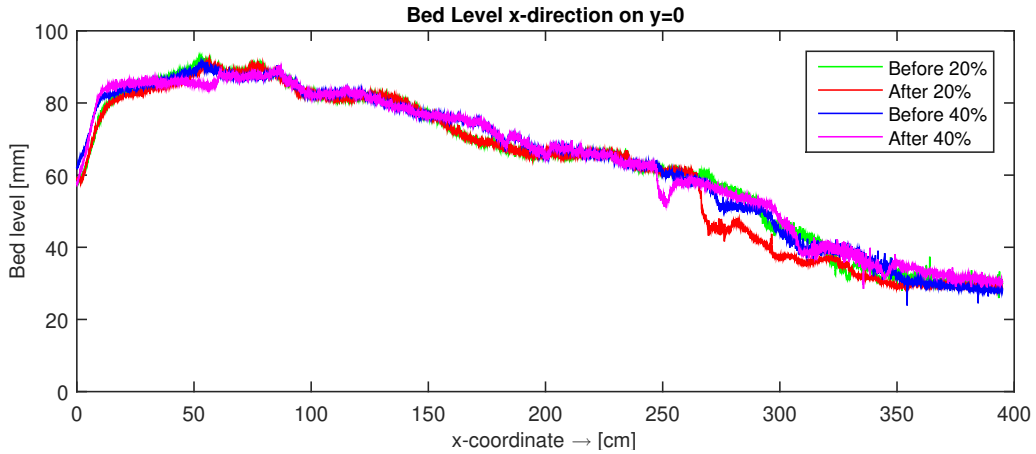

Figure 4.18: Longitudinal bed level before and after the narrowing the of upstream channel for experiment I20 and I40.

During both experiments the upstream width reduction resulted in asymmetrical reshaping of the island. During the 20% case the front slightly shifted towards the left, while the final section moved to the right. This caused the final section of the left channel to be wider than the right channel. In the final section of the left channel a bar formed, see Figure 4.20b. During the 40% case the front of the island moved approximately 4 cm towards the left, see Figure 4.20a. This shift in location was accompanied with some accretion at the left front of the island and erosion at the right front of the island. This resulted in a wider right channel and narrower left channel. This is probably due to the change in location of the upstream confluence as the reduction of width was in the inner bend of the upstream confluence. A clear elevation in front of the right channel can be observed. Further it was noticed that similar to the experiment with 20% reduction the left channel became wider at the final section. The downstream confluence scour hole is also influenced and is in opposite direction as the upstream confluence scour hole. Similar to the 20% case a bar formed in the final section of the left channel, see Figure 4.20c.
More images of the experiment can be found in Appendix B section B.8 and section B.9.

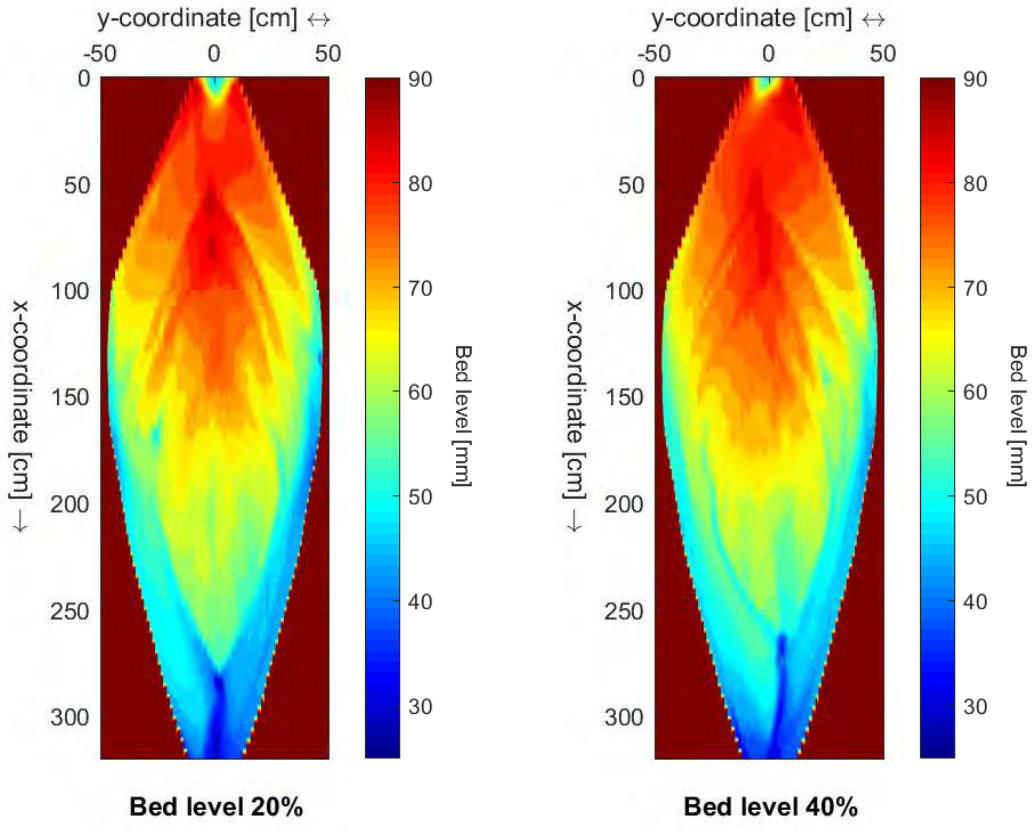

Figure 4.19: The bed level in the widened section after the width reduction for experiment I20 and I40.

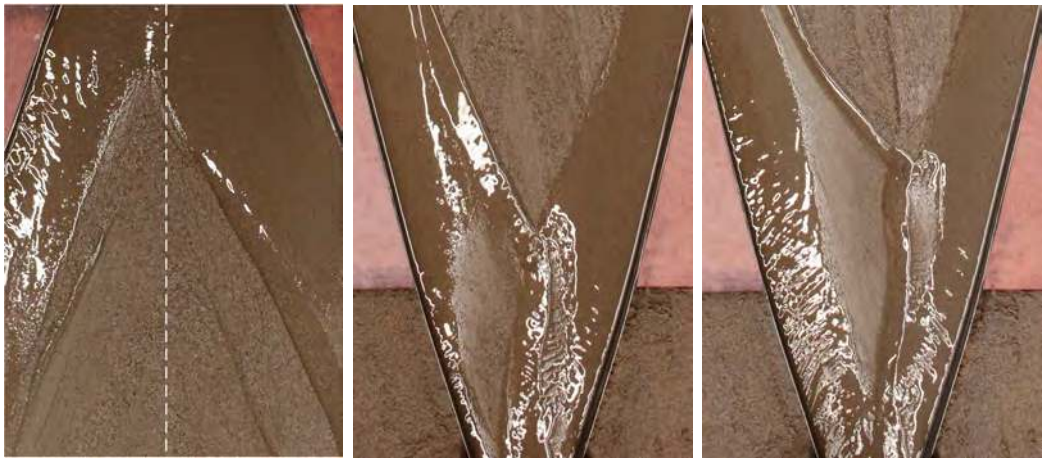

(a) (b) (c)

Figure 4.20: Images after the experiment with inner width reduction, while the flume drained. The front of the island with the 40% case (a) and the final section of the island for I20 (b) and I40 (c).

Outer bend width reduction

In Figure 4.21 the overview of the longitudinal bed levels before and after the 20% and 40% width reduction of the upstream outer bend are shown. The bed levels before the width reductions show the longitudinal slope after the island formation. The bed levels after the width reduction show for the 20% case some erosion at the front of the island while with the 40% case there is some sedimentation for the island. From Figure 4.22 it can be seen that this is caused by the increase in bed level at the begin of the right channel. Around the final section of the island, around $x = 275$, there is a difference between the 20% and 40% case. It can be seen that the final section of the island moved further upstream for the 40% case and the drop in bed level is more significant.

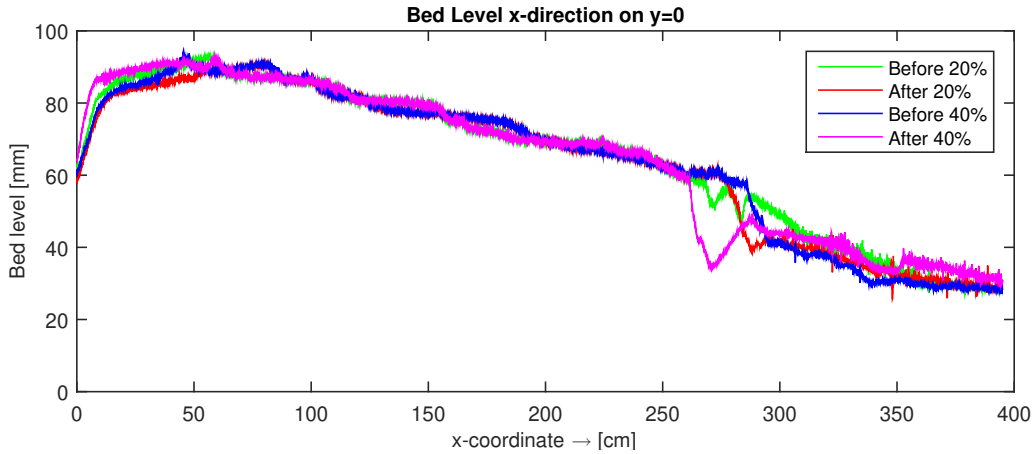

Figure 4.21: Longitudinal bed level before and after the narrowing the upstream channel for experiment O20 and O40.

From the bed level profiles after the width reduction measures in Figure 4.22 other observations are made. During both experiments the upstream confluence scour was influenced by the width reduction. As expected the dominant upstream channel mainly influenced the direction of the scour hole. During both experiments the scour hole clearly pointed towards the left, in line with the upstream dominant channel, during the whole experiment.

Compared to the width reductions in the inner bend, here the asymmetrical reshaping of the island was less significant. During the experiments a small bar formed at the beginning of the right channel. This bar caused the right channel to divert into two different streams, of which one eroded on the side of the island, see Figure 4.23a. Further it can be seen that for the 40% case an elevation formed from the upstream confluence to the island, blocking the flow for a large part to the right channel. A clear reduction in discharge was notices for the right branch, but no channel closure. In the final section of the right channel some sedimentation is visible for both cases, see Figure 4.23b and Figure 4.23c. For the 40% the difference with the left channel is even more noticeable. The downstream scour hole was directed towards the right for the 40% case, opposite to that of the upstream confluence scour hole and in line with the dominant channel.

More images of the experiment can be found in Appendix B section B.10 and section B.11.

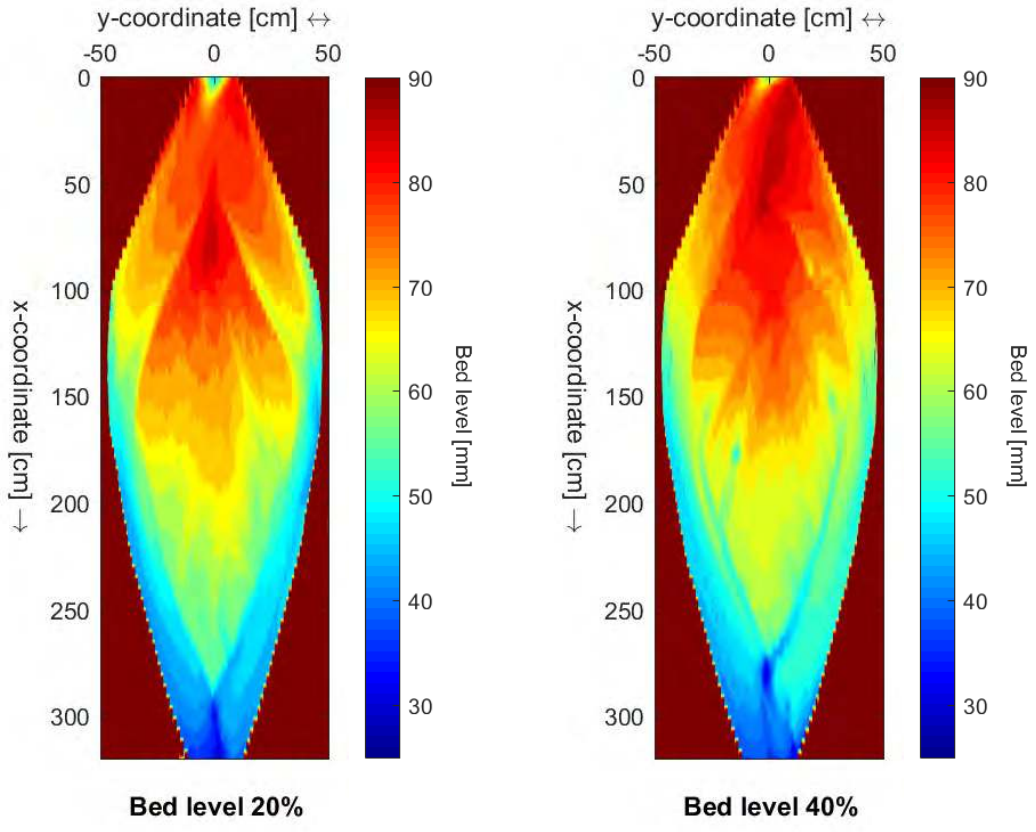

Figure 4.22: The bed level in the widened section after the width reduction for experiment O20 and O40.

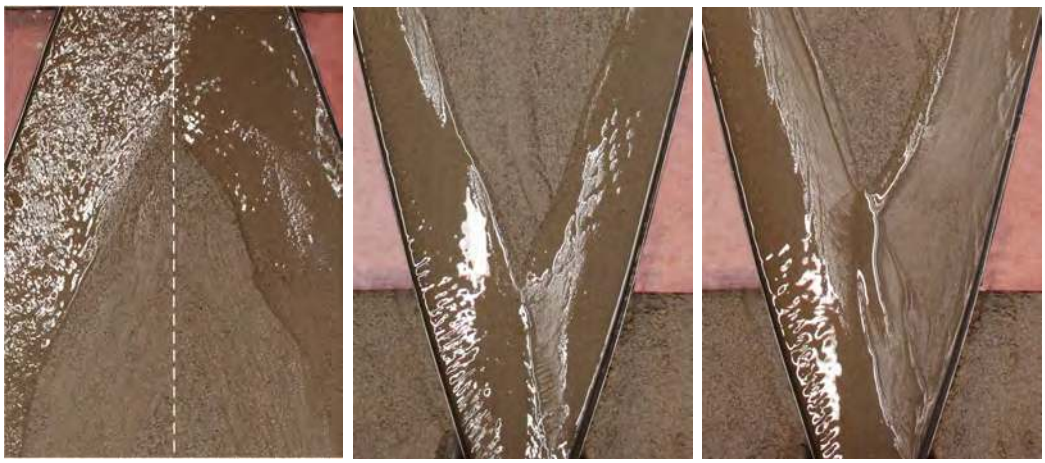

(a) (b) (c)

Figure 4.23: Images after the experiment with outer width reduction, while the flume drained. The front of the island with the 40% case (a) and the final section of the island for O20 (b) and O40 (c).

Discharge distribution

Besides the planform changes observed during and after the experiments, the discharge distribution over the two channels should be analyzed. An estimate of the discharge was obtained as explained in subsection 4.2.1. More details of the calculation can be found in Appendix D. Figure 4.24 shows the estimate of the discharge considered experiments for the low flow stage. The figure can be interpreted as followed: positive bed level differences indicate a deeper left channel and width ratio values larger than 1 indicate a wider left channel. Meaning that a point located in the upper right corner indicates that the discharge is mainly distributed to the left channel.

For the experiments with inner bend width reduction both the bifurcation and confluence of the island show a trend. At the bifurcation the difference in bed level is minimal. The width ratio at this location shows that the right channel conveys more water, especially for the 40% case. At the confluence of the island the bed level differences are significant, for both cases the left channel is shallower. However, the width ratio shows that for for both cases the left channel is wider. For the experiments with outer bend width reduction the bifurcation and confluence section of the island show more similarities. For the 20% case the width ratio is almost similar and the bed level difference is minimal. However, for the 40% case the left channel is deeper while at the front the right channel is wider.

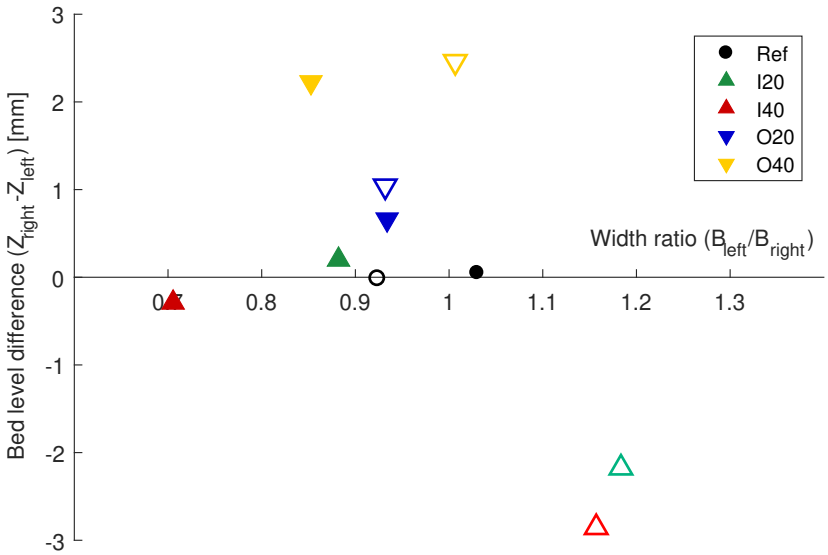

Figure 4.24: The difference of the average bed level and width ratio of the left and right channel at the bifurcation (filled makers) and confluence (open makers). The results are obtained after the low-discharge stage for the closure measures at the upstream confluence.

5 Discussion

In this chapter the experimental setup and the results of the experiments, presented in the previous two chapters, are discussed. The obtained results are compared with numerical studies and are used to address the research questions.

5.1 Selection of setup

The experimental setup was selected to systematically study the local effects of channel closure. The design of the laboratory experiments was based on the consideration that a reproducible and stable simplified section of a braided river should be considered. As a starting point a simplified system was taken with a channel, splitting and rejoining around an island. It was determined that this island should be self-forming in order to obtain a stable system. A self-forming island was obtained in a laboratory flume by initially forming a mid-channel bar which emerged as the discharge decreased. The mid-channel bar was formed by using a combination of non-erodible banks with a planform consisting of an upstream Y-shaped confluence followed by a widening. For the selection of the experimental setup several preliminary experiments were conducted. These experiments were designed on the basis of existing research on the development of mid-channel bars with planform forcing.

5.1.1 Planform forcing

The research of Repetto et al. (2002) and Wu and Yeh (2005) was initially used for the design of the setup. By using a planform with fixed outer banks and a single sinuous widening an elevation in the middle of the widening developed. However, this mid-channel bar only formed in the final section of the widening, downstream of the widest section. Moreover, the flow was mainly directed in the middle of the flume which prohibited the settlement of sediment in the upper region of the widening. It was concluded that the flow should be diverged in order to form an elevation in the upper section of the widening. This was obtained by using the planform forcing with an upstream confluence after the research of Ashworth (1996). A so-called confluence-diffluence unit was obtained due to the diverging streamlines downstream of the confluence. These observations from preliminary experiments have been confirmed with two experiments. For these two experiments

the influence of the upstream forcing was compared. During the experiments a clear difference was visible in the upper section of the widening. For the case with a straight upstream channel the main flow was concentrated in the middle, while this was not the case with the upstream confluence. However, at the final section both experiments show similar planforms. These results show that the upstream confluence diverges the streamlines, which is necessary for the development of an elevation in the upper section of the widening.
During the experiments an elevation formed downstream of the confluence, where bedload sheets stalled in the middle of the widening and merged into a single elevation. This stalling of the sediment can be attributed to the divergence of the streamlines downstream of the confluence, which resulted in a reduction of the shear stresses and hence in a decrease in sediment transport rate. The processes observed agree with the central bar mechanism as mentioned in subsection 2.2.3. Further it was observed that at the front of the bar the coarse sediment particles settled, forming a stable front in the middle. These results are similar to the results of Ashworth (1996) and the sediment sorting processes as mentioned in Figure 2.5. However, a difference with these previous studies is the mechanism of the increase in size of the bar. With these studies the bar increase in size due to downstream addition of sediment, which was accompanied with lateral migration of the channels. During this study the upstream addition of sediment was responsible for the increase in size of the elevation. This difference is probably due to the fixed outer banks, which prohibit the lateral migration of the channels.
Further it was observed that the setup with the upstream confluence is very sensitive to perturbations from upstream. The tributaries should be constructed very precise as small deviations results in an asymmetric formation of the elevation. In order to assure a symmetric forcing the tributary angle, discharge ratio and channel width should be similar for both tributaries. These outcomes agree with the observations of Yalin (1992) and Mosley (1976).

5.1.2 Reproducibility and stability

The overall obtained planform of the island formation stage shows much similarities for the different experiments. The bed level measurements indicate that the general shape and bed levels are quit similar. However, the analysis with the standard deviation of the bed level also indicates that at some locations there was quite some variation from the average. At the final section of one of the channels this deviation was significant. The estimate of the discharge distribution after the island formation also shows that the obtained planform was very similar. The results shows that one of the channels was repeatedly deeper than the opposing channel and the width ratio shows some scatter between $0.9 - 1.1$. In general it can be concluded that the obtained planform is reproducible enough to compare the different experiments. Some deviations should be taken into account when analyzing the results.
Due to the hydrodynamic forcing on the island some evolution of the planform was observed. After the low discharge stage it can be seen that some erosion took place around the outer edges of the island. The results of the reference experiment show that some erosion took place at the front and back of the island, which was also observed for most of the other experiments. This erosion was approximately 5 to 10 cm, which in total is in the order of 5% of the average 220 cm long island. Further it was observed that after the

low discharge stage the estimate of the discharge distribution changed for the reference experiment. The bed level difference was nearly non-existing, while the width ratio of the two channels changed. These results differ from the previous obtained estimate of the discharge distribution after the island formation. It can be concluded that due to the hydrodynamic forcing the planform changed shape. The observations show that these changes mainly took place at the beginning of the low discharge stage and the final obtained planform is very similar. In order to improve the stability of the planform the final phase of the island formation stage can be extended. By doing so the observed evolution can take place during the island formation stage, which results in a more stable planform for the subsequent low discharge stage. Further the sediment input could be compared with the sediment output, in order to verify whether an equilibrium was obtained.

5.1.3 Comparison theoretical model

The two experiments conducted for selection of the setup were mainly used to analyze the outcomes of the preliminary experiments. The qualitative observations agree with the overall conclusions of the preliminary experiments. However, it should be taken into account that the shape of the widening was not based on the research of Repetto et al. (2002) and Wu and Yeh (2005), which was the case for the preliminary experiments. When we simplify the asymmetrical shape of the widening it is possible to make a qualitative comparison with the model of Wu and Yeh (2005).
In Table 5.1 the different parameters for the comparison are calculated. The average depth is determined on the basis of the Phase 1 of the first stage, as here the complete planform was submerged. As mentioned before are the parameters β and λ_b the main controlling factors determining the type of elevation formed. In the research of Wu and Yeh (2005) several models were compared. The outcome of one of these models has very similar values of β and λ_b with the experimental results, see Figure 5.1. The different cross-sections in the figure are taken at different values in longitudinal direction, with 0 at the wide section and π/λ_b at the narrow section.
The overall shape of elevations per cross-section show much similarities. For both cases side bars are observed in the widest section and a central bar downstream of this region. However, it should be taken into account that, besides the β and λ_b, the other parameters are quit different. Therefore a quantitative comparison, of for example the bed level, is not possible.

Parameter	**Value**	**Unit**
Wavelength of width variation (L_b^*)	3.30	m
Wavenumber of width variation (λ_b^*)	1.90	m
Average half-width of channel (B_0^*)	0.24	m
Average depht (D_0^*)	0.02	m
Dimensionless wavenumber (λ_b)	0.45	-
Average aspect ratio (β)	12	-

Table 5.1: The parameters for the comparison with the model of (Wu and Yeh, 2005). With $\lambda_b^* = 2\pi/L_b^*$, $\lambda_b = \lambda_b^* \cdot B_0^*$ and $\beta = B_0^*/D_0^*$.

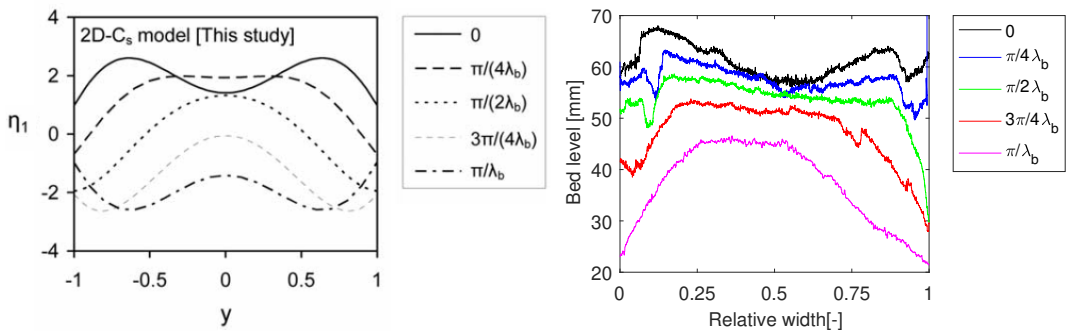

(a) $\lambda_b = 0.5$, $\beta = 10$ (b) $\lambda_b = 0.45$, $\beta = 12$

Figure 5.1: Cross-sections at different locations within the widening, comparison between the model of Wu and Yeh (2005) (a) and results of experiment *Str* (b).

5.2 Channel closure on island scale

The morphodynamic effects of channel closure on island scale have been analyzed by installing a closure measure in one of the channels surrounding the island. This closure measure was installed at three different locations and has been analyzed both during the low and high-discharge stage.

5.2.1 Closure measure

For the experiments the closure measure, a weir, was installed in phases with toothpicks. This method was selected as instantaneous installation of a weir resulted in erosion at this location. However, this method of weir installment still had some problems that should be addressed. These problems were the construction height and the connection with the fixed banks. As the toothpicks were installed the water upstream of the measure increased due to backwater effects. Because the water level was used as reference height the precise construction height of the weir was problematic. By initially placing some toothpicks with more distance this problem was solved. However, the final obtained weir was not perfect and differed per experiment. During one of the experiments the incorrect height of the weir caused the direct bypassing of the closure measure, see Figure 5.2, which resulted in a failed test. The connection of the weir with the fixed outer banks was also difficult. As most of the erosion took place here, the toothpicks needed to be installed very precise in order to prevent flow bypassing the weir.

Figure 5.2: Direct bypassing of the weir.

In order to compare the different locations the use of a constant width of the closure measures is advisable. The width of the weir was determined on the basis of the channel width. However, as the width of the channel surrounding the island was not constant, this resulted in three different weir lengths. The varying width along the island is not representative for natural braided river and therefore a constant width should be used.
Further it should be taken into account that several closure measures can be used to

close off a channel. In this experimental study only use was made of a weir. However, roughness elements such as porcupines and jack jetties show potential in their ability to close off channels. By installing a grid of toothpicks the local increase of roughness can be simulated, similar to the research conducted by Vargas Luna (2016). Due to time constrains these experiments were cancelled from the current study.

5.2.2 Low-discharge stage

During the low-discharge stage the installment of the closure measure at the different locations resulted in a reduction in discharge for the closed branch. For all three locations the reduction in discharge was accompanied with sedimentation in the closed branch, both in front of and after the measure. Further it was observed that the velocity reduced due to the closure measure. In general this asymmetrical distribution of the discharge is preferable for channel closure as this can improve the navigational conditions and prevent bank erosion.
However, there was a difference observed in the inner and outer bend morphology. Upstream of the measure sedimentation took place in the inner bend, followed by erosion downstream of the measure. At the outer bend erosion took place around the measure, while sedimentation took place downstream of the measure. The sedimentation in front of the measure is induced by backwater effects, which where visible for all three experiments. This sequence of sedimentation in front of the measure, erosion around the measure and sedimentation after the measure agrees with the model of (Schuurman et al., 2016). However, the difference between the inner and outer bend morphology is probably an effect of the scale experiment. It was observed that the main flow was directed along the stainless steel outer banks, which explains the erosion at the outer bend around the structure. In natural bends the main flow is also concentrated in the outer bend, however the smooth fixed outer banks amplify this difference between the outer and inner bend.
The morphological response to the closure measure explains the difference in discharge distribution for the different experiments. For the closure measures at the begin and middle the sedimentation upstream of the measure influenced the distribution at the bifurcation. For both experiments a clear elevation at the bifurcation redirected most of the flow towards the other channel. The closure measure at the downstream part did not induce as much sedimentation at the bifurcation. In the research of Ostanek Jurina (2017) a closure effectiveness for the different measures was determined based on several parameters, including the near bank velocity, discharge ratio and water level difference. For the dry season, which coincided with the low-discharge stage, the closure effectiveness of the entrance and middle was in the order of 100% while the downstream measure in the order of 60%. It should be taken into account that for the numerical study the weir length was constant for the different locations and an embankment was used perpendicular to the weir. From the estimate of the discharge distribution in this study it is difficult to quantify the closure effectiveness. However, it can be concluded that channel closure at the begin and middle is more effective than at the downstream part.

5.2.3 High-discharge stage

During the high-discharge stage the complete planform changed as the discharge increased and most of the planform submerged. Erosion took place mainly at the front of the island, resulting in a shorter and narrower elevation in the middle. The closure measure affected the system such that the elevation in the middle reshaped asymmetrical. For all three locations of the weir the elevation moved towards the closed branch, resulting in directing most of the discharge towards the open branch. For channel closure these effects are preferable as the main discharge is shifted towards the other channel.

Formation bypass channel

For the different experiments it was observed that the closure measures were bypassed as time proceeded. Initially it was observed that sediment was deposited in front of the weir as discharge increased. The associated higher water level resulted in a higher elevation before the measure in the inner bend. This process continued until the elevation was similar to that of the island. For the experiments with the weir installed at the begin and middle the measure was slowly bypassed as discharge increased. When time proceeded more sediment was eroded from upstream and the bypass slowly developed further downstream and increased in width. However, during the experiment with the weir installed at the downstream section the bypass channel developed different. Here the channel developed from downstream and took the full high-discharge stage to develop.

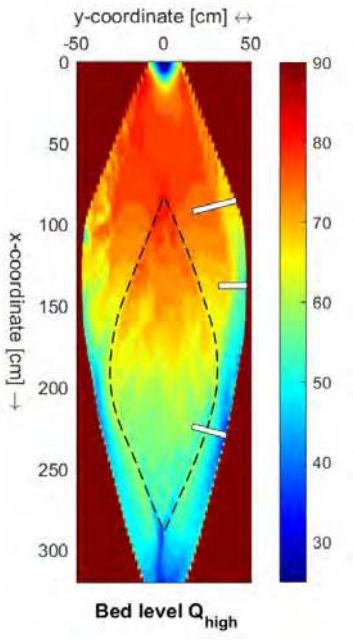

Figure 5.3: The bed level in the widened section after Q_{high} for the reference experiment with location and length of closure measures.

Initially, the final bed levels after the experiment seem quite similar to that observed in the numerical research of Ostanek Jurina (2017). However, as mentioned were the developments of the bypassing channels not similar. Figure 5.3 indicates the location and length of the closure measures with the bed level after the high-discharge stage of the reference experiment. It can be seen that, due to the reshaping of the island, the first two closure measures would be bypassed during this stage. Although the reshaping of the reference experiments is not the same for the experiments with channel closure, it does indicate that measures are easily bypassed with such reshaping. In braided rivers the wet season is accompanied with planform changes as well, see Figure 5.4a. However, the overall planform of an island is quite stable and does not reshape to this extent. The planform in the numerical research of Ostanek Jurina (2017) shows some erosion at the front but not a complete reshaping, see Figure 5.4b.

The bypass channel formed during the experiment with the weir at final section does seem to be caused by the water level gradient. During the experiment it was observed that the bypass channel developed with headward erosion. At this location a clear acceleration of the flow was observed, which was probably due to the water level difference. The final obtained planform is similar to the results of Ostanek Jurina (2017). However, the bypass channel developed from upstream for the numerical simulations while it developed with headward erosion during the experiment. The difference in erosion mechanism can be

explained by the difference in sediment mobility. The numerical simulations were based on large sand-bed braided rivers, while for the experiments gravel-bed similarity was obtained. This headward erosion was also found in other scale experiments with gravel-bed similarity (Leddy et al., 1993).

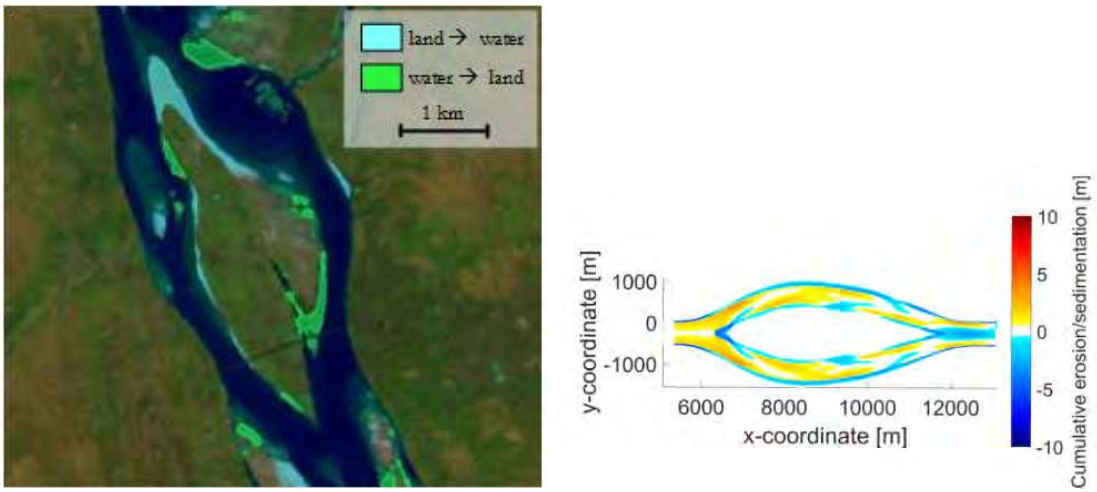

(a) Changes in one year of the Ayarwaddy River, flow from upper left corner. From AquaMonitor (Donchyts et al., 2016)

(b) Cumulative erosion and sedimentation after the wet season in the numerical simulation, from (Ostanek Jurina, 2017)

Figure 5.4: Reshaping of the planform after the wet season.

Ripples

During this discharge stage the development of bedforms was observed in the form of ripples. These ripples formed near the non-erodible banks at the beginning of the widening and further downstream in the channel with the closure measure. As mentioned in subsection 3.1.2 is the development of ripples undesirable as they provide unrealistic morphology in the small-scale experiment. In order to prevent these bedforms from developing hydraulic rough conditions are needed during the experiment. It was calculated that the particle Reynolds number at the measured locations was in the range of 32-36 for this flow stage, which should provide hydraulic rough conditions.

A possible explanation for the development of bedforms were the smooth outer banks and the velocity reduction in the closed off branch. From the equation of the particle Reynolds number, Equation 3.4, it can be seen that most of the parameters remain constant during the experiments (ρ, ν, D_{50}). A reduction in shear stress is mainly of influence for the local transition to hydraulic smooth condition. For the shear stress, $\tau = \rho \cdot g\frac{u^2}{C^2}$, the ratio of velocity and Chézy is of importance. Therefore the smooth stainless steel outer banks, which increase the Chézy value, might be an explanation for the development of bed forms. In addition, the decreased velocity of the closed off branch might be another reason for the formation of ripples.

Prevention bypass channel

The research of Ostanek Jurina (2017) concludes with recommendations on channel closure based on the pursued goals and the conditions in the particular river section, see Appendix F. The recommendations from the model study are elaborate and propose different closure measures at different locations. In addition, the construction of a long

embankment at the end of the closure measure, parallel to the island banks, was recommended in order to decrease the water level gradient around the structure. Based on this experimental study most of these recommendations cannot be verified. First of all considerably less channel closure options were considered. Further the results obtained from the high-discharge stage with this experimental setup cannot be analyzed properly. The large-scale reshaping of the island makes it very difficult to analyze channel closure measures at the begin and middle. For future research it is of importance to redesign this high discharge stage. Besides an increase in flume length, as explained in section 5.4, perhaps an increase in size of the island would limit the reshaping.

5.3 Channel closure effects on successive island

The morphodynamic effects of channel closure on the successive island have been analyzed by narrowing one of the channels in the upstream confluence. The width reductions resulted in the asymmetric distribution of the discharge over the tributaries. These width reductions were installed at the inner and outer bend of the tributary.

5.3.1 Closure measure

By narrowing one of the channels in the upstream confluence the effects of channel closure on the downstream successive island have been simulated. The width reductions of 20% and 40% for the experiments were chosen based on practical considerations. The resulting redistribution of the discharge was not necessarily representative for channel closure. At most a difference of $1/8Q$ was obtained, which is not considered as a full closure measure. Moreover, the difference between the considered cases was not significant ($1/9Q$ for 20% and $1/8Q$ for 40%). However it should be taken into account that the cross-sectional area also decreased for the overall discharge (90% against 80%). With this setup the reduction of the flow velocity in the closed branch was also not taken into account. However, the asymmetric distribution of the discharge gives an indication on how the successive planform is influenced.

5.3.2 Planform changes

During the experiments the planform changed in response to the asymmetric discharge distribution at the confluence. The results show that the planform changes were more significant for the experiments with larger discharge ratio's, so for the 40% cases. The dominant tributary from the upstream confluence could be recognized from the parallel alignment of the scour hole with this tributary. This alignment with the dominant branch was observed in three of the four experiments. For the experiment with 20% width reduction in the inner bend this planform change did not remain till the end of the experiment. Further it was observed that the location of the width reduction, the inner or outer bend, resulted in a different development of the planform. This difference in development was observed both with planform indicators and the estimate of the discharge distribution. As mentioned before were the observed differences more significant for the experiments with 40% width reduction. For the 20% cases the observed differences were

less pronounced, or even not observed.
The results of the inner bend width reduction indicate that the channel in line with the upstream closed channel became dominant. The main contribution to this unexpected development was the shift of the bifurcation towards the other channel. The reason for this shift of the bifurcation was probably the shift of the upstream confluence, which was the result of the inner bend width reduction. This shift was more significant for the 40% case. Further it was observed that the scour hole downstream of the island was also in line with the dominant channel. In addition, an elevation formed in the final section of the other channel. The estimate of the discharge distribution also shows that it is plausible that this channel became dominant.
For the experiments with outer bend width reduction the results indicate that the channel in line with upstream dominant channel became dominant. It was observed that both the upstream and downstream confluence scour holes aligned with this dominant channel. In addition, an elevation formed at the opposite channel near the bifurcation for the 40% case which directs the flow towards the dominant channel. At the final section of the same channel an elevation formed, while the final section of the island remained approximately in the middle. The estimate of the discharge distribution shows that the non-dominant channel was a fraction wider at both the bifurcation and the confluence. On the other hand the figure also shows that the dominant channel at these locations is slightly deeper. These results show the planform indicators are more convincing than the estimate of the discharge distribution for the dominance of the left channel.

5.3.3 Comparison numerical simulation

The result of the experiments can be compared with some of the qualitative aspects of the numerical simulations of Schuurman et al. (2016). The differences and similarities of the studies should be taken into account for the comparison. First of all the differences in scale: the numerical study focused on the braided network on the scale of the river reach while this experimental study focused on the downstream successive island. Moreover, the fixed banks resulted in very a different development of the system. The fixed outer banks prevented the branches from re-aligning, rotating, migrating or the merging of the bars with the outer bank. On the other hand the asymmetrical inflow and channel closure simulated in the numerical study show much similarity with this experimental study. For the comparison only the general qualitative evolution is considered.
From the numerical simulation Schuurman et al. (2016) found that a disturbance can induce far downstream effects in the braided channel network. The asymmetrical division of discharge and sediment over the bifurcation branches leads to the elongation of the bar tail limbs along the dominant branch and a change in approaching flow towards the downstream successive bifurcation. The asymmetrical reshaping of mid channel bars was found to have a crucial affect on the downstream propagation of disturbances. Figure 5.5 shows the evolution within the braided network with an asymmetrical inflow.

Some of the mechanism observed in the numerical study can be observed for the downstream successive island during the experiments. The asymmetrical inflow at the confluence resulted in the asymmetrical division of discharge at the bifurcation branches. Subsequently one of the branches became dominant. The elongation of bar tail limbs along the dominant branch was not observed during the experiments. This absence is probably due to the fixed outer banks, which prohibits the formation of bar tail limbs.

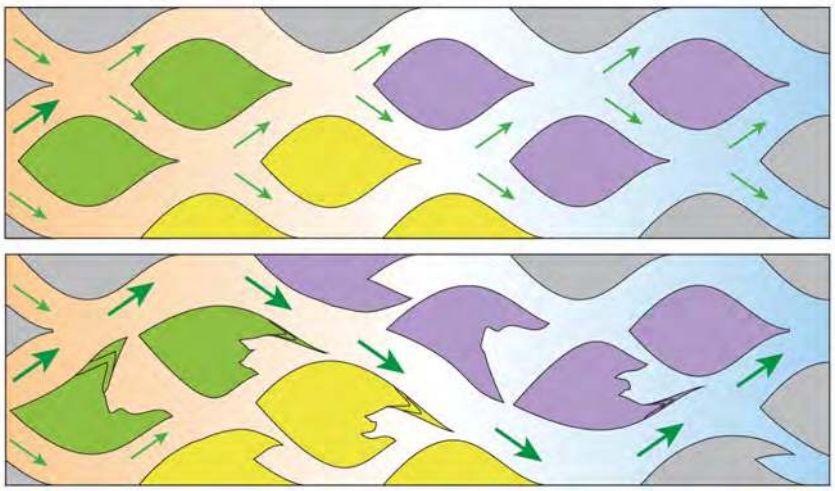

Figure 5.5: The evolution of morphological units in response to the prevailing flow, from (Schuurman and Kleinhans, 2015).

However, the asymmetrical reshaping of the island has been observed. Especially the experiment with 40% inner bend width reduction was accompanied with an asymmetrical reshaping. Here the shift of the bifurcation towards the non-dominant channel and the shift of the confluence towards the dominant channel was observed. Further it can be seen that the dominance of one of the branches influenced the downstream confluence. Here it was observed that the dominant channel was deeper while an elevation formed in the non-dominant channel. It can by hypothesized that this would influence the approaching flow towards the successive bifurcation and so influence the network. In addition, without the fixed banks the channels would be able to re-align, rotate or migrate which would have influenced the system even more.
From the numerical study it can be observed that dominant branches develop in line the dominant branches from upstream. This evolution was also observed with the outer bend width reduction, while for the inner bend width reduction the opposite was observed. The results of the inner bend width shows that the planform of the experimental setup is very sensitive to a change in the location of the upstream confluence. The location of the upstream confluence and the fixed outer banks have large effects on the development of the planform.

5.4 Limitations and improvements

For the interpretations of the findings of this experimental study the limitations of the research should be taken into account. The experimental conditions were designed such that the flow pattern and general processes of the braided rivers were reproduced. However, due to practical reasons and scale effects the experimental conditions were limited, as mentioned in subsection 3.1.2 and subsection 3.2.3. Some of these limited conditions are repeated here for comparison of the results. In the final section possible improvements of the experimental setup are discussed.

5.4.1 Limitations

- The experiments conducted had gravel-bed similarity which is not necessarily representative for braided rivers. The decrease in sediment mobility was visible in the obtained results. For the comparison with numerical studies, which simulated sand-bed braided rivers, this differene should be taken into account.
- The braided planform in the experiments only had two channels, while in natural braided rivers more channels are possible. The interaction with the rest of the river was not taken into account in the experiments. Moreover, in practice it would be possible to have an adjacent channel next to the closed off channel. This would result in additional problems for channel closure due to bypassing from two sides.
- The braided planform in the experiments did not include erodible floodplains. The fixed outer banks prevented the interaction with the adjacent banks.
- Large-scale morphodynamics of braided rivers are not included. The processes of channel shifting, re-aligning, rotating, migrating or the bar dynamics are not represented here. These processes influence the distribution at bifurcations and therefore have a significant effect on channel closure.
- The initial planform of the island was not exactly the same for the different experiments. The differences between the self-forming islands should be taken into account for the interpretation of the results.
- On the island the influence of vegetation or cohesion is not taken into account. The homogeneous topography of the island is not representative for natural rivers. These limitations influence the sediment mobility on the island surface. However, the sediment mobility is most likely more influenced by the gravel-bed similarity.

5.4.2 Improvements

In this section some possible improvements of the characteristics of the setup and the measurement techniques are discussed. In the previous sections some improvements were mentioned, which are shortly mentioned here.

Pump
The pump should be suitable for the discharge stages of the experiments. The submersible pump used in the experimental setup had a maximum discharge of 13 L/s. However, for the experiments a range of 0.7 to 2.1 L/s was needed, which is in the order of 5-15% of the maximum capacity. In practice this resulted in setting a certain minimum discharge threshold in order to reintroduce water to the flume after bed level measurements. The desired discharge was set when water was reintroduced to the flume. However, this setting of the discharge required exact timing, otherwise the high-discharge would ruin the obtained planform. This practical constrain resulted in one failed experiment and was sub-optimal for the experiments.

Length flume
The influence of the downstream boundary condition can be minimized by increasing the channel length after the widening. During the experiments the height increase of the weir at the downstream boundary condition was limited due to the constrains of the channel

length after the widening. Due to this constrain the design of the high-discharge stage was limited.

Sediment feeder
The use of an automatic sediment feeder would improve the experiments. The manual sediment input in batches has practical drawbacks and is not so accurate. A constant automatic sediment input is more realistic and results in more time during the experiment to observe and record developments.

Shape and material widening
The overall shape of the widening and material properties of the sides should be improved. Small deviations of the shape of the widening resulted in deviations in the obtained elevation. By laser cutting the shape of the widening these deviations can be minimized. In addition, the stainless steel sides gave an unrealistic smooth surface at this location. By covering the sides with sediment a more realistic roughness can be obtained.

Bed laser
The bed laser measurements can be improved by using a bed laser sheet instead of a single laser. For the bed level measurements of the widened section cross-sections were measured every 5 cm with a single laser. These measurements were used to obtain an overview of the bed level by interpolation between the cross-sections. Although these measurements give a good indications of the morphological development, the use of a bed laser sheet is more accurate and practical. First of all is the interpolation between the cross-section not necessary as the laser sheet measures over the complete longitudinal direction. Moreover, the measurements with a laser sheet can be obtained within a short time span, while with a single laser the measurements took up to 20 minutes.
An additional improvement would be the possibility to measure the bed level during the experiments, with water present in the flume.

Closure measures
The problems addressed with the closure measures have been discussed in subsection 5.2.1 and subsection 5.3.1.

6 Conclusions and recommendations

The objective of this research was to obtain a better understanding of the local morphodynamic effects of interventions aiming at channel closure in a braided river. The research questions stated in section 1.3 are repeated and answered in this chapter. Recommendations on channel closure and future research are given in the final section of this chapter.

6.1 Conclusions

How can an experiment be designed to study the local morphodynamic effects of interventions aiming at channel closure in a braided river?

In order to systematically study the local effects of channel closure a reproducible, stable and simplified section of a braided river was considered. This simplified system consisted of a channel, splitting and rejoining around an island. The planform was obtained by forming a mid-channel bar, which emerged as the discharge decreased. The bar developed with the flow stages and sediment used and a combination of non-erodible banks with a planform consisting of an upstream Y-shaped confluence followed by a widened section. Downstream of the confluence bed sheets stalled in response to the divergence of streamlines, causing a decrease in shear stress and hence in sediment transport rate. The bed load sheets merged and formed into a single elevation in the downstream section of the widening. By decreasing the discharge the mid-channel bar emerged and the island increased in size by upstream addition of sediment. During the phase with minimum discharge the finally obtained planform developed, with an island surrounded by two similarly sized channels. The formation of the elevation showed much variation for the different experiments, however the finally obtained planform is very similar. Further it was observed that the hydrodynamic forcing reshaped the planform slightly during the subsequent experimental stage. However, in general it was concluded that the final planform was reproducible and stable enough to systematically study the local effect of channel closure.

What are the morphodynamic effects of interventions aiming at channel closure on island scale, during low and high water?

During the low discharge stage the sequence of sedimentation in front of the measure, erosion around the measure and sedimentation behind the measure was observed. This sequence was also observed in numerical simulations. However, the results show that the inner and outer bend developed differently. This is probably due to the smooth fixed outer banks, where most of the flow was concentrated. For effective channel closure it is important to redistribute the discharge at the bifurcation point. By inducing sedimentation at the bifurcation of the closed branch most of the discharge is redirected towards the open branch. Therefore the closure measures at the upstream side of the island, at respectively the begin and middle, were most effective for channel closure. The channel closure measure at the final section had significantly less influence on the redistribution at the bifurcation.

The development of the island during the high discharge stage could not be used to properly analyze the effects of channel closure. During this stage the island completely reshaped and became shorter and narrower. The closure measures at the begin and middle were bypassed as a result. However, the closure measure at the final section was not influenced by the reshaping and could be analyzed. During this experiment a bypass channel was eroded with headward erosion. This erosion was caused by the water level gradient between the two channels. With numerical simulations of Ostanek Jurina (2017) the bypass channel formed with erosion from upstream as a result of the water level gradient. This difference can be attributed to the difference in sediment mobility of the two studies.

What are the morphodynamic effects of interventions aiming at channel closure on the downstream successive island?

The system obtained from the experimental setup was sensitive to the discharge distribution from upstream. An asymmetric discharge distribution resulted in an asymmetrical distribution of discharge over the bifurcation branches. This resulted in one of the channels becoming dominant and subsequent asymmetrical reshaping of the island. It can be hypothesized that the flow for the successive bifurcation would change as well and so would influence the braided network far downstream. This sequence of morphodynamic changes on the successive island corresponds with the numerical simulation of Schuurman et al. (2016). The formation of bar-tail limbs was not observed, which is probably due to the fixed outer banks.
During the experiments two different reshaping mechanisms were observed, which differently influenced the distribution at the bifurcation. The first reshaping mechanism was the shift of the front due to the shift of the upstream confluence. The reshaping in line with the upstream dominant channel is the second reshaping mechanism. This second mechanism is also observed in numerical studies. The sensitivity to perturbations in the upstream confluence is likely due to the experimental setup, which prohibits the migration, rotation and reshaping of channels.

6.2 Recommendations

The recommendations of this study are split into recommendations on channel closure and recommendations for further research.

Channel closure
For effective channel closure during the dry season a closure measure should be placed at the upstream side of the island, at respectively the begin and middle. By installing a closure measure here the sedimentation in front of the measure influences the discharge distribution at the bifurcation the most. These results agree with the more elaborate recommendations and guidelines of Ostanek Jurina (2017), see Appendix F.
Furthermore the effects of channel closure on the braided network should be taken into account. The experimental study shows that adjusting the discharge distribution has large local effects on the successive downstream planform. It can be hypothesized that the flow for the successive bifurcation is changed and so influences the braided network far downstream , similar to the results of Schuurman et al. (2016). Channel closure projects should consider the possible large effect on the braided network.

Future research

- *Experimental setup*
  Several characteristics of the setup and measurement techniques should be adjusted or improved for future research, as discussed in subsection 5.4.2. For the setup a suitable discharge pump and an automatic sediment feeder should be considered to improve the experiments. Furthermore it is recommended to improve the overall shape of the widening and the material properties of the stainless steel sides. The measurements of the bed level can be improved by using a bed laser sheet which is capable of measuring with water in the flume. Finally the channel length behind the widened reach should be increased in order to minimize the influence of the downstream boundary condition.

- *Closure measures*
  In this experimental study a weir consisting out toothpicks was used as closure measure. It is recommended to use a constant width for the closure measures. In addition, an alternative method for the installment of the weir is recommended. Finally it should be considered to test other types of closure measures, such as porcupines and jack jetties, in their ability to close off channels.

- *Large-scale experiments*
  The laboratory experiments in this study were conducted with a widened planform with a length of 3.3 m, resulting in an island of approximately 2.2 m long. This small-scale model simulated gravel-bed similarity. For future research it would be interesting to increase the scale of the experiments and eventually perform a full-scale pilot test. With an increase in scale it would be possible to simulate sand-bed rivers. The work of Parker (2004) can be used in order to design such an experiment with the correct scaling. With several dimensionless parameters the bankfull characteristics of natural sand-bed rivers can be simulated in a scale model. By increasing the scale of the experiments it is likely that the system will be less sensitive to small perturbations. The observed large-scale reshaping of the island during

the high-discharge stage might be acceptable with an increase in scale. Another advantage is the increase in water depth of the experiments. Hydrodynamic and morphological processes in the vertical, such as secondary flow, are represented more accurately with water depths close to nature. The average water depth was in the order of 1 to 3 cm, whereas water depths in rivers are in the order of metres.
With increasing the scale of the experiments it should be taken into account that the accompanied timescales become longer and costs become higher. Therefore it is important to obtain sufficient knowledge of the processes with small-scale experiments and numerical models, which require less time and money. Before conducting a full-scale pilot project it is important to obtain more information on the long-term and network effects of channel closure.

- *Stability of self-forming island*
  In order to create a more stable planform after the formation of the island two recommendations are considered. First of all the sediment input can be compared with the sediment output, in order to verify if an equilibrium situation is obtained. Secondly, the time of the final phase of the island formation stage can be extended. During the low-discharge stage some reshaping of the planform was observed. By extending the island formation stage this reshaping is prevented during the subsequent stages.

- *High-discharge stage*
  A new method should be designed to simulate the high discharge stage. The large-scale reshaping of the island during this phase makes it impossible to analyze the closure measures. Possible design considerations that can be taken into account are: to minimize the influence of the downstream boundary condition or to increase the scale of the experiment.

- *Numerical research*
  The planform used during the experiments, with an upstream confluence followed by a widening with fixed banks, should be tested with a numerical model. First of all it could be tested whether a self-forming island can be obtained by using similar flow conditions. Furthermore the sensitivity to upstream perturbations, such as tributary asymmetry or angle, could be tested more elaborately.

References

Ashmore, P. and Parker, G. (1983). Confluence scour in coarse braided streams. *Water Resources Research, Vol. 19, No. 2, Pages 392-402, 1983.*

Ashmore, P. E. (1982). Laboratory modelling of gravel braided stream morphology. *Earth Surface Processes and Landforms, Volume 7, Issue 3, May/June 1982,Pages 201–225.*

Ashmore, P. E. (1991). How do gravel-bed rivers braid. *Canadian Journal of Earth Sciences 28:326-341.*

Ashmore, P. E. (1993). Anabranch confluence kinetics and sedimentation processes in gravel-braided streams. *Bristow and Best (1993), pages 129-146.*

Ashmore, P. E., Ferguson, R. I., Prestegaard, K. L., Ashworth, P. J., and Paola, C. (1992). Secondary flow in anabranch confluences of a braided, gravel-bed stream. *Earth Surface Processes and Landforms 17:299-311.*

Ashworth, P. J. (1996). Mid-channel bar growth and its relationship to local flow strength and direction. *Earth Surface Processes and Landforms, Vol 21, 103-123.*

Ashworth, P. J., Best, J. L., Roden, J. E., Bristow, C. S., and J., K. G. (2000). Morphological evolution and dynamics of a large sand braid-bar, Jamuna River, Bangladesh. *Sedimentology 47: 533–555.*

Ashworth, P. J., Ferguson, R. I., and Powell, D. M. (1992). Bedload transport and sorting in braided channels. *Dynamics of Gravel-Bed Rivers, John Wiley, Chichester etc.*

Ashworth, P. J., Sambook Smith, G. H., Best, J., Bridge, J. S., Lane, S. N., Lunt, I. A., Reesink, A. J. H., Simpson, C., and Thomas, R. E. (2011). Evolution and sedimentology of a channel fill in the sandy braided South Saskatchewan River and its comparison to the deposits of an adjacent compound. *Sedimentology 58: 1860–1883.*

Baki, A. B. M. and Gan, T. Y. (2012). Riverbank migration and island dynamics of the braided Jamuna River of the Ganges-Brahmaputra basin using multi-temporal landsat images. *Quaternary International, Volume 263, pp. 148-161.*

Bertoldi, W., Zanoni, L., , Miori, S., Repetto, R., and Tubino, M. (2009). Interaction between migrating bars and bifurcations in gravel bed rivers. *Water Resources Research, volume 45.*

Best, J. L. (1987). Flow dynamics at river channel confluences: Implications for sediment transport and bed morphology. *The Society of Economic Paleontologists and Mineralogists, 1987.*

Best, J. L. (1988). Sediment transport and bed morphology at river channel confluences. *Sedimentology 35:481-498.*

Best, J. L., Ashworth, P. J., Bristow, C. S., and Roden, J. E. (2003). Three-dimensional sedimentary architecture of a large, mid-channel sand braid bar, Jamuna River, Bangladesh. *Journal of Sedimentary Research 73, 516–530.*

Bolla Pittaluga, M., Repetto, R., and Tubino, M. (2003). Channel bifurcation in braided rivers: equilibrium configurations and stability. *Water Resources Research 39(3): 1046.*

Bresse, J. (1860). Cours de mécanique appliquée professé à l'ecole des ponts et chaussées. *Mallet-Bachelier, Paris, France (in French).*

Brice, J. E. (1964). Channel patterns and terraces of the loup rivers in Nebraska. *United States Geological Survey Professional Papers, 422'D.*

Bridge, J. (1993). The interaction between channel geometry, water flow, sediment transport and deposition in braided rivers. *Braided Rivers (Eds J.B. Best and C.S. Bristow), pp. 13–71. Special Publication 75, Geological Society Publishing House, Bat.*

Bristow, C. S. (1987). Brahmaputra River: Channel migration and deposition. *Ethridge, F. G., Flores, R. M. and Harvey, M. D. (eds.) Recent Developments in Fluvial Sedimentology.*

Bristow, C. S. and Best, J. (1993). Braided rivers: perspectives and problems. *Geological Society, London, Special Publications, 75, 1-11, 1 January 1993.*

Burge, L. M. (2006). Stability, morphology and surface grain size patterns of channel bifurcation in gravel-cobble bedded anabranching rivers. *Earth Surf. Processes Landforms, 31, 1211–1226.*

Chabert, J., Remillieux, M., and Spitz, I. (1961). Application de la circulation transversal a la correction des rivieres et a la protection des prises d'eau [in french]. *Ninth Convention (pp. 1216–1223). Dubrovnik: IAHR.*

Church, M. (1972). Baffin Island Sandurs: A study of Arctic fluvial processes. *Baffin Island Sandurs: A study of Arctic fluvial Processes. Geological Survey of Canada Bulletin 216.*

de Vries, M. (1973). On measuring discharge and sediment transport in rivers. *Publication no. 106, Delft Hydraulics Laboratory.*

Directorate of Water Resources and Improvement of River Systems (2016). Ayeyarwady integrated river basin management project: Environmental and social management plan - final. Technical report, Directorate of Water Resources and Improvement of River Systems, Myanmar.

Donchyts, G., Baart, F., Winsemius, H., Gorelick, N., Kwadijk, J., and van de Giesen, N. (2016). Earth's surface water change over the past 30 years. *Nature Climate Change, Volume 6, pp. 810-813.*

Douma, D. and Mosselman, E. (2005). Field application of bottom vanes in the Elanjani River, Tangail, Bangladesh. *NCR-days 2005, Research on river dynamics from geological to operational time scales.*

Duró, G., Crosato, A., and Tassi, P. (2015). Numerical study on river bar response to spatial variations of channel width. *Advances in Water Resources, doi: 10.1016/j.advwatres.2015.10.003.*

Egozi, R. and Ashmore, P. (2008). Defining and measuring braiding intensity. *Earth Surf. Process. Landforms 33, 2121–2138.*

Engelund, F. and Skovaard, O. (1973). On the origen of meandering and braiding in alluvial streams. *Teksnisk Forlag, Copenhagen.*

Ferguson, R. (1987). Hydraulic and sedimentary controls of channel pattern. *Richards, K., editor, River channels: environment and process, Institute of British Geographers Special Publication 18, Oxford: Blackwell, 129–58.*

Flood Management Organisation (2012). Handbook for flood protection, anti-erosion and river training works. Technical report, Government of India, New Delhi, India.

Hooning, E. (2011). Flooding and sediment management on the Koshi alluvial fan, Nepal. Master's thesis, Delft University of Technology.

Hoque, M. M., Rahman, M. R., Hoque, M. A., Rahman, M. M., H. M. A., Sarker, M. H., Hossain, M., and Uddin, M. N. (2008). Field based applied research for the stabilization of major rivers in Bangladesh. *Technical Report 1(R05/2008), June-2008, IWFM, BUET.*

Jagers, H. R. A. (2003). *Modelling Planform Changes of Braided Rivers.* PhD thesis, University of Twente.

Jha, M. M. (2014). Permeable structures for river training works. *Department of Water Induced Disaster Prevention, Bulletin. July 2014, Series XV.*

Karmaker, T. and Dutta, S. (2016). Prediction of short-term morphological change in large braided river using 2D numerical model. *Hydraulic Engineering, 2016, 142(10): 04016039.*

Klaassen, G. J., Douben, K. J., and van der Wal, M. (2002). Novel approaches in river engineering, river flow 2002. *Bousmar and Zech (eds.), ISBN 90 5809 5096, pp. 27-43.*

Klaassen, G. J. and Masselink, G. (1992). Planform changes of a braided river with fine sand as bed and bank material. *Karlsruhe, World Association for Sedimentation and Erosion Research.*

Kleinhans, M. G., Ferguson, R., Lane, S. N., and Hardy, R. (2013). Splitting rivers at their seams: bifurcations and avulsion. *Earth Surface Processes and Landforms, 38,47-61.*

Kleinhans, M. G., van Dijk, W. M., van de Lageweg, W. I., Hoendervoogt, R.and Markies, H., and Schuurman, F. (2010). From nature to lab: scaling self-formed meandering and braided rivers. *River Flow 2010 - Dittrich, Koll, Aberle & Geisenhainer (eds) - 2010 Bundesanstalt für Wasserbau ISBN 978-3-939230-00-7.*

Koomen, E. (1992). Remote sensing study of morphological processes in the Jamuna River, Bangladesh. Master's thesis, Delft University of Technology.

Leddy, J. O., Ashworth, P. J., and Best, J. L. (1993). Mechanisms of anabranch avulsion within gravel-bed braided rivers: observations from a scaled physical model. *In: J. L. Best & C. S. Bristow, eds. Braided Rivers. London: Geological Society, pp. 119-127.*

Leopold, L. B. and Wolman, M. G. (1957). River channel patterns: braided, meandering and straight. *Physical and Hydraulic Studies of Rivers 14: 283–300.*

Meyer-Peter, E. and Muller, R. (1948). Formulas for bed load transport. *paper presented at 2nd Meeting, Int. Assoc. for Hydroaul. Environ. Eng. and Res., Madrid.*

Mosley, M. P. (1976). An experimental study of channel confluences. *Journal of Geology 84:535-562.*

Mosselman, E. (2001). Morphological development of side channels. *CFR project report 9, IRMA-SPONGE and Delft Cluster.*

Mosselman, E. (2006). Bank protection and river training along the braided Brahmaputra–Jamuna River, Bangladesh. *Delft University of Technology and WL/Delft Hydraulics.*

Mosselman, E. and Sloff, K. (2002). Effect of local scour holes on macroscale river morphology. *Proc. River Flow 2002 Vol 2, pages 767-772.*

Nakagawa, H., Zhang, H., Baba, Y., Kawaike, K., and Teraguchi, H. (2013). Hydraulic characteristics of typical bank-protection works along the Brahmaputra/Jamuna river, Bangladesh. *Journal of Flood Risk Management, Volume 6, pp. 345-359.*

Nayak, A., Sharma, N., Mazurek, K. A., , and Kumar, A. (2016). Design development and field application of RCC jack jetty and trail dykes for river training. *River system analysis and management.*

Northwest Hydraulic Consultants & Mott MacDonald (2014). Flood and riverbank erosion risk management investment program – Project 1. Technical report, Institutional Strengthening and Project Management Consulting Services, Bangladesh.

Odgaard, A. J. (2009). *River training and sediment management with submerged vanes.* American Society of Civil Engineers.

Odgaard, A. J. (2015). River channel stabilization with submerged vanes. *Advances in Water Resources Engineering Volume 14 of the series Handbook of Environmental Engineering pp 107-136.*

Odgaard, A. J. and Kennedy, J. F. (1983). River-bend bank protection by submerged vanes. *Journal of Hydraulic Engineering, Vol. 109, pages 1161-1173.*

Odgaard, A. J. and Spoljaric, A. (1986). Sediment control by submerged vanes. *Journal of Hydraulic Engineering, Vol 112, pages 1164-1180.*

Ostanek Jurina, T. (2017). Channel closure in large sand-bed braided rivers. Master's thesis, Delft University of Technology.

Parker, G. (2004). 1D sediment transport morphodynamics with applications to rivers and turbidity currents, Ch. 3 bankfull characteristics of rivers. *retrieved from http://hydrolab.illinois.edu/people/parkerg/powerpoint*$_{l}$*ectures.htm.*

Rahman, M., Nakagawa, H., Khaleduzzaman, A. T. M., and Ishigaki, T. (2003). Channel stabilization using bandalling. *Annuals of Disas. Prev. Res. Inst., Kyoto Univ., No. 46 B,*.

Repetto, R., Tubino, M., and Paola, C. (2002). Planimetric instability of channels with variable width. *Journal of Fluid Mechanics, 457, pp. 79–109.*

Richardson, W. R. R. and Thorne, C. R. (1998). Secondary currents around braid bar in Brahmaputra River, Bangladesh. *Journal of Hydraulic Engineering 124(3):325-328.*

Richardson, W. R. R., Thorne, C. R., and Mahmood, S. (1996). Secondary flow and channel changes around a bar in the Brahmaputra River, Bangladesh. *Coherent Flow Structures in Open Channels, John Wiley & Sons Ltd.*

Sarker, M. H., Thorne, C. R., Aktar, M. N., and Ferdous, M. R. (2014). Morphodynamics of the Brahmaputra-Jamuna River, Bangledesh. *Geomorphology, Volume 215, pp. 45-59.*

Schmuck-Widmann, H. (2001). *Facing the Jamuna River: Indigenous and Engineering Knowledge in Bangladesh.* Bangladesh Resource Centre for Indigenous Knowledge.

Schuurman, F. and Kleinhans, M. G. (2015). Bar dynamics and bifurcation evolution in a modelled braided sand-bed river. *Earth Surface Processes and Landforms 40: 1318–1333.*

Schuurman, F., Kleinhans, M. G., and Middelkoop, H. (2016). Network response to disturbances in large sand-bed braided rivers. *Earth Surface Dynamics, 4, 25-45.*

Schuurman, F., Marra, W. A., and Kleinhans, M. G. (2013). Physics-based modeling of large braided sand-bed rivers: Bar pattern formation, dynamics, and sensitivity. *Journal of Geophysical Research: Earth Surface, Volume 118, pp. 2509-2527.*

Seminara, G. and Tubino, M. (1989). Alternate bars and meanders: free, forced and mixed interactions. *River meandering, edited by Syunsuke Ikeda and Gary Parker. AGU, Washington, DC, chapter 10, pages 267–320.*

Uddin, M. N. (2010). *Flow and Erosion Processes at Bends and Around River Training Works in a Sand Bed Braided River.* PhD thesis, Bangladesh University of Engineering and Technology.

van der Velden, J. (2015). Understanding river dynamics of the Ayeyarwady River; how dynamic behaviour contributes to adapting the river morphology for navigational purposes. Master's thesis, Utrecht University.

Vandenberghe, J. (1995). Timescales, climate and river development. *Quaternary Science Reviews 14, 631–38.*

Vargas Luna, A. (2016). *Role of Vegetation on River Bank Accretion.* PhD thesis, Delft University of Technology.

Wang, Z., Fokkink, R., de Vries, M., and Langerak, A. (1995). Stability of river bifurcations in 1D morphodynamic models. *Journal of Hydraulic Research 33(6): 739–750.*

Whipple, K. (2004). Surface processes and landscape evolution. *MIT Open Course Ware, Ch. 1 Flow Mechanics, retrieved from: https://ocw.mit.edu/courses/earth-atmospheric-and-planetary-sciences/12-163-surface-processes-and-landscape-evolution-fall-2004/lecture-notes/.*

Wu, F. and Yeh, T. (2005). Forced bars induced by variations of channel width: Implications for incipient bifurcation. *Journal of Geophysical Research, VOL. 110.*

Wyrick, J. R. (2005). *On the formation of fluvial islands.* PhD thesis, Oregon State University.

Yalin, M. S. (1992). River mechanics. *Pergamon Press, Oxford.*

Yu, T., Wang, P., and Zheng, J. (2011). Study on the beach protection with the tetrahedron like penetrating frame groups. *Applied Mechanics and Materials, 90-93, 2533–2536.*

Zolezzi, G., Bertoldi, W., and Tubino, M. (2006). Morphological analysis and prediction of river bifurcations. *Braided Rivers: Process, Deposition, Ecology and Management, Smith GHS, Best JL, Bristow CS, Petts GE (eds), Blackwell: Oxford; 177–197.*

A Details experimental setup

In this Appendix the details of the experimental setup are discussed. In addition photo's of the different sections of the setup are shown.

Flume sections
A submersible pump was located in the downstream water basin, see Figure A.1a. Water was pumped in a system of pipes to the upstream stilling basin, see Figure A.1b. The amount of discharge pumped was controlled with a frequency controller, see Figure A.1c. The downstream water basin had an external constant supply of water from a tap, see Figure A.1d. An overflow pipe of the water basin prevented the basin from overflowing.

(a) The downstream basin

(b) The upstream basin

(c) The frequency controller

(d) Tap for external water supply

Figure A.1: Sections at the upstream side of the flume.

An upstream and downstream weir were installed as boundary conditions for the water level. The upstream weir was installed just after the stilling basin, see Figure A.2a. Additional weirs were installed at the point where the flow divided over the two tributaries of the confluence. The downstream weir was installed at the final section of the flume. During the high flow stage this weir was increased in height, which can be seen with the lighter piece of wood in Figure A.2b.

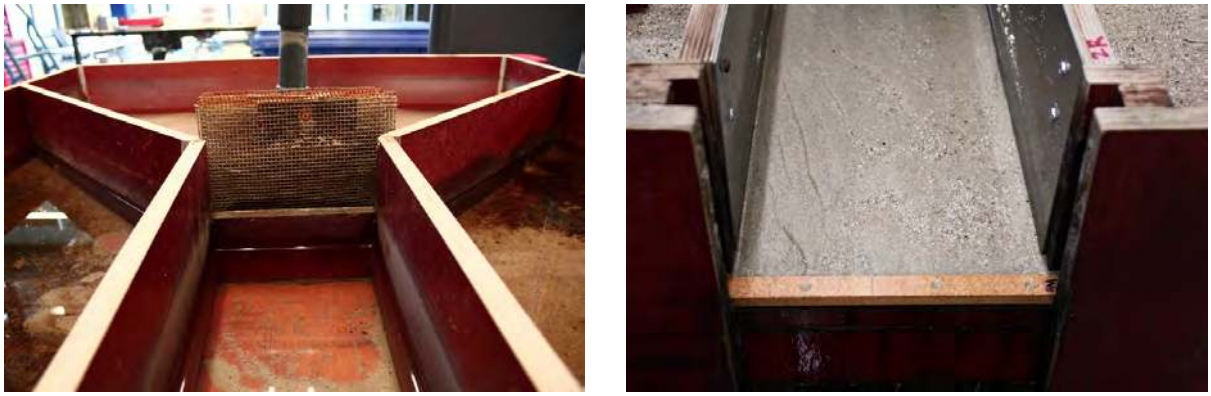

(a) Upstream installed weir (b) Downstream installed weir

Figure A.2: Installed weirs along the flume

Digital camera

A digital camera was installed approximately 6 m above the flume, on a movable crane. The camera was installed on a wooden frame and aligned with a bottom hatch on the crane, see Figure A.3.

Figure A.3: The camera was installed on a frame on the crane.

Laser platform
On the laser platform two lasers were installed which were both connected with a rotating wheel. The first laser was installed in the middle of the platform, which measured in the longitudinal direction, see Figure A.4a. The second laser was installed on a second rail system in the lateral direction, see Figure A.4b.

(a) Laser for the longitudinal direction

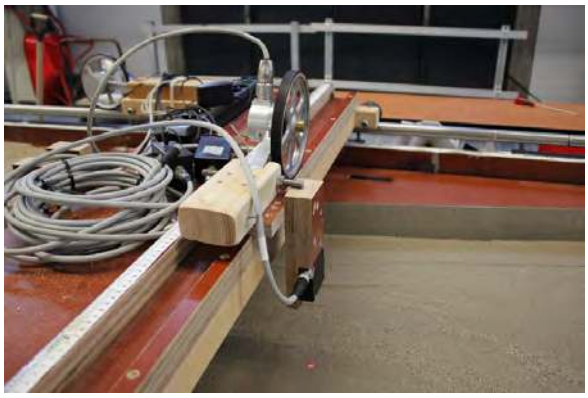

(b) Laser for the lateral direction

Figure A.4: The platform to measure the bed level.

Discharge measurements
The discharge was measured with a ultrasonic flow meter from Prosonic. The measuring system consisted out of one transmitter and two sensors. The two sensors were clamped outside the pipe between the pump and the upstream basin, see Figure A.5a. With this measurement method, acoustic (ultrasonic) signals were transmitted between two sensors. The transmitter received these signals and converted these in discharge measurements, see Figure A.5b.

(a) Two sensors connected to pipe

(b) Prosonic transmitter

Figure A.5: Measurement equipment for the discharge.

Upstream confluence and downstream channel
The upstream confluence was constructed with two tributaries of 10 cm wide, joining with an angle of 90°. The channels were 70 cm long and constructed from wood, see Figure A.6a. Downstream of the widened section a straight channel of 130 cm long and 20 cm width was constructed, see Figure A.6b. This was constructed with rigid stainless steel (1.5 mm thick) outer banks.

(a) Upstream confluence (b) Downstream straight channel

Figure A.6: The sections upstream and downstream of the widened section.

Widened section
The widened section had a total length of 330 cm and was constructed with fixed outer banks. The shape of the fixed outer banks was provided by stainless steel strips connected to wooden molds, see Figure A.7. The stainless steel strips of 1.0 mm thick were flexible and could be adjusted to the shape. The strips were 10 cm high and were placed into the bed. The wooden molds were 250 cm long and placed in the middle of the widened section. By doing so 40 cm of the fixed banks on both sides of the widening was not supported by the wooden molds. The exact shape of the widening can be reproduced with the help of Figure A.8 and Table A.1. In Figure A.8 one half of the widened section is shown, with the positive values of the y-axis. In this figure the upstream confluence is on the left of the figure, so flow is from left to right. The beginning and end of the widened section is straight with a curved shape in the middle. The coordinates of the points A till G are shown in Table A.1. The shape of the outer banks was streamlined along the mentioned coordinates.

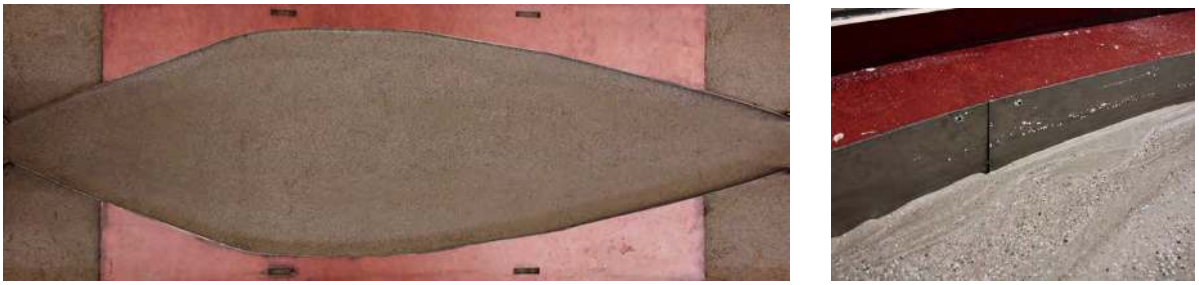

Figure A.7: The widened section with the wooden molds and stainless steel outer banks.

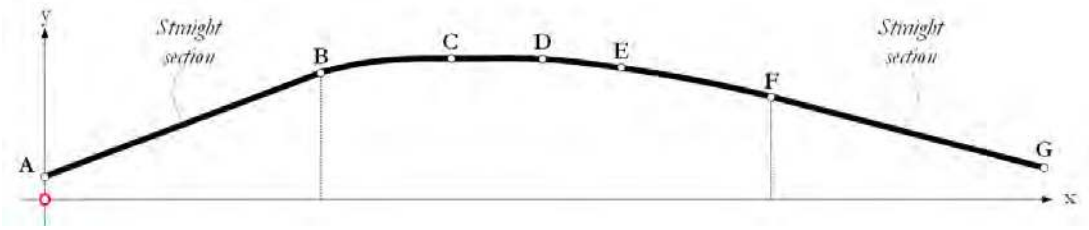

Figure A.8: Shape of the widened section with the coordinate system used in the graphs in the main report, with the x-direction the longitudinal direction.

	x-coordinate [cm]	**y-coordinate** [cm]
A	0	7.5
B	90	42.5
C	140	47.5
D	165	47.5
E	190	42.5
F	240	34
G	330	10

Table A.1: Coordinates of the points shown in Figure A.8.

B Photo's experiments

In this Appendix additional photo's of the experiments are shown. The photo's indicate the evolution of the bed at distinctive moments during the experiments. Besides the photo's of the main experiments, photo's of a preliminary experiments are shown in Figure B.1. The photo's of the main experiment are ordered similar as the results in the main report, with experiment: Str, Con, Ref, W1, W2, W3, I20, I40, O20 and O40.

B.1 Channel within widening

Preliminary experiment in order to determine whether an initial flat bed in the widening gave the same results as an initial channel within the widening.

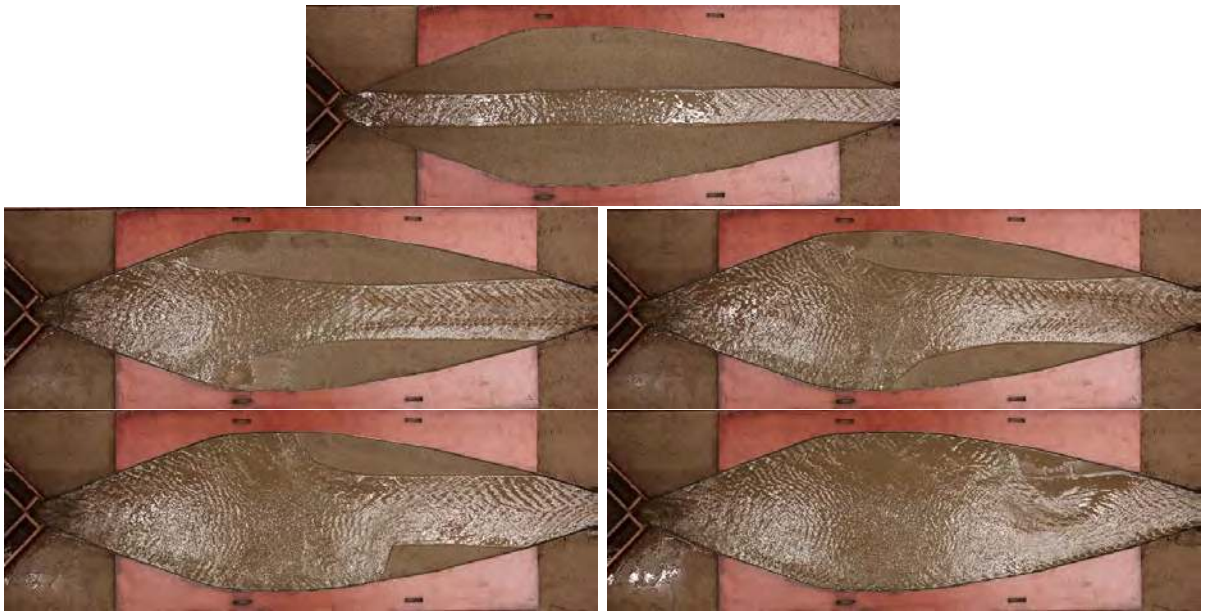

Figure B.1: Photo's taken at distinctive moments during the experiment. Starting up top: Begin 20 cm wide at t=0, at t=30 min, at t=60 min, at t=90 min, at t=120 min.

B.2 Straight channel (Str)

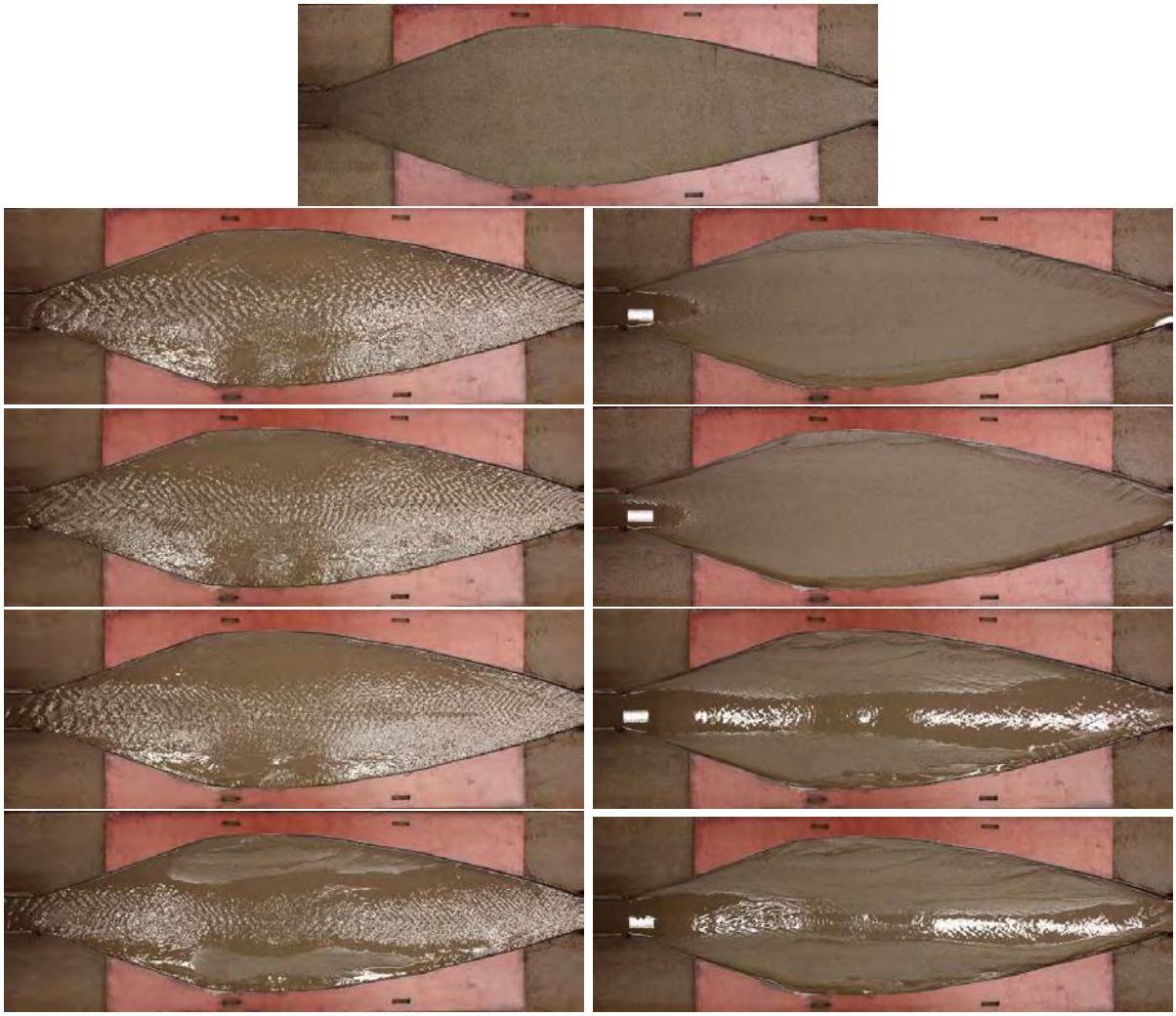

Figure B.2: Photo's taken at distinctive moments during the experiment.
Starting up top: Begin empty, Phase 1 flow, after Phase 1, Phase 2 flow, after Phase 2, Phase 3 flow, after Phase 3, Phase 4 flow, after Phase 4.

B.3 Y-shaped confluence (Con)

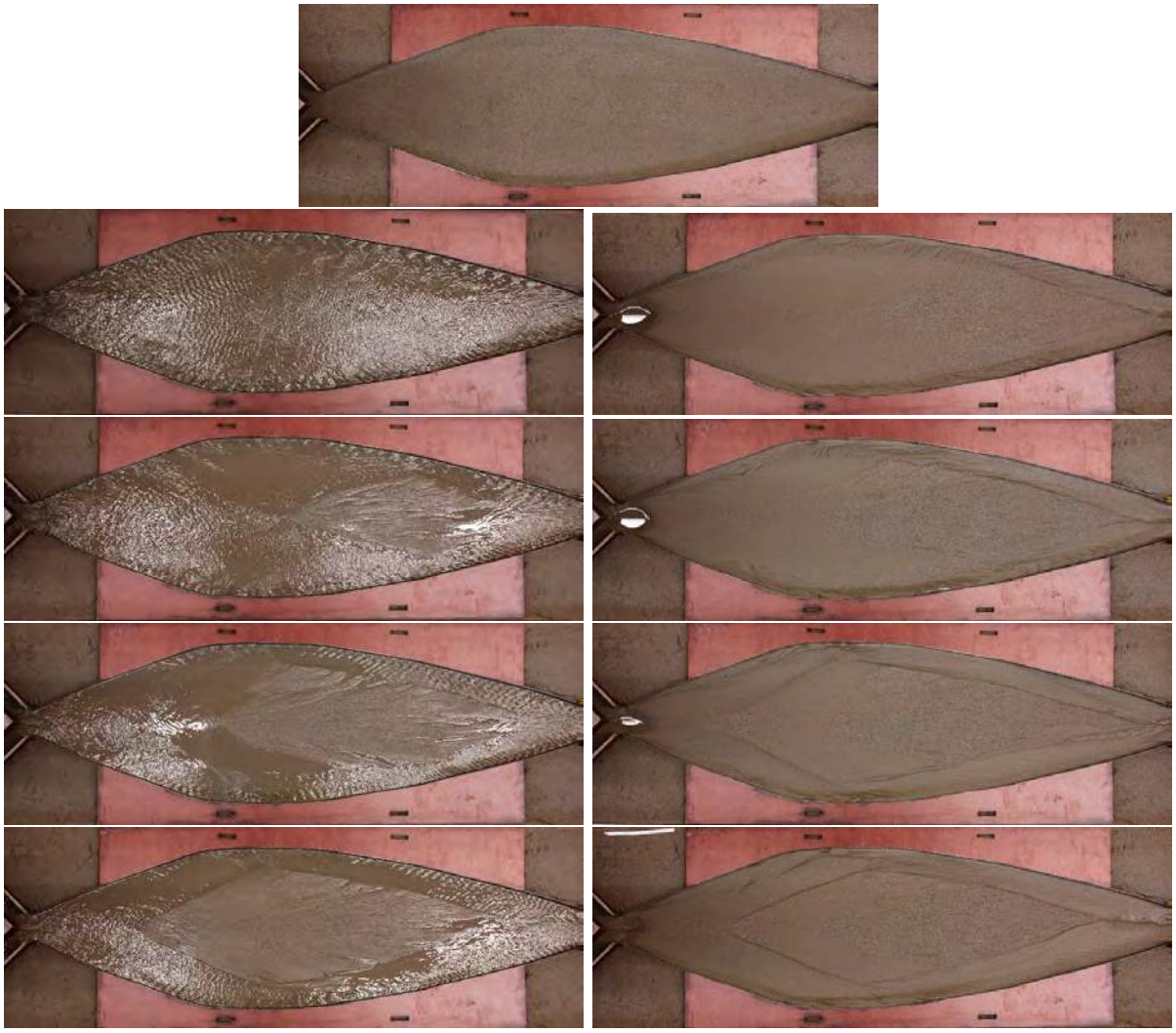

Figure B.3: Photo's taken at distinctive moments during the experiment.
Starting up top: Begin empty, Phase 1 flow, after Phase 1, Phase 2 flow, after Phase 2, Phase 3 flow, after Phase 3, Phase 4 flow, after Phase 4.

B.4 Reference (Ref)

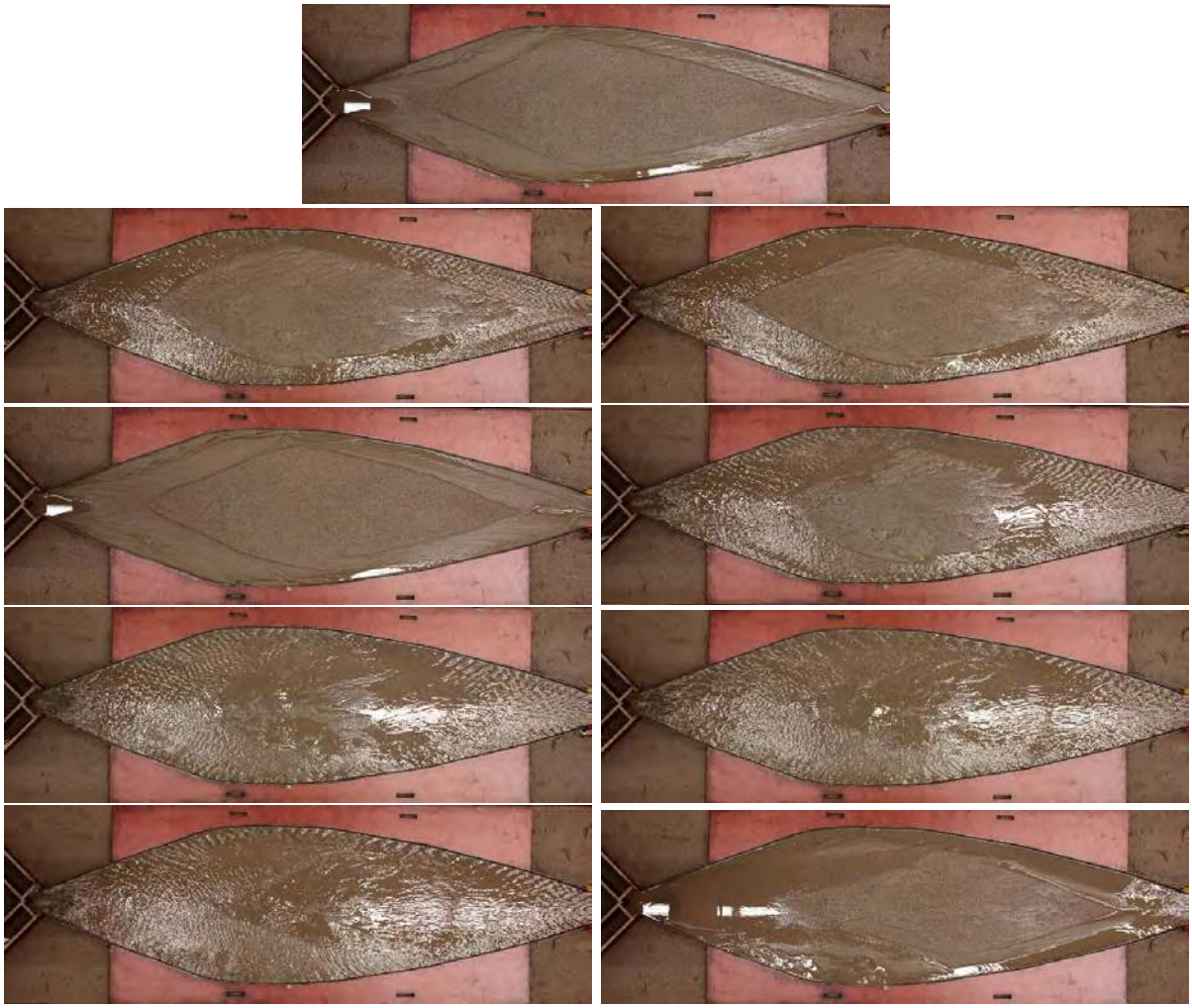

Figure B.4: Photo's taken at distinctive moments during the experiment.
Starting up top: formation island.
The low flow stage at t=15 min, at t=75 min, at t=75 min empty.
The high flow stage at t=15 min, at t=30, at t=60, at t=90, at t=90 empty.

B.5 Weir begin (W1)

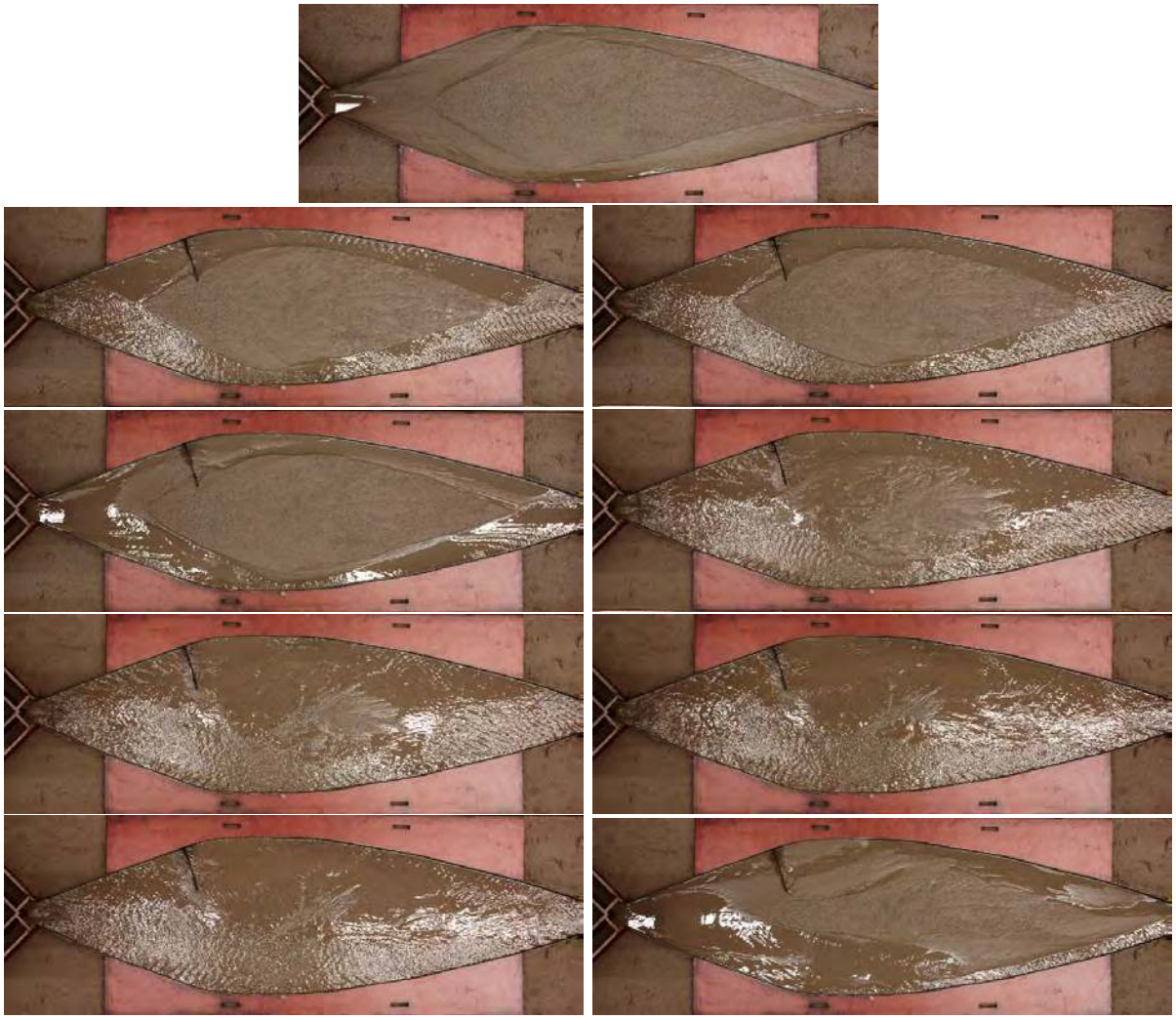

Figure B.5: Photo's taken at distinctive moments during the experiment.
Starting up top: formation island.
The low flow stage at t=15 min, at t=75 min, at t=75 min empty.
The high flow stage at t=15 min, at t=30, at t=60, at t=90, at t=90 empty.

B.6 Weir middle (W2)

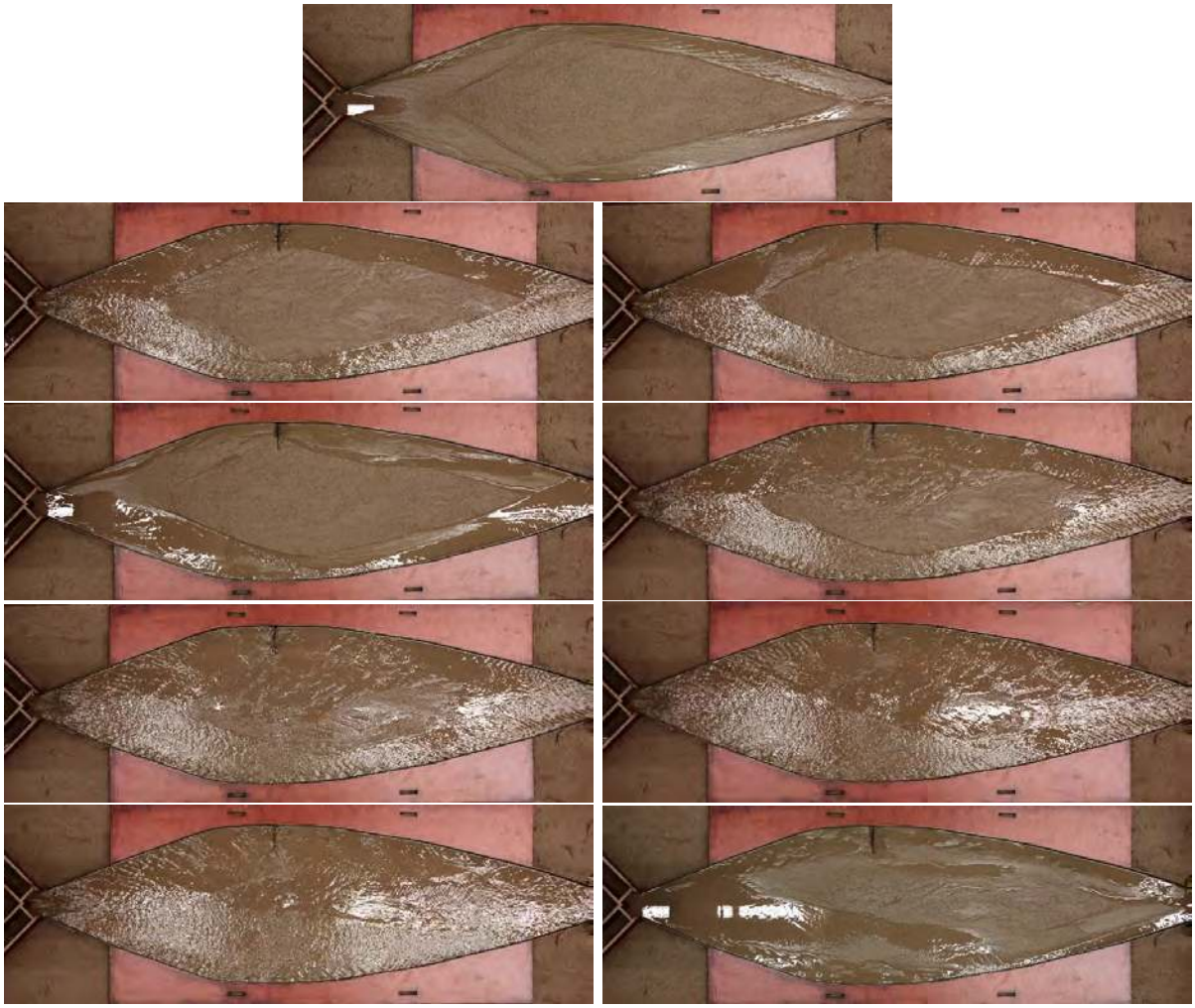

Figure B.6: Photo's taken at distinctive moments during the experiment.
Starting up top: formation island.
The low flow stage at t=15 min, at t=75 min, at t=75 min empty.
The high flow stage at t=15 min, at t=30, at t=60, at t=90, at t=90 empty.

B.7 Weir end (W3)

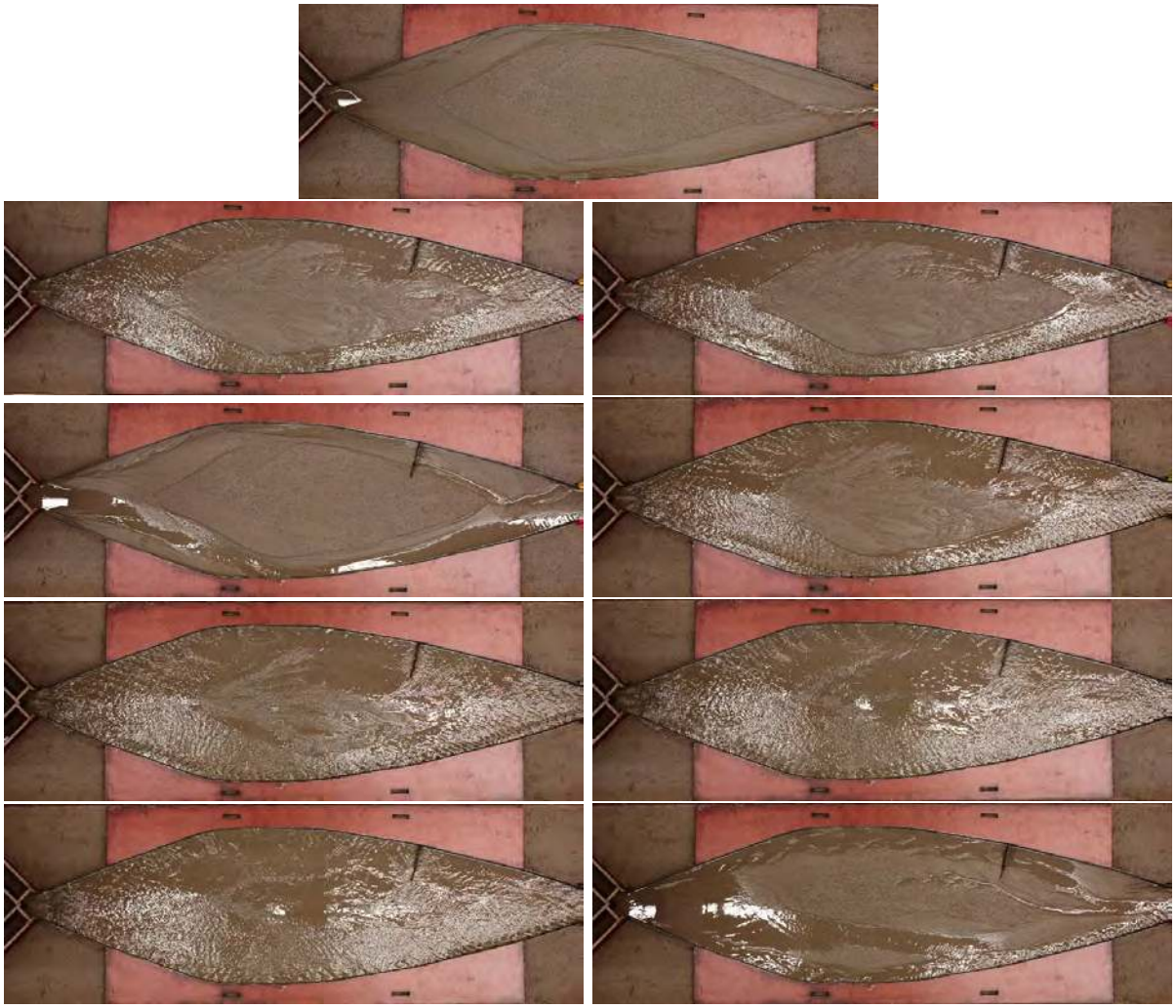

Figure B.7: Photo's taken at distinctive moments during the experiment.
Starting up top: formation island.
The low flow stage at t=15 min, at t=75 min, at t=75 min empty.
The high flow stage at t=15 min, at t=30, at t=60, at t=90, at t=90 empty.

B.8 Inner bend 20% (I20)

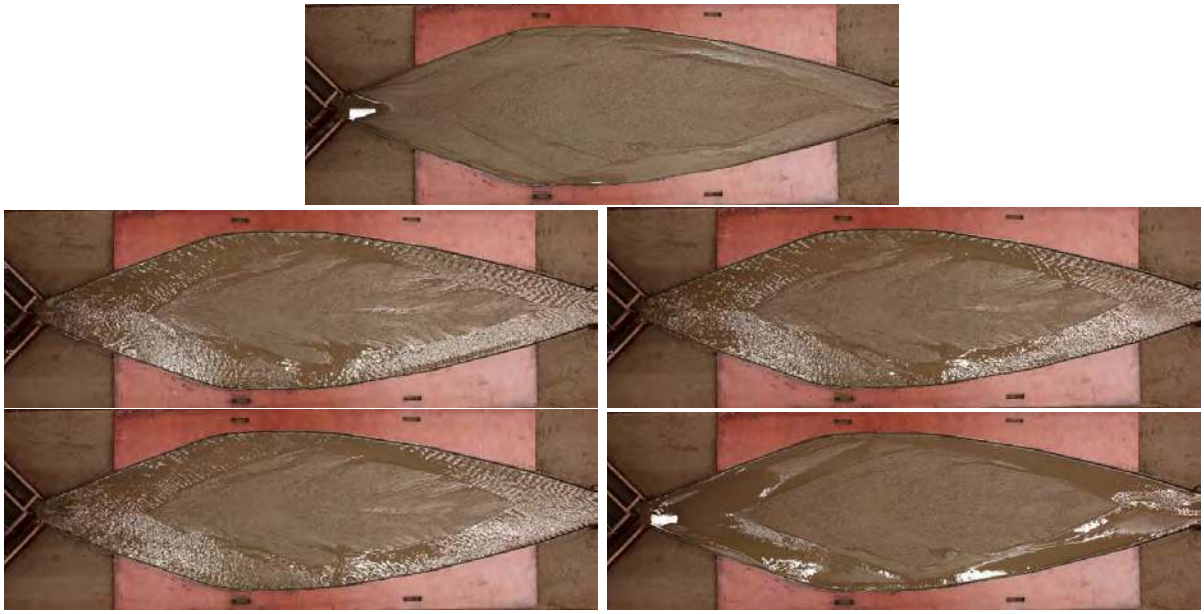

Figure B.8: Photo's taken at distinctive moments during the experiment.
Starting up top: formation island.
The low flow stage at t=15 min, at t=45 min, at t=75 min, at t=75 min empty.

B.9 Inner bend 40% (I40)

Figure B.9: Photo's taken at distinctive moments during the experiment.
Starting up top: formation island.
The low flow stage at t=15 min, at t=45 min, at t=75 min, at t=75 min empty.

B.10 Outer bend 20% (O20)

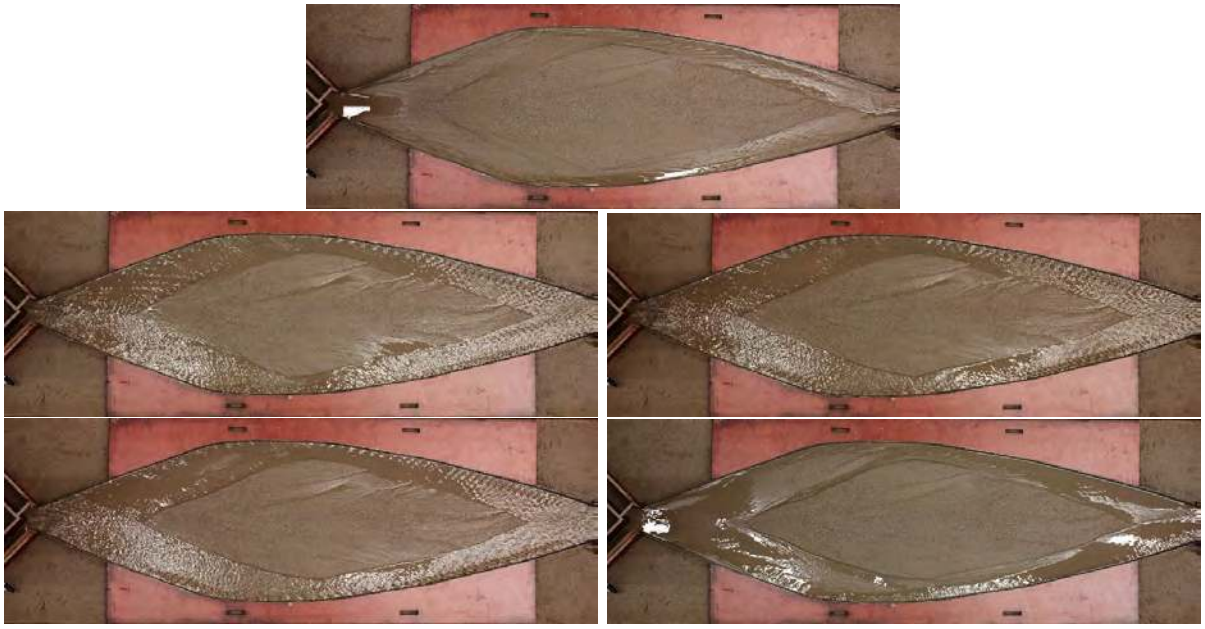

Figure B.10: Photo's taken at distinctive moments during the experiment.
Starting up top: formation island.
The low flow stage at t=15 min, at t=45 min, at t=75 min, at t=75 min empty.

B.11 Outer bend 40% (O40)

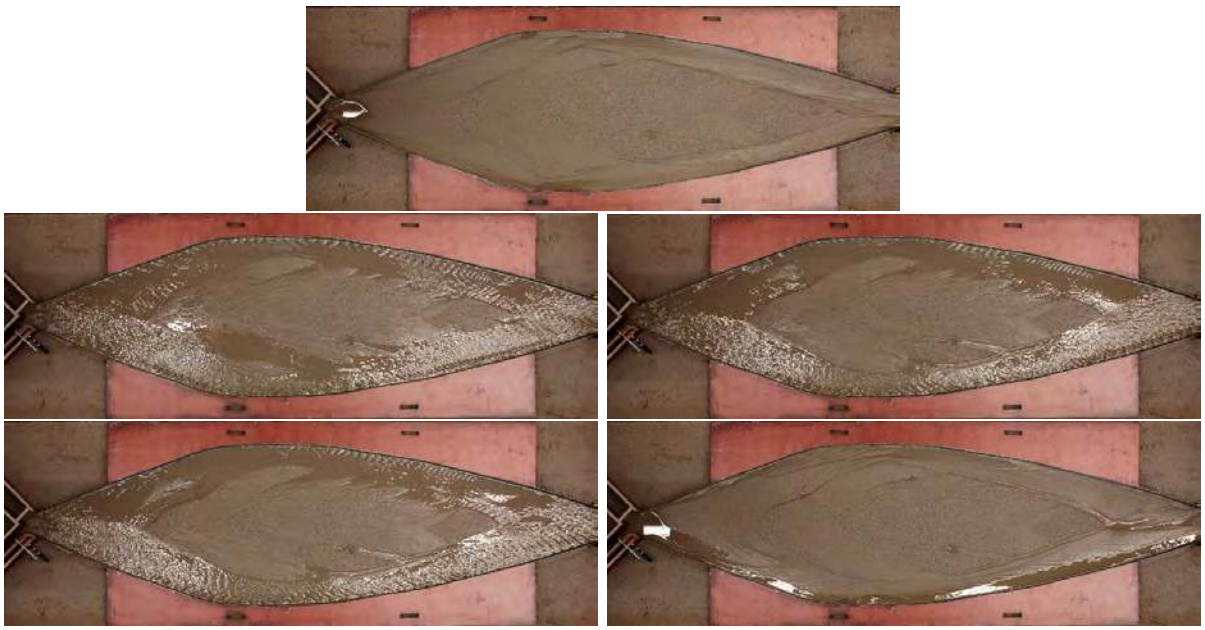

Figure B.11: Photo's taken at distinctive moments during the experiment.
Starting up top: formation island.
The low flow stage at t=15 min, at t=45 min, at t=75 min, at t=75 min empty.

C Island formation

C.1 General

In Table C.1 a summary is given of the four phases used to form the island with the first flow stage, the island formation. The time for each phase and distance of the front of the island/bar to the upstream confluence, indicated with X_f, are shown in the table. The location of the front was only applicable for the last three phases, as during the first phase no front forms. The final row shows the standard deviation for the different parameters per stage.
It can be seen that the formation of the island for each experiment was different. Both the time needed for each phase as the location of the front of the island/bar differ per experiment. The reason for this difference is the development of the island, which was different for each experiment. The final row shows the standard deviation per parameter for all experiment. The standard deviation, σ, is defined as the square root of the variance of X, $\sigma = \sqrt{E[(X-\mu)^2]}$. The total time needed for the different phases ranges from approximately 130 to 150 minutes. For the different experiments the standard deviation of the time for the first and third stage is relatively small, while it is larger for the second and fourth stage. For the different experiments the standard deviation of the location of the front decreases when the subsequent phases are conducted. As the island develops the difference in standard deviation decreases from 15, 6 and finally 2 cm. This development can be seen in Figure C.1 as well. It shows that the initial development is different, however the final obtained planform is very similar.

C.2 Bed level

The obtained bed level after the island formation was measured for all experiments, see Figure C.3 and Figure C.4. From the plots it can be seen that the obtained bed levels differ per experiment. It should be taken into account that these plots are based on 65 cross-sections in the y-direction taken every 5 cm. The plots obtained with Matlab® interpolate the bed level between the cross-sections.
With the data obtained from these measurements the standard deviation was calculated, see Figure C.2a. The figure shows the amount of variation of the bed level in the widened section. The average bed level for all island formations, see Figure C.2b, is used to calculate the standard deviation. From the calculation of the standard deviation two

Experiment	**Phase**							
	1		*2*		*3*		*4*	
	Time [min]	X_f [cm]	Time [min]	X_f [cm]	Time [min]	X_f [cm]	Time [min]	X_f [cm]
Ref	25		51	165	22	95	42	60
W1	27		62	180	23	95	40	60
W2	23		57	195	34	95	38	60
W3	17		52	190	28	105	42	65
I20	29		46	160	28	85	27	60
I40	22		51	155	25	95	33	65
O20	18		68	185	26	95	24	60
O40	28		42	160	26	105	36	60
Standard deviation	4		8	15	3	6	6	2

Table C.1: The time and location of the front per phase of the island formation stage for all experiments. The final row shows the standard deviation of the parameters for the different experiments.

main area's within the planform show above average variations; at the right channel in the middle/front and at the left channel at the end. In subsection 4.2.1 the standard deviation for the longitudinal profile at $y = 0$ was calculated, see Figure 4.3. This figure also shows that at the final section of the island the most variation can be seen. For the analysis of the results this area should be taken into account.

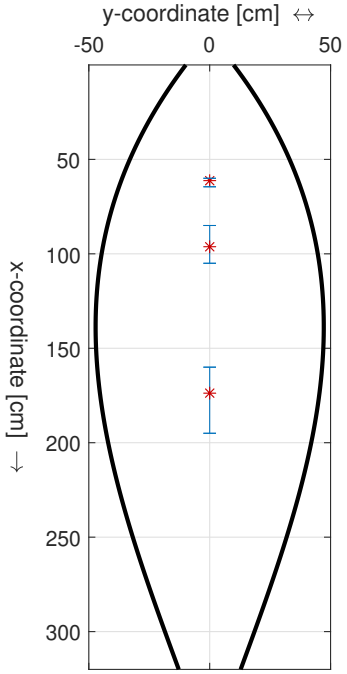

Figure C.1: Variation of the location of the front, X_f, for Phase 2, 3 and 4.

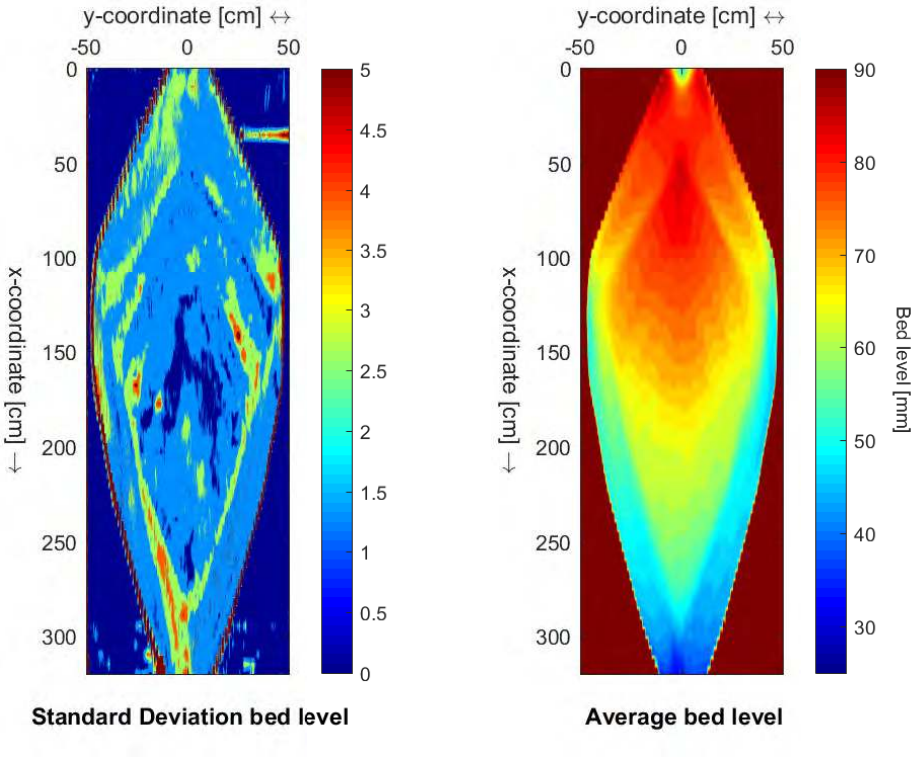

(a) (b)

Figure C.2: The standard deviation of the bed level (a) and the average bed level (b) after the first flow stage, the formation of the island, for all experiments.

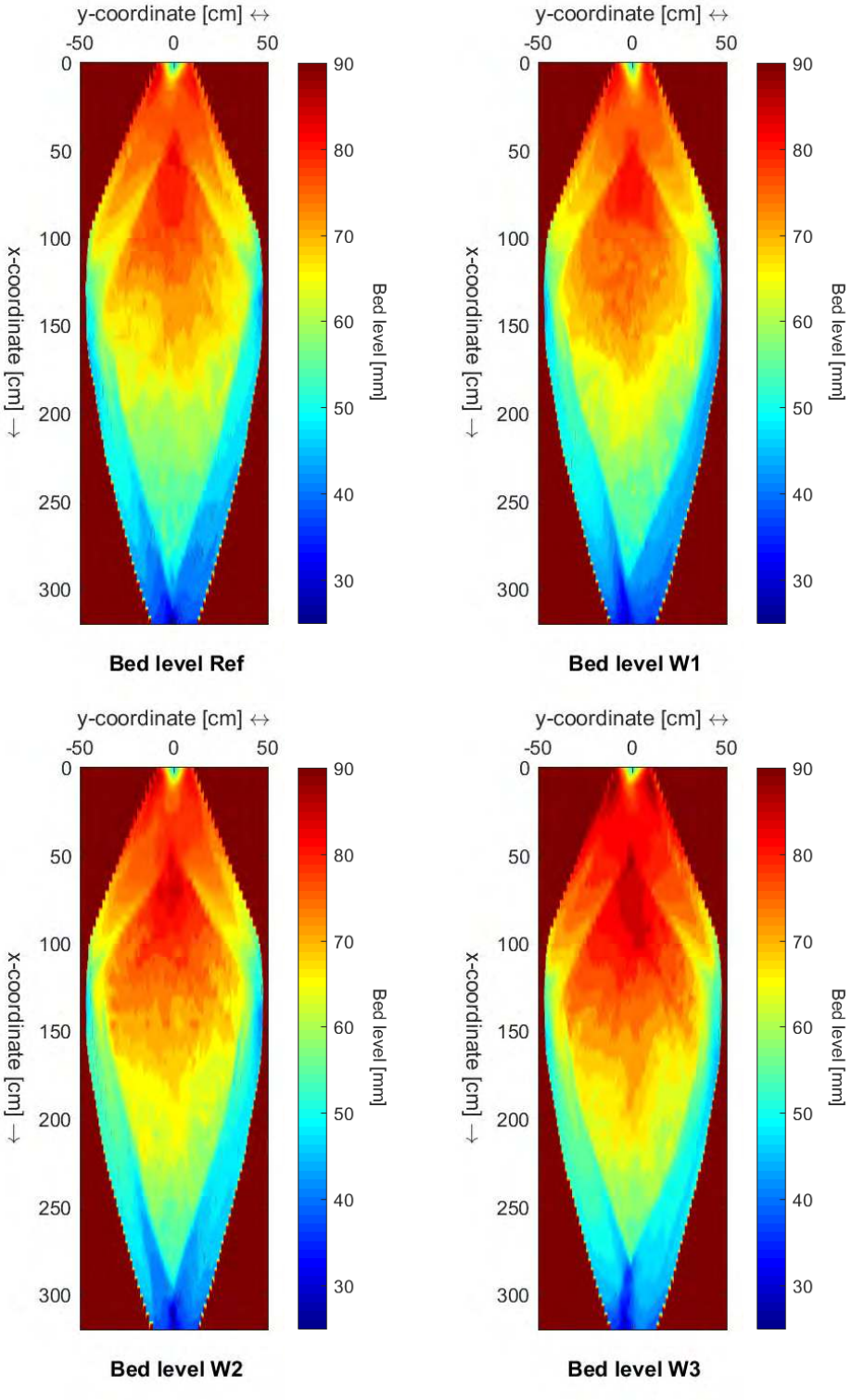

Figure C.3: The bed level in the widened section after the first flow stage, the formation of the island, for the experiments Ref, W1, W2 and W3.

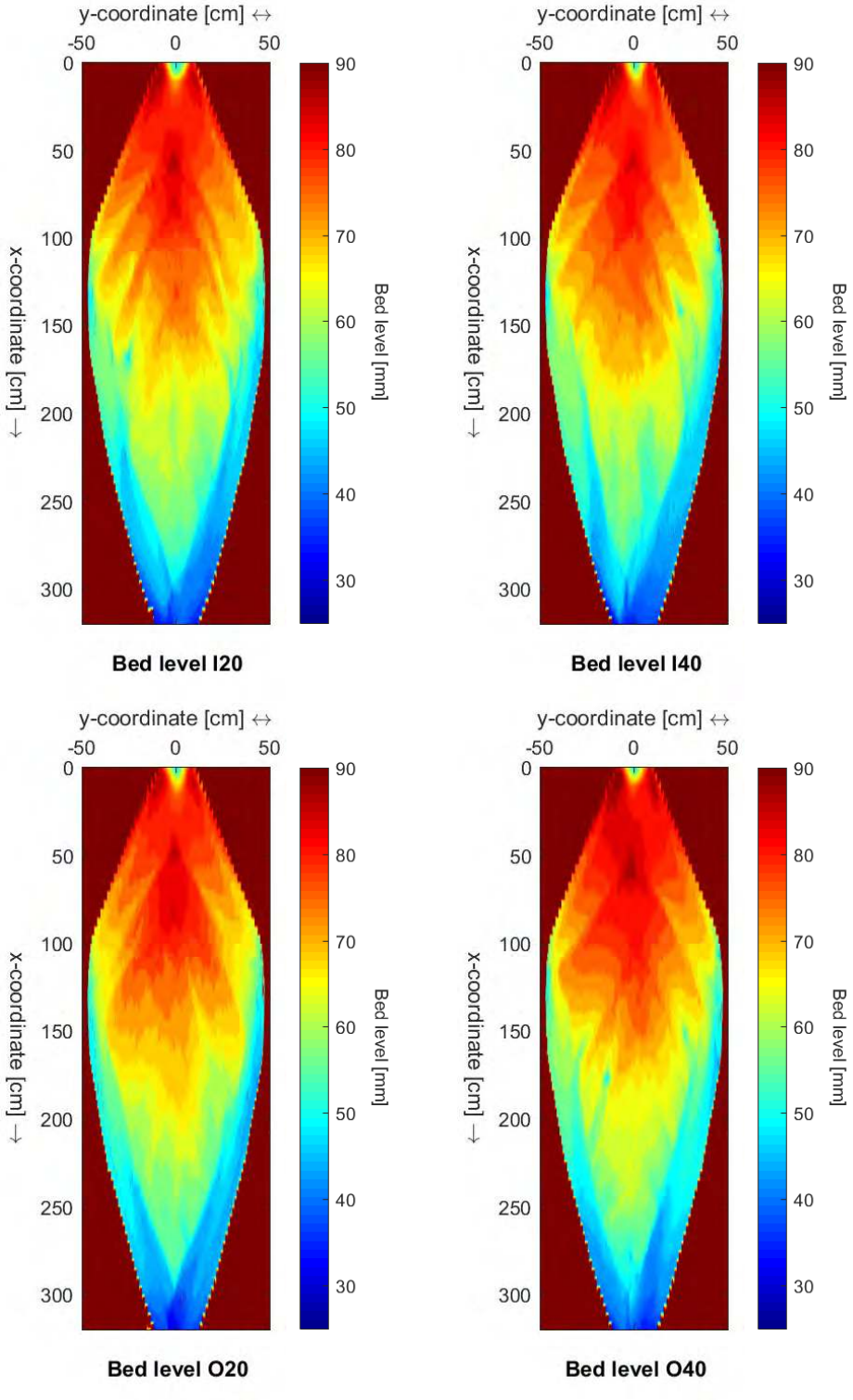

Figure C.4: The bed level in the widened section after the first flow stage, the formation of the island, for the experiments I20, I40, O20 and O40.

D Estimate discharge distribution

D.1 Method

The discharge distribution over the two channels surrounding the island is estimated in order to analyze the effects of the closure measures on the system. The distribution is estimated by comparing the cross-sectional area's and flow velocities in the two channels. The cross-sectional area's can be calculated from the water depth and channel width. Determining the water depth is not straight forward as the water levels were only measured upstream and downstream of the widened section. In the widened section only the bed levels were measured. Moreover, the velocities for the different channels were also not measured. For this estimate of the distribution it is therefore assumed that velocities and water depths were equal at the considered cross-sections. The cross-sectional area is therefore determined at the bifurcation and confluence, as here these assumption of equal water level is assured. The assumptions of equal velocity is assured for most of the experiments, with the exceptions of experiments W1, W2 and W3.

The bed levels and channels widths are determined based on two cross-sections at both the bifurcation and confluence. These cross-sections are obtained from the bed level measurements. As these bed level measurements were taken every 5 cm, a single cross-section might not represent the distribution well. Therefore two cross-sections are taken into account to assure a correct calculation. From these cross-sections the channel width and average bed level is determined, which are used to calculate the width ratio and bed level difference.
In Table D.1 the values of these parameters are shown for the reference experiment after the island formation. For the reference experiments the cross-sections at the bifurcation, at x=55 and $x = 60$, and at the confluence, at $x = 285$ and $x = 290$, are taken into account. Two of these cross-sections are shown in Figure D.1. The channel width is calculated by determining the left boundary, middle and right boundary from these figures. The average bed level for a channel is calculated with a script in Matlab®. The calculated values of the two cross-section are averaged in order to determine the width ratio and bed level difference.
The rest of the data is shown in the next section and was used for Figure 4.4, Figure 4.17 and Figure 4.24.

Cross-section		**Datapoint** [10/mm]			**Channel width** [mm]		**Average bed level** [mm]	
		left	*middle*	*right*	*left*	*right*	*left*	*right*
Bifurcation	x=55	2108	4958	7688	308	286	75,99	74,30
	x=60	1920	5000	7860	285	273	76,12	75,33
Confluence	x=285	2843	4891	6847	205	196	44,22	43,42
	x=290	2717	4967	7065	225	210	45,62	44,43

Cross-section		**Width ratio** [-]	**Bed level difference** [mm]
		B_{left}/B_{right}	$Z_{right} - Z_{left}$
Bifurcation	x=55	1,06	-1,24
	x=60		
Confluence	x=285	1,06	-0,99
	x=290		

Table D.1: Data from the analysis of the discharge distribution of the Reference experiment.

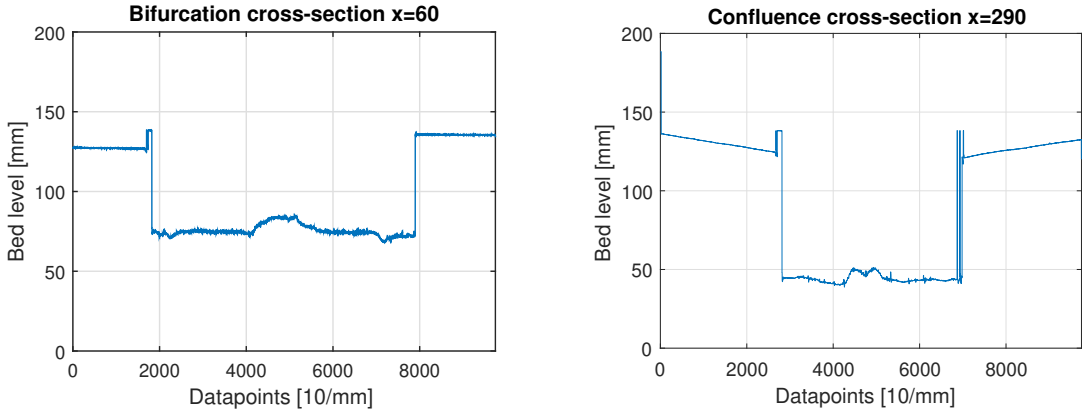

Figure D.1: The cross-sections taken at the bifurcation ($x = 60$) and the confluence ($x = 290$) in order to determine the parameters for the estimate of the discharge distribution.

D.2 Data

Experiment	**Cross-section**	**Channel width** [mm]		**Average bed level** [mm]		**Width ratio** [-]	**Bed level difference** [mm]
		left	*right*	*left*	*right*	B_{left}/B_{right}	$Z_{right} - Z_{left}$
Ref	x=55	308	286	75,99	74,30	1,06	-1,00
	x=60	285	273	76,12	75,33		
W1	x=55	304	290	74,88	73,94	0,96	-1,29
	x=60	276	281	75,18	74,00		
W2	x=55	304	284	77,56	75,17	0,98	-0,62
	x=60	281	269	77,00	76,30		
W3	x=55	297	289	80,82	79,22	0,97	-1,12
	x=60	281	273	81,70	80,53		
I20	x=55	289	304	79,44	78,36	0,97	-1,26
	x=60	270	279	80,23	79,41		
I40	x=55	298	306	78,66	77,34	0,92	-1,56
	x=60	283	274	79,55	77,85		
O20	x=55	298	285	78,89	77,37	0,99	-1,10
	x=60	281	273	79,61	78,23		
O40	x=55	289	303	81,30	80,05	0,95	-0,85
	x=60	290	267	82,40	80,37		
Ref	x=285	205	196	44,22	43,42	1,06	-1,24
	x=290	225	209	45,62	44,43		
W1	x=285	194	209	43,97	43,12	1,01	-1,06
	x=290	210	211	45,52	43,80		
W2	x=285	191	204	44,80	44,64	1,06	-1,65
	x=290	214	208	46,34	45,27		
W3	x=275	216	236	48,35	47,68	1,03	-1,39
	x=280	240	234	50,14	48,57		
I20	x=290	183	194	45,23	42,38	0,96	-0,95
	x=295	205	204	46,73	43,39		
I40	x=280	215	235	49,54	46,36	1,00	-1,51
	x=285	207	224	49,46	45,46		
O20	x=285	200	202	45,71	44,92	1,04	-1,45
	x=290	212	214	46,86	45,38		
O40	x=290	183	192	45,40	43,05	1,02	-1,64
	x=295	193	204	46,54	43,61		

Table D.2: Data from the analysis of the discharge distribution of Figure 4.4, after the island formation. The upper part shows the data of bifurcation and the lower part the data of the confluence.

Experiment	**Cross-section**	**Channel width** [mm]		**Average bed level** [mm]		**Width ratio** [-]	**Bed level difference** [mm]
		left	*right*	*left*	*right*	B_{left}/B_{right}	$Z_{right} - Z_{left}$
Ref	x=60	304	299	73,77	73,89	1,03	0,05
	x=65	321	308	73,17	73,15		
W1	x=65	341	286	73,04	75,27	1,17	2,75
	x=60	333	288	72,82	76,09		
W2	x=65	334	296	74,34	77,33	1,11	2,97
	x=70	342	313	74,26	77,21		
W3	x=65	340	290	78,24	79,10	1,15	0,99
	x=70	354	313	77,57	78,69		
Ref	x=285	205	226	44,53	45,07	0,92	-0,02
	x=280	217	231	46,01	45,44		
W1	x=285	225	206	43,57	45,26	1,10	1,26
	x=280	237	215	44,55	45,37		
W2	x=280	233	222	45,41	46,40	1,03	1,12
	x=275	237	235	46,25	47,50		
W3	x=270	268	237	48,61	48,36	1,10	0,06
	x=265	273	255	49,31	49,68		

Table D.3: Data from the analysis of the discharge distribution of Figure 4.17, after the measures around the island. The upper part shows the data of bifurcation and the lower part the data of the confluence.

Experiment	**Cross-section**	**Channel width** [mm]		**Average bed level** [mm]		**Width ratio** [-]	**Bed level difference** [mm]
		left	*right*	*left*	*right*	B_{left}/B_{right}	$Z_{right} - Z_{left}$
Ref	x=60	304	299	73,77	73,89	1,03	0,05
	x=65	321	308	73,17	73,15		
I20	x=60	282	314	76,57	76,62	0,88	0,20
	x=55	260	300	77,27	77,62		
I40	x=60	233	362	77,61	77,85	0,71	-0,29
	x=65	273	356	77,79	76,97		
O20	x=60	287	308	76,30	77,29	0,93	0,66
	x=65	302	323	76,16	76,49		
O40	x=60	265	322	77,28	79,81	0,85	2,23
	x=65	295	334	77,20	79,12		
Ref	x=285	205	226	44,53	45,07	0,92	-0,02
	x=280	217	231	46,01	45,44		
I20	x=280	246	206	47,25	44,93	1,18	-2,18
	x=275	258	221	48,22	46,19		
I40	x=260	304	245	51,89	48,93	1,16	-2,86
	x=255	298	279	52,51	49,76		
O20	x=285	208	221	44,78	45,97	0,93	1,04
	x=280	217	235	46,46	47,35		
O40	x=270	253	255	48,05	50,84	1,01	2,46
	x=265	262	257	49,59	51,72		

Table D.4: Data from the analysis of the discharge distribution of Figure 4.24, after the measures upstream of the island. The upper part shows the data of bifurcation and the lower part the data of the confluence.

E Grain size distribution

For the experiments a well mixed sediment mixture was used. In Figure E.1 the grain size distribution of the mixture is shown. From this grain size distribution the characteristic D_{50}=1 mm and D_{90}=1.55 mm were determined.

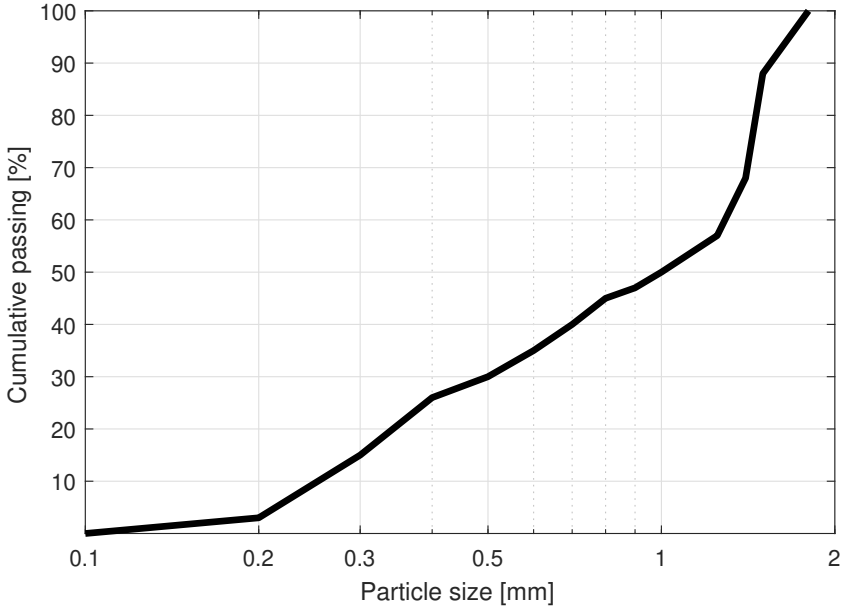

Figure E.1: Grain size distribution of the sediment mixture.

F Guidelines Ostanek Jurina (2017)

The research of Ostanek Jurina (2017) concludes with recommendations on channel closure based on the conditions of the particular river section and pursued goals of the intervention. In this Appendix the recommendations from the numerical study, based on these two criteria, are repeated. A schematic overview of the recommendations are shown in Figure F.1. The sections below are quotations from the report of Ostanek Jurina (2017, p. 81-82) of chapter 9.2 *Recommendations for channel closure.*

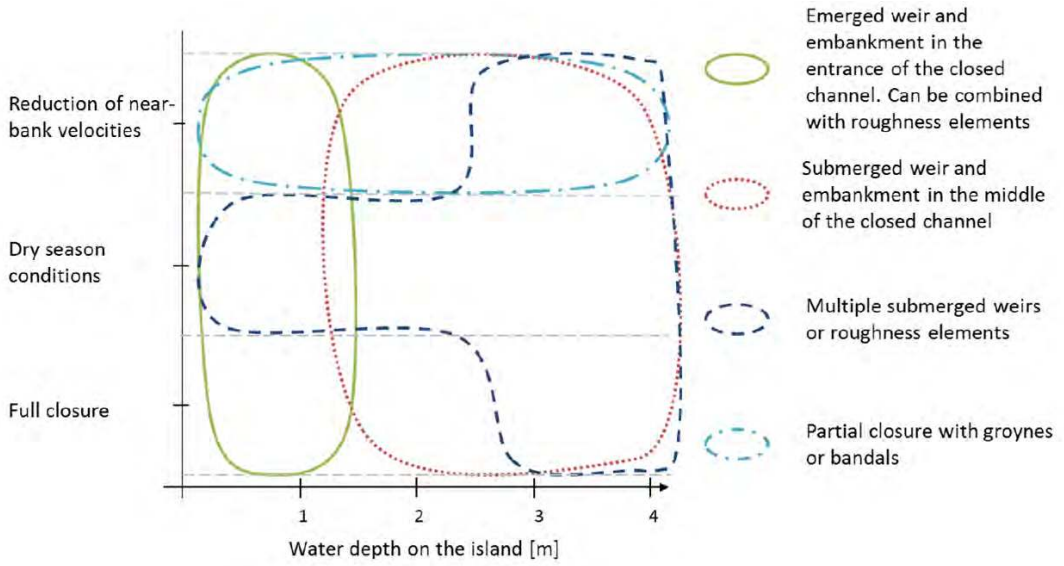

Figure F.1: Schematic representation of recommendations for channel closure derived from the results of the model study, from (Ostanek Jurina, 2017).

Conditions river section

When water levels relative to the island are low (below 1 m water depth on the island in this study), the best option for full closure is a weir in the upstream part of the channel combined with a long embankment parallel to the island banks that reduces the gradient around the structure. The embankment should reach the entrance of the closed branch to prevent the formation of a channel across the island upstream of the intervention. The alternative is a combination of multiple structures at appropriate intervals in the closed branch. Only one structure needs to block the channel completely, while the rest can be replaced with roughness elements for a similar effect.

When water levels are relatively high (2 or more above island level), the best option is to use multiple submerged weirs in the closed branch or alternatively one submerged weir and a long embankment in the middle of the closed channel, where the water level gradient across the island is the lowest. Complete closures with emerged weirs are not recommended, as significant erosion occurs in those cases. The choice between different options would likely depend on economic considerations. Where the closed channel is wide and deep and the flow on the island is shallow, embankments are probably a better option. On the other hand, if the channel is narrow and the water depth on the island is substantial, combining weirs with permeable structures can be a cheaper alternative.

Pursued goal

Whenever complete closure is not required, it is advised to reduce the discharges in the channel only partially and rely on gradual closure due to deposition in the channel. This can be done with a combination of low weirs and roughness elements. Single weirs with short embankments are not recommended due to bypass erosion. Gradual closure due to deposition needs to be studied further before recommendations can be elaborated further.
Near-bank velocities can be most effectively reduced by pushing the flow away from the bank using bandals or groynes that partially block the channel. Constriction of the channel could cause gradual channel abandonment over the course of a few years as well. If this is not an option, the best results are achieved with a combination of a weir and a long embankment on the island.
If the main goal is that the channel remains closed during the dry season, the most important consideration is that channels on the island do not develop. This can be best guaranteed by using multiple low or permeable structures, with at least one of them fully closing the branch during the dry season. A combination of a submerged weir and a long embankment works as well. Improvement of navigability is correlated with dry-season discharge reduction, so the same approach works best for it as well. When the closed channel is much smaller than the open branch, navigability improvement is minimal.